

## **Copyright Warning & Restrictions**

The copyright law of the United States (Title 17, United States Code) governs the making of photocopies or other reproductions of copyrighted material.

Under certain conditions specified in the law, libraries and archives are authorized to furnish a photocopy or other reproduction. One of these specified conditions is that the photocopy or reproduction is not to be “used for any purpose other than private study, scholarship, or research.” If a user makes a request for, or later uses, a photocopy or reproduction for purposes in excess of “fair use” that user may be liable for copyright infringement,

This institution reserves the right to refuse to accept a copying order if, in its judgment, fulfillment of the order would involve violation of copyright law.

**Please Note: The author retains the copyright while the New Jersey Institute of Technology reserves the right to distribute this thesis or dissertation**

Printing note: If you do not wish to print this page, then select “Pages from: first page # to: last page #” on the print dialog screen

The Van Houten library has removed some of the personal information and all signatures from the approval page and biographical sketches of theses and dissertations in order to protect the identity of NJIT graduates and faculty.

## **ABSTRACT**

### **Microstructural Investigation of Surface Coating Developed by Electro-Spark Deposition Technology**

**by  
Tianzong Xu**

Electro-spark deposition (ESD) is a pulsed-spark micro-welding process using an electrode to apply a fused, metallurgically bonded coating with an extremely low heat input so as to eliminate thermal distortion or changes in metallurgical structure of the substrate. The deposited surface achieves an exceptionally fine-grained, homogeneous coating that may approach as amorphous structure which is believed to contribute to good wear and corrosion resistance.

In this research, an optical image analysis system, scanning electron microscope with computerized energy dispersive spectrometer, microhardness testing system and computerized surfanalyzer were employed to investigate the microstructure and properties of achieved surface coatings.

As the results of this work, a special sample preparation method was designed, and microstructure-composition-properties of the surface coatings were obtained, showing that good bonding of applied coating and substrate as well as desirable transition microstructure contributed by alloying and diffusion can be achieved by electro-spark deposition process.

**MICROSTRUCTURAL INVESTIGATION  
OF SURFACE COATING DEVELOPED BY  
ELECTRO-SPARK DEPOSITION TECHNOLOGY**

**by  
Tianzong Xu**

**A Thesis  
Submitted to the Faculty of  
New Jersey Institute of Technology  
in Partial Fulfillment of the Requirements for the Degree of  
Master of Science in Mechanical Engineering**

**Department of Mechanical Engineering**

**January, 1993**



**APPROVAL PAGE**

**Microstructural Investigation of Surface Coating  
Developed by Electro-Spark Deposition**

**Tianzong Xu**

*12/16/92*

---

Dr. Roman Dubrovsky, Thesis Adviser/  
Associate Professor of Mechanical Engineering, NJIT

*Dec. 18, 92*

---

Dr. Nouri Levy, Committee Member  
Associate Professor of Mechanical Engineering, NJIT

*12/18/92*

---

Dr. R. Y. Chen, Committee Member  
Professor of Mechanical Engineering, NJIT

## **BIOGRAPHICAL SKETCH**

**Author:** Tianzong Xu

**Degree:** Master of Science in Mechanical Engineering

**Date:** January, 1993

**Date of Birth:**

**Place of Birth:**

**Undergraduate and Graduate Education:**

- Master of Science in Mechanical Engineering,  
New Jersey Institute of Technology, Newark, NJ, U.S.A., 1993
- Graduate Study in Materials Engineering,  
Shanghai Jiao Tong University, Shanghai, China, 1991
- Bachelor of Science in Materials Science and Engineering,  
Shanghai Jiao Tong University, Shanghai, China, 1988

**Major:** Mechanical Engineering

**This thesis is dedicated to  
my parents: Mr. Weibin Xu and Mrs. Ruihu Zhou**



## ACKNOWLEDGMENT

The author wishes to express his sincere gratitude to his thesis advisor, Professor Roman Dubrovsky, for his guidance, friendship, and moral support throughout this work.

Special thanks to Professors Nouri Levy and R. Y. Chen for serving as members of the committee.

Thank you to the technician of Electron Microscopy Laboratory in Materials Science and Engineering Department of Stevens Institute of Technology, and Dr. Gongyao Zhou in Mechanical Engineering Department of NJIT for their help.

The author is grateful to the Mechanical Engineering Department of NJIT for support of this research.

The author appreciates the timely help and suggestions from Surface Engineering Laboratory members, including Mr. Wenge Yang (former member), Peng Chen, Miss Ning Li and Dr. I-Tsung Shih. Also thanks to Mr. Don Rosander, Joseph Glaz, and David Singh for their help.

And finally, the author would like to express his special gratitude to his parents, his uncle and aunt Mr. & Mrs. Richard Zhou for their care and support for my study in the United States of America.

## TABLE OF CONTENTS

Chapter	Page
1 INTRODUCTION.....	1
2 BACKGROUND .....	3
2.1 History of Electro-Spark Deposition (ESD).....	3
2.2 Role and Problems of ESD.....	5
2.2.1 Improvement of Wear Resistance .....	6
2.2.2 Improvement of Corrosive Resistance.....	8
2.2.3 Fatigue Resistance of ESD Surface Coating.....	10
2.2.4 Problems .....	10
2.3 Application.....	11
2.4 Goal and Objectives .....	14
3 FUNDAMENTALS OF ELECTRO-SPARK DEPOSITION .....	15
3.1 Physical Concept of Electric-Discharge and Spark .....	15
3.2 Practical Electric-Discharge in Media.....	16
3.2.1 In a Gaseous Medium.....	16
3.2.1.1 Initiation by Electric Field .....	16
3.2.1.2 Initiation by Contact.....	16
3.2.2 In a Liquid Medium.....	17
3.2.3 Comparison .....	17
3.3 General Principles of Electro-Spark Deposition.....	18
3.4 Mechanism of Hardening by Electro-Spark Deposition .....	19
3.4.1 Thermal Effect of Spark .....	19
3.4.2 Surface Alloying.....	21
3.4.2.1 Influence of Atmospheric Gas Medium.....	21
3.4.2.2 Carbon Absorption .....	22
3.4.2.3 Electrode Transfer .....	24

<b>Chapter</b>	<b>Page</b>
4 METHODOLOGY .....	28
4.1 Surface Engineering by Electro-Spark Deposition .....	28
4.1.1 ESD Equipment and Processing.....	28
4.1.1.1 Polarity Feature .....	29
4.1.1.2 Function of Ballast Resistor.....	29
4.1.1.3 Energy Input.....	30
4.1.2 Modern Equipment.....	30
4.1.3 Material Systems and Environment Media.....	31
4.1.3.1 Electrode Materials.....	31
4.1.3.2 Substrate.....	32
4.1.3.3 Environment Media .....	32
4.1.4 ESD Processing .....	33
4.2 Analysis of ESD Coating.....	33
4.2.1 Introduction.....	33
4.2.2 Microscopic Analysis .....	35
4.2.2.1 Optical Metallurgical Analysis .....	35
4.2.2.2 SEM and EDS Analysis.....	38
4.2.3 Surface Topography .....	44
4.2.3.1 Introduction.....	44
4.2.3.2 Methodology .....	45
4.3 Performance Evaluation.....	50
4.3.1 Microhardness Test .....	51
4.3.2 Bonding and Strength Evaluation.....	52
4.3.2.1 Simple Bending Test.....	53
4.3.2.2 Indentation Test.....	53

<b>Chapter</b>	<b>Page</b>
5 RESULTS .....	54
5.1 Microstructure of ESD Surface Coating.....	54
5.1.1 General Structure.....	54
5.1.2 Microstructure of Specimen 1.....	54
5.1.2.1 Fusion Zone.....	59
5.1.2.2 HAZ .....	61
5.1.2.3 Fusion Line .....	61
5.1.3 Microstructure of Specimen 2.....	61
5.1.3.1 Fusion Zone.....	61
5.1.3.2 HAZ and Fusion Line .....	65
5.1.4 Specimen 3 .....	65
5.1.4.1 Fusion Line .....	65
5.1.4.2 HAZ and Fusion Line .....	69
5.1.5 Microstructure of Specimen 4.....	69
5.1.5.1 Fusion Zone.....	69
5.1.5.2 HAZ and Fusion Line .....	73
5.2 Surface Topography .....	74
5.2.1 Surface Morphology.....	74
5.2.2 Surface Roughness .....	78
5.2.2.1 Specimen 1 .....	82
5.2.2.2 Specimen 2 .....	83
5.2.2.3 Specimen 3 .....	83
5.2.2.4 Specimen 4 .....	83
5.3 Microhardness Test .....	84
5.3.1 Specimen 1 .....	84
5.3.2 Specimen 2.....	89

<b>Chapter</b>	<b>Page</b>
5.3.3 Specimen 3 .....	89
5.3.4 Specimen 4 .....	90
5.4 Simple Bend Test .....	92
5.5 Indentation Test.....	95
6 DISCUSSION .....	99
6.1 Surface Alloying and Microstructure of ESD Coating System .....	99
6.1.1 Surface Alloying.....	99
6.1.2 Materials Systems.....	100
6.1.2.1 Electrodes.....	100
6.1.2.2 Substrates .....	102
6.1.2.3 Environment Medium .....	103
6.1.3 Microstructure of ESD Coating Systems.....	105
6.1.3.1 General Description.....	105
6.1.3.2 Distinguishment of ESD Coating Structure .....	106
6.1.3.3 Coating Thickness .....	110
6.1.3.4 Softening in ESD Coating System.....	111
6.2 Diffusion in ESD.....	112
6.3 Metallurgical Bonding.....	113
6.4 Microcracking of ESD Coating System .....	114
6.5 Process Parameters and Their Effects .....	117
6.5.1 Electrical Power and Energy.....	117
6.5.1.1 Production .....	117
6.5.1.2 Dissipation .....	117
6.5.1.3 Distribution .....	118
6.5.1.4 Effect.....	118

<b>Chapter</b>	<b>Page</b>
6.5.1.5 Limitation.....	118
6.5.2 Capacitance .....	119
6.5.3 Voltage and Spark Gap.....	122
6.5.4 Duration of the Sparking.....	122
6.5.5 Sparking Time .....	123
6.5.6 Amplitude and Frequency of the Vibrating Electrode .....	124
7 CONCLUSIONS.....	126
8 RECOMMENDATIONS FOR FUTURE WORK .....	128
WORKS CITED.....	129

## LIST OF TABLES

<b>Table</b>	<b>Page</b>
4.1 ESD coatings applied to date .....	31
4.2 Information of electrode materials .....	32
4.3 Methods of thickness testing.....	48
5.1 Surface roughness parameters.....	81

## LIST OF FIGURES

<b>Figure</b>	<b>Page</b>
2.1 Results of wear tests on steel sparked with carbide electrode.....	7
2.2 Wear test results for sparked copper and nickel .....	7
2.3 Corrosion of chromiumcarbide coatings in sodium at 625 <sup>o</sup> C.....	9
2.4 Thermogravimetric test data for the dulfidation of ESD coated and uncoated Type 310 SS in a H <sub>2</sub> /H <sub>2</sub> S atmosphere at 875 <sup>o</sup> C .....	9
3.1 Basic RC circuit for electro-spark deposition.....	18
3.2 General structure of ESD surface coating .....	20
3.3 Influence of environment on the hardness of sparked iron .....	21
3.4 Cast-iron structure on iron sparked with a graphite electrode.....	23
3.5 Influence of cover gas on ESD mass transfer mechanism.....	26
3.6 Localized transfer causing protuberance on the surface of steel workpiece .	27
4.1 Basic circuit diagram.....	28
4.2 Sketch of manually operated ESD .....	33
4.3 Sketch of some techniques in metallographic sample preparation .....	36
4.4 Interaction between incident electron beam and solid sample .....	39
4.5 Histogram of energy dispersive diagram.....	40
4.6 Basic component of SEM .....	42
4.7 Schematic diagram of the detector of ESD.....	42
4.8 Sketch of doing spot analysis using SEM and EDS.....	44
4.9 Illustration of some surface roughness parameters .....	46
5.1 Optical micrograph of Specimen 1 deposited with Eltd1.....	55
5.2 Optical micrograph of Specimen 1 deposited with Eltd1.....	55
5.3 Optical micrograph of Specimen 1 deposited with Eltd1.....	56
5.4 Optical micrograph of Specimen 1 deposited with Eltd1.....	56



<b>Figure</b>	<b>Page</b>
5.5 SEM micrograph of Specimen 1 .....	57
5.6 Variation in concentration with respect to micrograph of Specimen 1.....	58
5.7 SEM micrograph of Specimen 2 .....	62
5.8 Variation in concentration with respect to micrograph of Specimen 2.....	63
5.9 SEM micrograph of Specimen 3 .....	66
5.10 Variation in concentration with respect to micrograph of Specimen 3.....	67
5.11 SEM micrograph of Specimen 4 .....	70
5.12 Variation in concentration with respect to micrograph of Specimen 4.....	71
5.13 Surface micrographs .....	75
5.14 Surface profiles of ESD deposited specimens .....	79
5.15 Bearing area curves .....	81
5.16 Variation in microhardness with respect to tape-sectioned micrograph of Specimen 1 .....	85
5.17 Variation in microhardness with respect to tape-sectioned micrograph of Specimen 2.....	87
5.18 Variation in microhardness with respect to tape-sectioned micrograph of Specimen 3 .....	88
5.19 Variation in microhardness with respect to tape-sectioned micrograph of Specimen 4.....	91
5.20 Optical micrographs of cross-sectioned specimen after 90 <sup>o</sup> simple bend test	93
5.21 Optical micrographs of cross-sectioned specimen after indentation test .....	96
6.1 Variation in stress relief cracking in chromium carbide deposited on Type 394 SS as a result of varying ESD parameters .....	115
6.2 Cr <sub>3</sub> -15% ESD coating on Type 316 SS .....	115
6.3 Material transfer vs. circuit capacity .....	120
6.4 Material transfer vs. spark energy .....	120
6.5 Material transfer vs. discharge inductance .....	121

<b>Figure</b>	<b>Page</b>
6.6 Spark duration vs. spark energy for maximum transfer .....	121
6.7 Increase in weight of the workpiece depending on the specific welding time, for different electrical powers $P_m$ .....	122

# CHAPTER 1

## INTRODUCTION

All engineering materials are usually characterized by those of their properties which are of practical value to the designer, production engineer, toolmaker, etc. These properties are related to the condition of surface layer and usually are: wear, corrosion, fatigue, heat resistance; hardness and roughness of the surface; thermal conductivity of the surface layer and their resistivity [1]. The wear, corrosion and fatigue resistance are the most commonly encountered industrial problems leading to the replacement of components and assemblies in engineering practice.

Naturally, each operation which alters the surface is bound to affect the corresponding properties of the material by intensifying or weakening them. So improvement of surface performance is of most practical importance to extend the useful life of tools and machine components which are subjected to wear, corrosion, galling, etc. The best way combining surface performance with economy is to produce well-qualified surface coatings without interfering the basic properties of the bulk materials. This brings out the field of surface treatment.

Of various methods in this field, such as nitriding, case hardening, PVD, CVD, and electroplating which are well known and developed intensively, electro-spark deposition (ESD) which originated from electric-discharge machining (EDM), is not a new technique as having been in use for over 30 years, but with least development and gaining just a limited awareness in most of the western nations. However, it is a very unique, versatile and economically effective method for improving surface performance.

In the literatures, the process is known by a variety of other names, such as sparking hardening [2], electric spark toughening [3], electro-spark alloying [1], and similar terms. By scientific definition, it is a pulsed-arc micro-welding process

using short-duration, high-current electrical pulses to deposit an electrode material on a metallic substrate so as to produce an exceptionally fine-grained, homogeneous and metallurgically-bonded surface coating without interfering the basic properties of the bulk materials [4]. Its advantages and limitations can be described as the following [5]:

#### **A. Advantages**

- \* Metallurgically bonded coating
- \* Low heat input to substrate
- \* Distortion free
- \* Little or no substrate preparation required
- \* Little or no surface finishing required
- \* Little operator skill required
- \* Fast set-up, inexpensive equipment
- \* Portable equipment
- \* Applicable to ID surfaces and complex shapes
- \* Easily automated
- \* Can apply nearly all metals and cermets

#### **B. Limitations**

- \* Maximum coating thickness currently limited to 50 ~250  $\mu\text{m}$ , depending on materials
- \* Stress relief cracking inherent in some materials
- \* Minimum as-deposited roughness currently 2.5  $\mu\text{m}$  AA (100  $\mu\text{m}$ -in AA)
- \* Both substrate and coating material must be electrically conductive
- \* Maximum effective coating rate currently is  $\sim 15\text{cm}^2/\text{min}$  per applicator head used

With the rapid development of modern science and technology, ESD will gradually exhibit its promising prospect in High Tech areas as well as in commercial industry areas.

## **CHAPTER 2**

### **BACKGROUND**

#### **2.1 History of Electro-Spark Deposition (ESD)**

The first known reference to the influence of electric spark on metal surface appears in the discussion of a paper by H.S.Rawdon in 1924 [6]. When he did experiments with spark struck between contacts of electrolytic iron, he discovered that surface regions heated to fusion by the sparks became very hard as determined by a scratch-resistance test, while the repeated experiments with copper or nickel contacts showed no increase in hardness. He then concluded that the hardening of the iron, surprising for materials of such low carbon content (0.02%) was attributed to the formation of martensite as a result of rapid quenching of the minute spark-heated surface volume. This is also one of the earliest observations of the effects of extremely rapid solidification, because martensite formation in the pure iron he was using would have been unexpected under more normal heat-treatment conditions.

In 1957, N.C.Welsh at the Research Laboratories of Associated Electrical Industries in Great Britain [7], encountered the same phenomenon as Rawdon, while he attempted to simulate the effect of frictional heating on steel surfaces by the thermal action of electric sparks. In further work [7, 8], he showed that the surface hardness could be influenced by the choice of the medium in which the sparking occurred. Absorption of atmospheric elements such as nitrogen or oxygen contributed, sometimes markedly, to the hardness changes available. Sparking of titanium surfaces under oil, for example, resulted in high surface concentrations of titanium carbide and changed a very poor-wearing, galling-prone material to one with a hard, low-friction and durable surface. He and others went on to show that surface alloying by the transfer of matters from the electrode to the substrate

between the spark contacts is one of the great general importance, as it confers much great hardness and seems to be the sole means by which most non-ferrous metals can be hardened [2, 9, 10]. It was not until then that the detail descriptions of the constitutional changes produced by spark and the fundamentals of ESD process were demonstrated.

In fact, the first discovery of the principle of spark hardening should be attributed to the Russian researches. As early as 1944, two Russian people first demonstrated the value of spark treatment as a practical process for surface hardening [11]. Since then the process has been intensively studied in the U.S.S.R. and applied to a very wide range of tools and components. Commercial equipment was produced in Russia in the early 1950s. Subsequently, with improvement of the equipment, several versions of the ESD method of hardening with favorable results were described in a number of Russian publications, as well as some of Czechoslovakia and East Germany [3]. The ESD appeared to have become a commonly used method of increasing life of many cutting tool and machine components subjected to wear, such as lathe tools, drills, milling cutters, dies, files hacksaw blades, camshafts, tappets, wheel rim and turbine blades.

However, development in other countries was in a comparatively small scale, especially in the Western nations. By the end of 1950s, commercial equipment began to be available in Britain and other Western countries [3]. Two British firms marketed equipment for the ESD hardening of cutting tools in 1958. But early results obtained with these machines were inconsistent and not always favorable. While a certain measure of success was claimed, other cases were also cited in which there was no improvement or even a deterioration in performance of tools as a result of treatment [3].

In the 1960s, M.M.Barash and C.S.Kahlon [3,12] investigated in this field and presented some useful conclusions about the importance of parameters control

and their effects on surface quality, the relationship between the concentration of hard electrode material in the treated surface and the hardness of the surface, the relationship between the cutting performance of treated tools and the hardness & thickness of the strengthened layer.

In 1974, Roger N. Johnson at Westinghouse Hanford Company in U.S.A. reported on promising experiments with ESD coatings in support of applications on nuclear reactor components [13]. Whereas, he stated that further development was required for better coating uniformity, smoother surface finishes and improved reproducibility and control of the process before ESD coatings could be fully acceptable. It was shown that control of a large number of process parameters was a principle approach to achieve the goal. Since then, development of applications of ESD process has resulted in advances of electronic controls, significant increase of deposition rates and improvement of coating quality. R.N.Johnson, G.L.Sheldon (at Dept. of Mech. Eng. and Mat. Sci. of Washington State University) and E.A.Brown III (at Hewlett Parkard Co.) have contributed a lot to the development of ESD in the U.S.A. [4, 13, 14, 15, 16].

Now, ESD processes have been further improved by understanding and control of deposition and use of computer-controlled automation. As a result, ESD coatings that meet various rigorous demands of performance and consistency are being routinely applied to nuclear reactor and other components, more extensive applications appear to be assured in the near future.

## **2.2 Roles and Problems of ESD**

ESD is a surface coating process by micro-welding of material of applied electrode to substrate. The produced surface with alloyed structures, obtains properties approaching those of the electrode material. Therefore, a wide range of surface performances can be designed by applying appropriate electrode materials.

In engineering practice, the most important concerns are centered on the wear resistance, corrosion resistance and fatigue resistance of material surfaces. ESD as a unique surface coating technology can serve as a versatile and effective approach to improve surface performance. However, as mentioned before, ESD has always been lack of awareness since its early development. It is still less developed. Up to now, ESD is mainly applied for improvement of wear resistance while some advanced applications in corrosive environments have achieved success.

### **2.2.1 Improvement of Wear Resistance**

The final object of investigations into the surface properties of ESD coatings is usually the study of the wear resistance, i.e., of a property of considerable importance in engineering since on it depends the service life of tools and machine components [1].

Almost every paper dealing with the wear resistance of ESD coatings invariably records its substantial increase. The causes of the increased wear resistance of ESD coatings are, on the whole, these that cause an increase in their microhardness due to:

- a. intense heating and rapid chilling micro-volumes of surface materials
- b. surface alloying with matters from the electrode or atmospheric media.

All these principle causes at least result in a fine-grained metallurgically bonded ESD coating with prominent wear resistance.

Polyachenko lists a number of rules characterizing the dependence of increased wear on the technology of electro-spark hardening operations [17]. He pointed out that an increase of the relative duration of process in the initial stage, before a solid ESD coating has been produced, raises the wear resistance, but continuation of the process no longer increases the relative wear resistance. So that service life of deposited part remains dependently only on the thickness of the



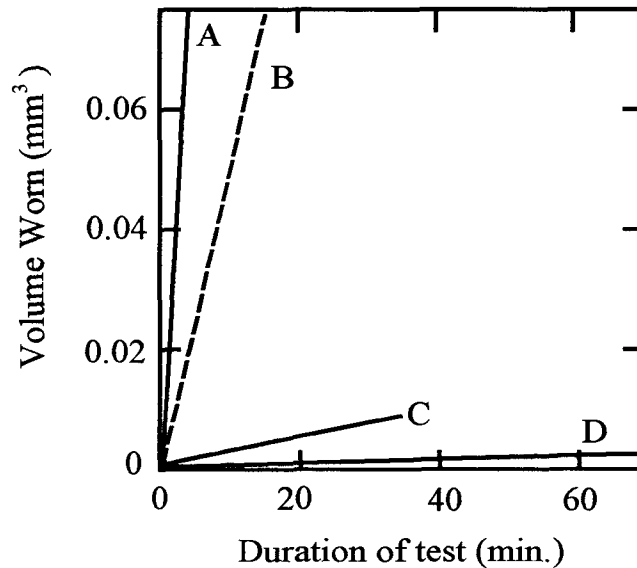


**Figure 2.1** Results of wear tests on steel sparked with carbide electrode: 68%WC-25%TiC-7%Co; test load 2 kg; sliding speed 200 cm/sec. A: Untreated steel (1.2%C); B: Case-carburized mild steel; C: Sparked for 4min/cm<sup>2</sup>; D: Sparked for 8 min/cm<sup>2</sup>.

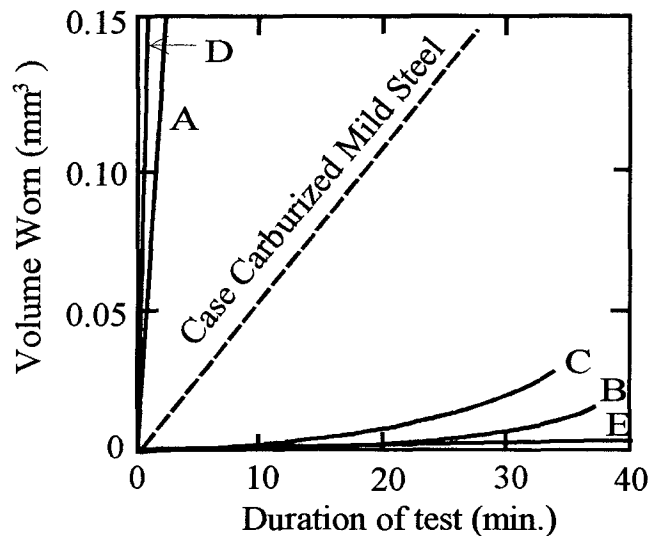


**Figure 2.2** Wear-test results for sparked copper and nickel. Test load 2 kg; sliding speed 200 cm/sec. A: Untreated copper; C: Copper sparked for 12 min/cm<sup>2</sup> with Ti electrode in nitrogen; B: Copper sparked for 27 min/cm<sup>2</sup> with WC electrode (6%Co); D: Untreated nickel; E: Nickel sparked for 3 min/cm<sup>2</sup> with WC electrode (6%Co).

applied coating. However, it is advisable to use thinner layers, applied at a low pulse energy, since they are usually denser, less brittle, smoother and therefore better wear resistance.

The curves of Figure 2.1 [2] show the very marked reduction of wear rate produced by alloying with matter transferred from an electrode of hard carbide.

In Figure 2.2 [2], curve C is of special interest, as it illustrated the effect of the transfer of a soft electrode material (Titanium) that is hardened by reaction with the environment medium (nitrogen). The hardness produced on the copper surface by the formation of titanium nitride is of magnitude similar to that conferred by sparking with a carbide electrode: the wear resistance is correspondingly high. The fact that the wear resistance of the ESD coating does not always reflect the properties of the original electrode material, presents to us two suggestions:

- a. try to avoid profound intermixing between hard-wear-resistant electrode material with workpiece materials.
- b. make use of hardening effect that results from the chemical reactions with atmospheric medium to develop electrode materials and the process in a more economical way.

### **2.2.2 Improvement of Corrosive Resistance**

The transformation of the structure of the surface layer and the change of the chemical composition during the ESD process invariably cause a reduction in the chemical activity of the metal of the layer concerned. Moreover, the rapid solidification that occurs in ESD coatings produces an exceptionally fine-grained (for some materials, amorphous), dense structure that is usually superior in corrosion resistance to that at the same or similar composition produced by other methods [4].

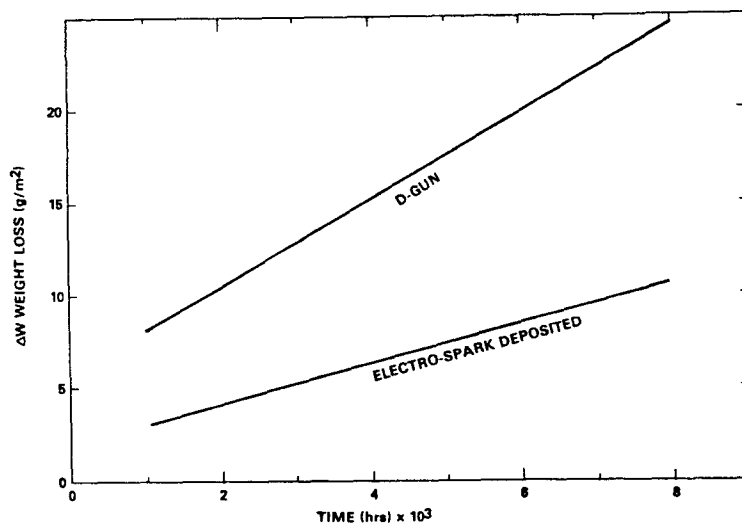


Figure 2.3 Corrosion of chromium carbide coatings in sodium at 625°C [14].

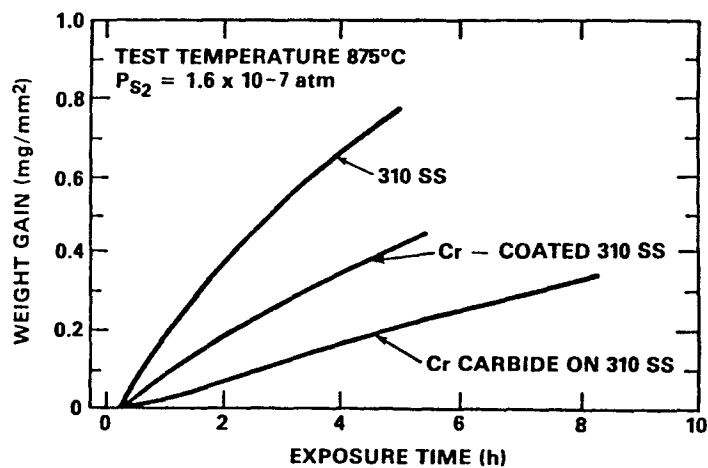


Figure 2.4 Thermogravimetric test data for the sulfidation of ESD coated and uncoated Type 310 SS in a  $H_2/H_2S$  atmosphere at 875°C [18].

Corrosion testing conducted on ESD coatings in some environments and comparing testing with other coatings all show the improvement of corrosion resistance of ESD coatings. Figure 2.3 [14] and 2.4 [18] illustrate such results.

However, ESD coatings obtained to date usually contain a certain number of pores and cracks. Therefore, this method has not, as yet, be widely recommended for applying protective coatings to surfaces, although some breakthroughs have been achieved. This may be one of the major reasons why ESD process receives a limited awareness in its development history. Further works are needed to develop new electrode materials and optimum process parameters so as to achieve good quality and well-performed coatings.

### **2.2.3 Fatigue Resistance of ESD Surface Coating**

A very important property of material, which depends on the quality of its surface to a considerable extent, is its fatigue strength. It is known that increasing the hardness and wear resistance of a surface is usually a radical as well as an effective means of increasing the fatigue strength as a whole. However, little work has been done in this aspects. Some early works [1] indicated that the fatigue strength of parts by ESD process in air was slightly lower than that of those machined by other methods. The decrease of fatigue strength was believed to be caused by the roughness of the surface, the non-uniform structure and tensile stresses in the surface, since ESD coatings often have pores and nonmetallic inclusions. Up to now, no papers dealing with ESD process cover this problem.

### **2.2.4 Problems**

Although, ESD has gradually received awareness for its unique advantages and has been applied in some advanced engineering practice, it is still mainly limited to some applications for improving wear resistance of metal parts, especially in tool

manufacturing or repairing work. Its great potentiality of applying a wide range of electrode materials to produce various surface performance, is lack of notice. The main reasons are that its deposition mechanism and process metallurgy are far beyond thorough understanding.

However, most of the present works are still conducted mainly on the study of process parameters and improvement of wear resistance. Therefore, more effort should be put on the investigation of ESD mechanism and study of the nature of ESD coating systems, based on which rapid development of the process can really be expected.

### 2.3 Applications

ESD process is first developed and widely used in U.S.S.R., and has also been applied in Japan, Czechoslovakia, China, Poland, Hungary, Germany, France, Britain, U.S.A., India and etc.

In the early time, ESD was often used for hardfacing, i.e., increasing the hardness and wear resistance of cutting tools and some machine parts, frequently with tungsten carbide or titanium carbide base electrodes. And due to the low deposition rate, practical applications were confined to relative small surface area where local wear occurred.

The list of ESD hardened items includes cutting tools, milling cutters, slotting tools, pneumatic drills, disc saws, dies, wood worksaws, pneumatic hammer chisels, drill bits, camshaft cams and pushrod end for internal combustion engines, tractor parts, diesel engine valve, nonsliding mating parts of bearings, gearbox forks, railroad engine wheels and rolling joints [1]. Besides, the specific properties of ESD coatings have been used to extend the application, for example, depositing on high-voltage power line contacts with silver to reduce contact resistance while improving the service life, or preparing the surface of fine structure for metal

spraying and electroplating [1]. Also ESD coatings were applied where a surface with a high degree of light scattering in all directions and where a high-finish matte surface was required.

With the development of ESD equipment and better understanding of the ESD process, coating quality and reproducibility and production rates have been improved a lot, and better-performed chromium carbide has been successfully applied in many areas.

### **1. In Nuclear Reactor Components [4, 19]**

One of the first successful reactor applications for wear resistant sodium valves was achieved by applying chromium carbide-based coatings with nickel or nickel alloy binders. The application on the reaction core component imposed stringent requirements on coating performance in corrosion, thermal cycling, wear, friction, self-welding and irradiation. The ESD process was found to be the only successful coating method that provided a metallurgically bonded coating without affecting the 20% cold-work condition required for irradiation swelling resistance in the Type 316 stainless steel. Currently ESD coatings are applied in qualification testing for high neutron fluence environments and are expected to see increasing use in a variety of reactor applications.

### **2. In Steam Generator Tubes [4]**

ESD are being considered for preventing of wear damage to steam generator tubes. It has been reported that 2.25Cr-1Mo steel steam generator tubes have been successfully coated with chromium carbide at an automated ESD work station.

### **3. In Gas Turbine Engine [4]**

ESD coatings are now being applied commercially to gas turbine engine components, such as:

- a. deposition of hardfacing alloys on "Z-Notch" surface of turbine blades;
- b. application of corrosion resistant coatings to turbine blade tips where

- protective diffusion coatings were removed in finish machining operations;
- c. application of platinum to selected areas of turbine blades as the first step in forming platinum-modified aluminide diffusion coatings;
  - d. repair of chipped or damaged diffusion coatings;
  - e. buildup of nickel-base superalloys to reclaim close-tolerance parts, such as curvic couplings, that are out of tolerance due to either wear or machining errors.

#### **4. Automotive Industry [4]**

Automotive application of ESD coatings are now appearing in racing engines. ESD coatings of titanium carbide are being used on titanium valve stems and valve guides of high-performance internal combustion engines. ESD coatings have also been used to buildup splines on critical shafts and to rebuild oil seal in close-tolerance over-running clutches.

#### **5. Fossil Energy and Petrochemical Industry [4]**

ESD coatings are currently being developed and tested for corrosive resistance, wear resistance and erosive resistance in fossil energy and petrochemical industry application. The ESD process allows a wide range of material coatings to be evaluated, including materials that would be difficult or impractical to apply by other process. Coatings being developed include duplex and multi-layer coatings that allow special properties to be designed into the coatings. For example, refractory metals such as niobium and tantalum are being applied to steels as diffusion barriers, then are followed with coatings to further improve wear resistance or erosive resistance. This ideas is of special importance to open up the future prospect of ESD process.

#### **6. Other Applications**

ESD chromium carbide coatings are replacing tungsten carbide inserts brazed into tips of surgical tools and needle-holders. Not only is the ESD coating significantly

less expensive, but the instrument also last several times longer because of the superior corrosion resistance of chromium carbide.

As we can expect, with further development of ESD process, its exceptional versatility and unique capabilities will be more widely recognized, and its increasing applications will appear in even widely expanding fields.

#### **2.4 Goal and Objectives**

The goal of this work is to investigate the surface microstructure-properties developed by Electro-Spark Deposition—a unique engineering approach to improve surface performance in a versatile and economical way.

The objectives are to make further understanding of the mechanism of Electro-Spark Deposition, reveal its metallurgical essence and surface microstructural properties.

The key approaches are to investigate the microstructure and surface topography with regard to material systems, operating method, process parameters and control.

To achieve the goal, a typical surface analysis methodology was developed as the use of optical image-analysis system, scanning electron microscope combined with energy dispersive spectrometer for study of microstructure, detection of alloyed resultants and element concentration; surfanalyzer to investigate surface topography; microhardness test, simple bend test and indentation test to examine microstructural properties. In this way, some inherent relations of materials-microstructure-surface finishes-process parameters-performance can be revealed.



## **CHAPTER 3**

### **FUNDAMENTALS OF ELECTRO-SPARK DEPOSITION**

#### **3.1 Physical Concept of Electric-Discharge and Spark [20]**

In general usage the term "spark" denotes the electric discharge—the passage of an electric current through a gas or liquid (in some case a solid) dielectric that taking place when the potential between contiguous bodies exceeds critical value. In suitable circumstances this discharge may perpetuate as an arc. For present purpose it is unnecessary to distinguish between initiation and propagation of the discharge and the spark can be consider simply as an arc of very short duration.

A necessary condition for producing a discharge is ionization of the dielectric, i.e. splitting up of its molecules into positively charged particles known as ions, and negatively charged particles as electrons. The ionization can be produced by many external factors (effect of dissimilar emissions, radiation, high temperature, high-energy electric field and presence of charged particles of dust, etc.). If the removal of these factors causes a cessation of discharge, this is known as a conditional or dependent discharge; if, however, due to certain factors, supports ionization of material while eliminating these factors itself (by its own powers) and through process accompanying the discharge, then it is called unconditional or independent. Both kinds of discharges, according to their type, may be stationary and nonstationary. When the electrical, thermal and other characteristics of the discharge during its passage remain uncharged, the discharge is stationary; if on the other hand, these characteristics change with time the discharge is non-stationary. As a special variant of the non-stationary type, an impulse discharge with a duration of  $10^{-4}$  to  $10^{-8}$ , is termed "spark" which is used in metal working technique.

## **3.2 Practical Electric-Discharge in Media [20]**

In electro-spark approach, the discharges are usually produced with close contiguity of electrode (anode) and substrate (cathode), both immersed either in a gas or a liquid dielectric medium, depending on the type of operation to be undertaken.

### **3.2.1 In a Gaseous Medium**

#### **3.2.1.1 Initiation by Electric Field**

When the close contiguity between anode and cathode reaches some pre-determined value, the potential intensity of the electrical field increases so much that individual electrons get enough energy and break loose from the surface of the cathode and are accelerated toward the anode. In their movement within the anode-cathode inter-space electrons will bump and initiate collisions with neutral molecules of gas and ionize them. When the ionization within the inter-space reaches such a level that a considerable flow (avalanche) of electrons along the channel thus is formed, towards the anode, constituting by such movement a momentary current impulse—discharge.

#### **3.2.1.2 Initiation by Contact**

In this case, the current impulse is produced by a short circuit at the moment of the contact of individual micro-peaks or projections on the surface of the anode and cathode. Accompanying the discharge, the liberation of energy leads to the production of extremely high temperature causing fusion and vaporization of metals at the point of discharge action. The liquid melting drop is then dispersed into the surrounding space exploded by the surge of explosive gaseous wave produced during discharge.

Thus discharge creates its own heat impulse, causing breakdown of electrode material. Moreover these momentary heat impulses in periodical sequence produce deep physical-chemical transformations in the surface layer of the substrate materials. The transfer of materials of the interacting electrode-substrate and diffusion of elements of the surrounding medium are also facilitated by this transformation of the surface layer.

### **3.2.2 In a Liquid Medium**

Under this condition, electro-spark operation is conducted with anode and cathode immersed in a liquid dielectric (such as mineral or paraffin oils, or kerosene) contaminated with various conductive substances. The particles removed from the anode and cathode by the spark discharge fall into the liquid medium, are cooled, and contaminate the space around the anode and cathode with colloidal suspensions of metals. These suspensions and also the products of decomposition of the liquid dielectric drawn into the inter-space under the action of the field during the preliminary phases of the discharge, are distributed along the electric lines of forces forming unique current conducting "bridge". Very rapid heating and therefore breakdown of one such bridge causes local gas formation in the liquid, ionization of a certain quantity of molecules, and consequently the discharge.

Discharge in a liquid brings about the same effects as in a gas, i.e. momentary fusion and vaporization of electrode material, whereby the gas formed as a result of decomposition of the working liquid forces the molten metal into surrounding liquid.

### **3.2.3 Comparison**

Comparing the effects accompanying discharge in both media, it is noted that the spark discharge in a gaseous medium leads to a partial transfer and diffusion of the

torn-off anode particles into the surface of the cathode while in liquid to a more intense ejection of anode particles into the surrounding space.

Both phenomena are utilized in the electro-spark processing of materials: the first in electric-discharge machining (EDM) and the second in operation connected with the strengthening or toughening of a substrate and building up of surfaces—electro-spark deposition (ESD).

### 3.3 General Principles of Electro-Spark Deposition (ESD)

In practical ESD process, as illustrated in the basic circuit diagram Figure 3.1, the electrode and substrate are connected to the poles of a condenser, charged from a rectified current source through a ballast resistance.

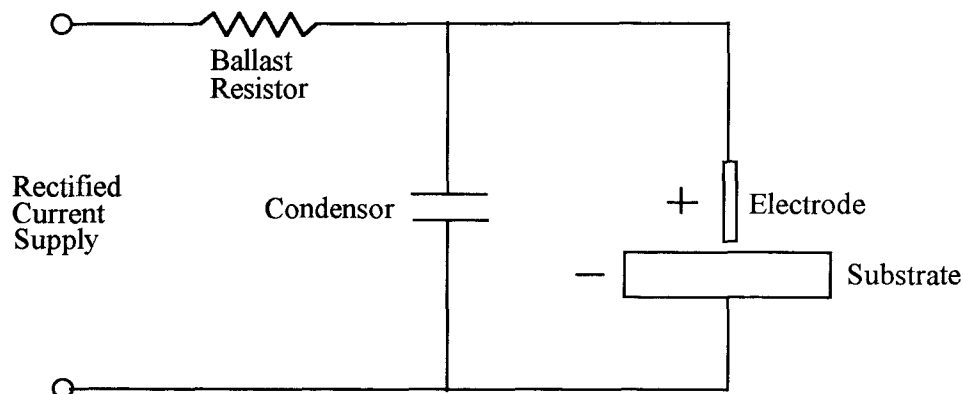


**Figure 3.1** Basic RC circuit for electro-spark deposition.

The electrode is vibrated electromagnetically, repetitively making and breaking contact with the substrate. The spark occurred immediately before "make", so discharging the condenser, which recharged again on "break". During sparking, electric pulses pass through the contacting surface asperities and also move across the very short ionized gas. The electrical pulse may be as high as 2000 amperes and thus provides an intense heat source sufficient to melt and

vaporize a portion of contacting electrode asperities and substrate in a very short amount of time [19]. It is assumed that at the time of sparking, the substrate is heated up to about some 1000°C in the zone of contact and is then quenched in a very short time [20]. At the same time, material of the electrode melts and is transferred to the substrate. The process causes a considerable physical-chemical change in the structure of the surface layer and effect the hardening of the treated spot. Some diffusion between the coating and substrate occurs and a true metallurgical bond results without significantly changing the temperature or properties of the bulk material. Coatings of nearly any electrically conductive metal, alloy or cermet can thus be deposited on electrically conductive substrates.

### **3.4 Mechanism of Hardening by Electro-Spark Deposition**

#### **3.4.1 Thermal Effect of Spark**

This factor is important in treating ferrous metals since the thermal cycling invokes the martensitic change. During ESD process the brief but intense heating of the spark produces extremely steep temperature gradients in the substrate surface, ranging from the boiling point of the metal to the ambient temperature over a few hundredths of a millimeter in depth. Two important structural zones can be recognized (Figure 3.2) [2]:

- 1) zone I—that in which the temperature is reaches some value between the melting point and boiling point of the metal;
- 2) zone II—that in which the temperature is less than the melting point, but high enough to modify the structure of the substrate.

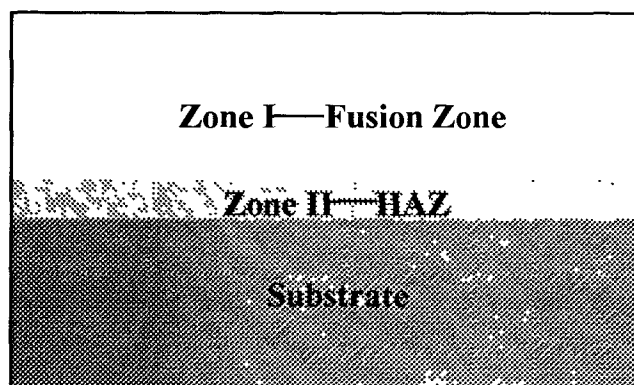


**Figure 3.2** General structure of ESD surface coating.

For steel, the lowest isotherm of interest, bounding zone II is that pertaining to the  $\alpha$ - $\gamma$  transformation. The mass of metal heated in each spark is minute in comparison with the bulk of cold metal, and the interval between heat pulse ( $10^{-2}$  sec) is large compared with the duration of pulse ( $<10^{-4}$  sec). Cooling is therefore extremely rapid and austenite formed in each zone can be expected to transform to martensite. This is one of the major reasons why even the iron with carbon content less than 0.02% can produce martensite which is impossible to obtain at normal heat treatment.

An important consequence of the short duration of each heat pulse is the fact that transferred materials penetrate appreciably only to the depth of melting area and little opportunity is available for solid diffusion to occur in zone II. Zone I is therefore of great interest in the ESD process. Moreover, the intense heating and rapid cooling of microvolume of surface material lead to the formation of extraordinary fine-grained or even amorphous structured coatings which is believed to contribute to the hardness, strength, wear and corrosion resistance more than that with the same composition of normal size.

### 3.4.2 Surface Alloying

This factor confers much greater properties and is the sole means by which most non-ferrous metals can be hardened. The source of alloying of the greatest general importance is matter transferred to the surface from the sparking electrode.

#### 3.4.2.1 Influence of Atmospheric Gas Medium

Figure 3.3 [2] shows the influence of the environment on the hardness of sparked iron.

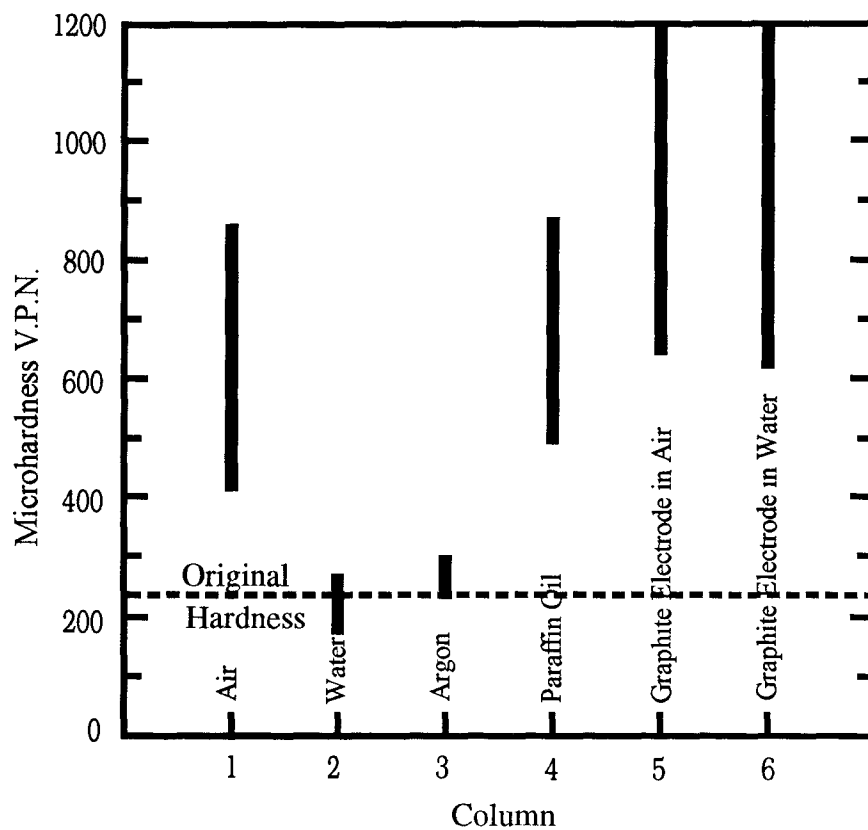


Figure 3.3 Influence of the environment on the hardness of sparked iron.

#### 1. Atmospheric Nitrogen

Air sparked surface of pure iron achieves an extreme hardness, usually associated only with quench-hardened steels of high carbon content. Further works [2, 5]

show such high hardness just exists in melt region known as zone I, but unmelted region (known as zone II) hardened only to the levels characteristic of the normally heat-treated steel. This contrasting behavior of both zones is evidently a consequence of contamination from air. It can be explained by the absorption of nitrogen and formation of nitrides in the sparked surfaces. Microchemical analysis have revealed a substantial increase in nitrogen content which are likely to affect profoundly the hardness of low carbon steels. The same effect has been achieved in ESD processing of non-ferrous materials.

## **2. Atmospheric Oxygen**

Evidence has been forthcoming which indicates that atmospheric oxygen also plays some part in the hardening process. Although the presence of oxygen does not accentuate the hardness of air-sparked surface, it has been established that oxygen can itself cause hardening, as shown in the experiment with titanium [2]. Titanium self-soaked in an "Air" mixture of argon-oxygen, is found to have hardened strongly with the formation of the oxide TiO in the surface.

### **3.4.2.2 Carbon Absorption**

The hardening by carbon absorption is in effect a small-scale case-carburizing process but one in which carburization and quenching take place simultaneously and only the surface material is heated.

#### **1. In Hydrocarbon Oil Environment**

When sparking is conducted in a hydrocarbon oils, thermal decomposition of the oil provides a strong carburizing environment. As shown in Figure 3.3, the hardness change is closely comparable to that produced by air-sparking. However, as in hydrocarbon oil, the erosion rate of substrate is comparatively high, it is normally employed in EDM in which rapid erosion of the substrate is the sole objective.



## 2. With Graphite Electrode

Carburization can also be effected by sparking the metal with a graphite electrode which involves the transfer of electrode matter. The hardening produced by sparking iron in air with a graphite electrode is shown in Figure 3.3. The hardness values range up to 1200 VPN, a level substantially greater than that observed on the surfaces self-sparked in oil. The exceptionally high hardness values can be attributed to the formation of a large proportion of iron carbide. A typical, extraordinary fine-grained, cast iron structure could often be resolved in the layer (Figure 3.4 [2]), and the carbon concentration evidently greatly exceeds that attained by conventional carburizing methods. Carbon is apparently more readily assimilated from a graphite electrode than from thermally decomposed oil. Moreover, using graphite electrode never increases the dimensions of the surface but forms a good alloy with substrate surfaces, producing a hard compound. Since, during machining, graphite also removes the highest peaks from the surface, it is sometimes used for improving the surface finish after ESD processing.

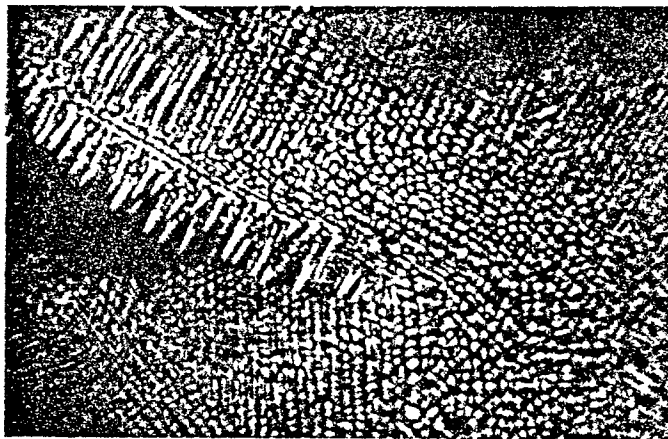


**Figure 3.4** Cast-iron structure on iron sparked with a graphite electrode.

### **3. With Graphite Electrode and Powder Additives**

Based upon the fact that many metal carbides have much greater intrinsic hardness than iron carbide, it is sure that by forming these carbides in the surface, even higher degree of hardness can be achieved. This has been accomplished by the expedience of introducing finely divided particles of hard-carbide-forming metals, in the form of a paste or a dry powder, to the spark zone. In the heat of spark, the particles are fused to the surface of the substrate and can be simultaneously carburized by sparking with a graphite electrode. Hardness values ranging up to 1350 (chromium powder), 1450 (molybdenum powder, 1800 (tungsten powder), and 2000 VPN (tantalum powder) have been recorded on surfaces treated in this way.

#### **3.4.2.3 Electrode Transfer**

##### **1. General Principle**

During the sparking matter may be transferred from one contact to the other by several processes, of which the most probable ones are:

- a. recondensation of vaporized metal;
- b. ionic transfer under the influence of the applied electric field;
- c. asymmetric rupture of liquid or solid junctions when the contacts separate.

The degree of alloying produced will be determined by the relative rates of self-erosion and of the transfer of electrode matter. While useful alloying might be achieved despite a net loss of matter, it is well known that contacts passing direct current often show a net gain on the cathode, as evidenced by the familiar "pip" and "crater". The same phenomenon can be utilized in ESD process to produce a built-up layer of high alloyed material on the substrate surface. This is a particularly desired result, offering ,as it does the possibility of restoring the dimension of worn articles. In practice, however, the process of electrode transfer

proves to be one of considerable complexity, influenced by specific characteristics of the materials employed and sensitive to numerous experimental factors. A detailed study thus is needed for further understanding.

## **2. General Transfer Characteristics**

In most circumstances sparking produce a loss of electrode (anode) and a net gain in the weight of the substrate, but at a progressively diminishing rate. Due to the splatter of melts and other factors, only a portion of the eroded electrode matter is retained by the substrate. The rate of workpiece gain will be referred to as the "transfer rate", the Ratio of substrate gain to electrode loss as the "transfer efficiency" [10].

If sparking is prolonged, although the electrode loss remains constant with minor deviations, the cathode gain will reach a definite maximum, beyond which the substrate weight diminishes, i.e., the transfer rate and transfer efficiency diminish with the time of sparking. This has been explained in the terms of thermal fatigue. It is postulated that the rapidly fluctuating temperatures tend to disintegrate the surface layers thereby setting up an erosive process which becomes increasingly pronounced as the time of sparking is prolonged and finally completely counteracts and dominates the transfer process. This phenomenon precludes the possibility of building up layers of indefinite thickness by continued sparking. An increase in the power of the spark generally increases the rate of anode erosion and cathode gain, but at the expense of surface roughening. Moreover, other factors such as movement of electrode, additional chemical reactions induced by dissociable gas, electromagnetic forces and material combinations also effect the material transfer and the surface roughness.

## **3. Globular Mass Transfer**

This type of transfer mechanisms dominates in the presence of dissociable gases (e.g., air, N<sub>2</sub>, CO<sub>2</sub>) which can be ionized to form a plasma of high thermal

conductivity promoting a molten globular transfer. In globular mass transfer, a molten droplet forms on the end of the electrode and is accelerated towards the substrate by the plasma jet. The droplets impact on the substrate with a typical "splash" appearance as seen in Figure 3.5(a) [4].

#### 4. Spray Transfer

Spray transfer usually occurs in the presence of the gases such as argon which is easily ionized and produce a plasma of relatively low thermal conductivity. This tends to produce a fine spray of molten electrode material and result in a fine matte appearance superimposed on the splashed surface.

Figure 3.5(b) [4] illustrates a typical deposit where both globular and spray transfer have occurred.

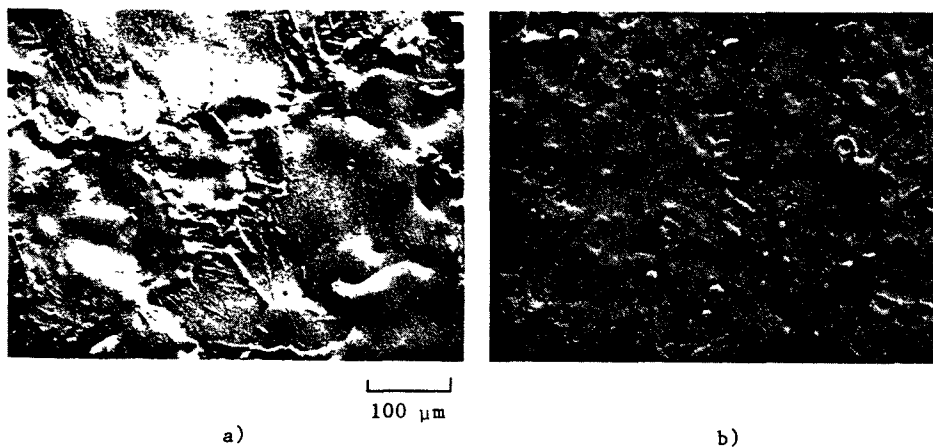


**Figure 3.5** Influence of cover gas on ESD mass transfer mechanism.

(a) Globular transfer in air;

(b) Mixed globular and spray transfer in argon.

#### 5. Comparison

The spray transfer mechanism is preferred for most of applications. It tends to produce a smoother and more uniform coating, helps eliminate electrode sticking, and gives a clear cathode etching effect, but less efficient in material transfer. The globular transfer mechanism appears to provide great deposition rate and higher

transfer efficiencies for all metallic materials except the refractory alloys and compounds where spray transfer appears to be more efficient. When the globular transfer mechanism predominates and relatively large amounts of electrode materials are being transferred, however, the coating tends to be rougher, and in the extreme cases can result in distinct islands or lump deposits, as shown in Figure 3.6 [2]. Lumping seems to be enhanced by the presence of oxygen. Exothermic reactions with electrode materials are believed to increase the temperature and the globular formations. Once small protuberance form from large globules, they continue to increase in size at the expense of the adjacent areas because electrode contact is restricted to these high points. Injecting argon into the spark displaces oxygen, thereby decreasing the cathode temperature and reducing both globular transfer and lumping tendencies.



**Figure 3.6** Localized transfer causing protuberance on the surface of steel workpiece ( $\times 10$ ).

## CHAPTER 4 METHODOLOGY

### 4.1 Surface Engineering By Electro-Spark Deposition

#### 4.1.1 ESD Equipment and Processing

The equipment of ESD has achieved great development since its inception in the 1950's. However, the basic spark generation and control circuit have remained unchanged. As shown in Figure 4.1, there are two kinds of basic structures for ESD equipment corresponding to the two kinds of deposition processes. In our research, the ESD processing is performed manually by interrupted electrode contact, which is of lower cost and convenient usage.

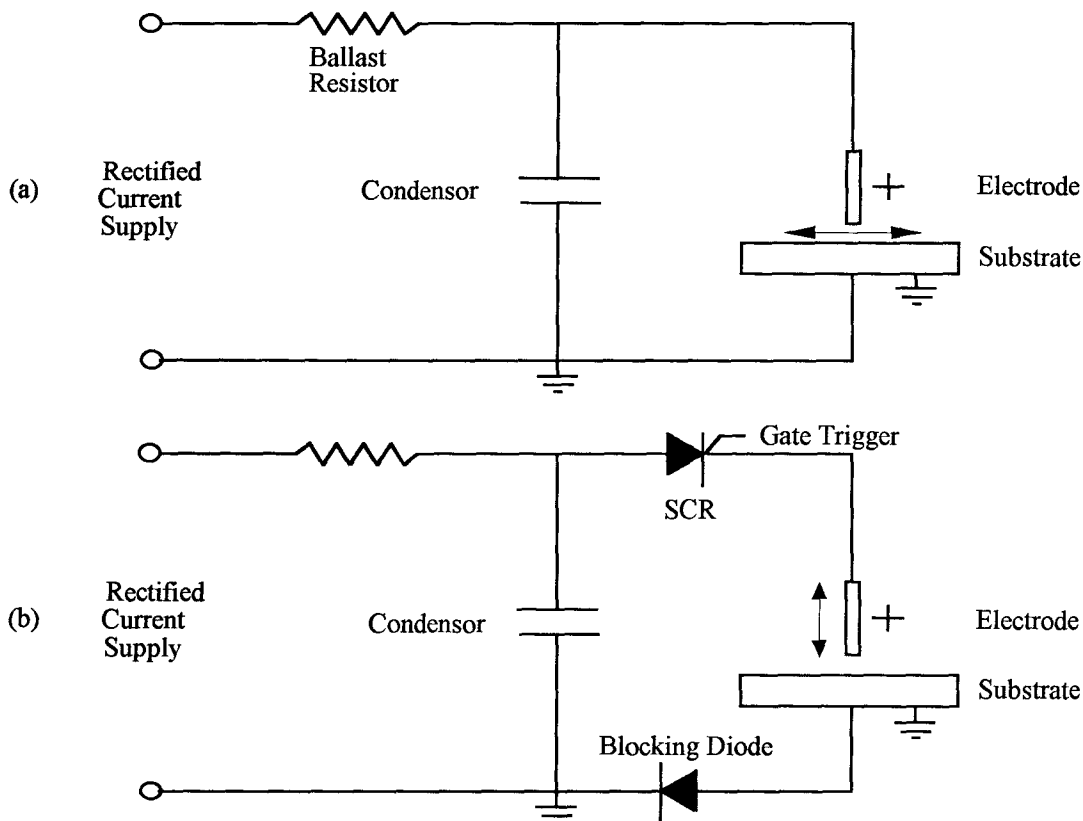


Figure 4.1 Basic circuit diagram.

The electrode (anode) and substrate (cathode) are connected to the poles of condenser, charged from a rectified current source through a ballast resistance. The electrode vibrating at a fixed frequency "make" and "break" contact between the electrode and substrate surface. At "make", the energy stored in the condenser begins to discharge through the electrode and the substrate, and continues to flow between them at break as a spark discharge.

#### **4.1.1.1 Polarity Feature**

The polarity that the electrode is made the anode favors the transfer of matter to the cathodic substrate. However, the temperature difference established between the small electrode and larger substrate itself promotes transfer in the desired direction and this important factor tends to dominate the transfer process. Early experiments have shown that transfer to the substrate often still occurs, though at a reduced rate, if the polarities are reversed. Indeed a useful rate of transfer can be produced with an a.c. circuit in which the polarities of the contact change in each spark and in some early Russian equipment the condensers are eliminated and an a.c. source employed. But the general d.c. sources or rectified transformers are used. More modern equipment utilizes components such as silicon controlled rectifiers and various triggering circuits to produce great control over the spark discharge characteristics.

#### **4.1.1.2 Function of Ballast Resistor**

The ballast resistor which charges the condenser functions to limit the working current, spark duration and the gap distance so as to eliminate the occurrence of arcs which are found to cause cracks and material softening in some kinds of materials. Moreover, an optimum gap distance for maximum transfer efficiency,

after which the substrate weight gain per unit of energy does not increase with voltage, can be achieved by the optimization of ballast resistance.

#### 4.1.1.3 Energy Input

The energy available at the time of occurrence of a spark is the charge stored in the condensers, which is given by:

$$E = \frac{1}{2}CU^2 \quad (4.1)$$

where C is the capacitance of the condenser, and U is the breakdown voltage.

The total electrical energy over a set period is given by:

$$Q = Ef = \frac{1}{2}CU^2f \quad (4.2)$$

where f is the spark frequency.

Therefore, the energy input can be controlled by three basic parameters—capacitance, voltage and frequency.

#### 4.1.2 Modern Equipment

Modern equipment tend to utilize the mechanism of continuous contact electrode deposition, which uses components such as silicon controlled rectifiers and various triggering circuits to produce greater control over the sparking characteristics. Spark frequency, for example, is controlled electronically rather than by electrode vibration. Computer-controlled work stations have been developed to provide control of substrate and electrode positions, motion and speed; electrode rotation speed; contact force between electrode and substrate; flow rate and flow geometry of protective cover gas; number of coating passes; and overlap of passes.

In our research, a manually operated ESD equipment patented in Russia and modified in our Surface Engineering Laboratory of Mechanical Engineering Department, is employed for the work.



### 4.1.3 Material Systems And Environment Media

Up to now, a wide range of materials system have been used satisfactorily in ESD process, as a summary is shown in the following Table 4.1.

**Table 4.1** ESD Coatings Applied to Date

Coatings	Coatings	Coatings	Substrates
Chromium Carbide*	Iron Alloys	Tungsten Alloys	Low-Alloy Steels
Tungsten Carbide*	Chromium	Niobium Alloys	High-Alloy Steels
Titanium Carbide*	Aluminum	Tantalum Alloys	304 and 316 SS
Niobium Carbide*	Copper	Zirconium Alloys	Copper
Tantalum Carbide*	Antifriction Bronze	TiB <sub>2</sub> , ZrB <sub>2</sub> , TaB <sub>2</sub>	Molybdenum
Stellite 6, 12 and 21 <sup>+</sup>	Silver		Niobium
Tribaloy 400, 700, 800 <sup>+</sup>	Nickel		Mo-Re Alloys
Ni-Cr-B Alloys	Gold		Ni-Base Alloys
Ni-base Superalloys	Platinum		Co-Base Alloys
Fe-36Ni	Iridium		Zirconium Alloys
Nickel Aluminide	Palladium		Titanium Alloys
FeCrAlY & NiCrAlY	Molybdenum		Aluminum
304 and 316 SS	Mo Alloys		Cast Iron

\*With metal binders, usually 5% to 15% Ni or Co.

+Trademarks, Stoody Deloro Stellite Co., Industry, CA.

According to the availability of materials, we choose for investigation the material systems of less cost and more potentiality for wide application.

#### 4.1.3.1 Electrode Materials

Electrodes for ESD process may be nearly any electrically conductive metal or cermet capable of being melting in electric sparks. We choose the commercially available bare metals and welding electrodes. Four kinds of hardfacing materials shown in the following Table 4.2 are used.

Detail information about the composition and geometry of the electrodes made in Russia is not available.

**Table 4.2** Information of Electrode Materials

<b>Code</b>	<b>Composition Information</b>	<b>Deposited Specimen</b>
Eltd1	Ni-Ti-Cr base alloys	Specimen 1
Eltd2	WC-Co-Ti alloy	Specimen 2
Eltd3	WC with Co binder(I)*	Specimen 3
Eltd4	WC with Co binder(II)*	Specimen 4

\*Eltd3 contains a little more Co than Eltd4.

#### 4.1.3.2 Substrates

As with electrodes, substrate materials must also be electrically conductive and capable of being melted.

Most structural alloys, such as iron-, nickel-, cobalt-, copper-, aluminum-, titanium-, zirconium-, and refractory metal-base alloys have been successfully coated by ESD process.

A low carbon content alloy steel (AISI 4030) containing fewer percent of Mn is used in our research.

#### 4.1.3.3 Environment Media

Environment can have significant effect on the matter transfer and alloying of the ESD process. Just as welding, ESD are usually performed in gas media, among which argon and air are two of the most popular media being used.

Due to our limitation, all the ESD processes are performed in the air which is of direct meaning and great importance to engineering practice. If air can be fully utilized in ESD to produce well-qualified surfaces, ESD will present even greater prospect in surface engineering.

#### 4.1.4 ESD Processing

All the ESD processes are empirically and manually performed according to the selected electrodes. A two-stage deposition technique, namely a rough and fast deposition followed by a fine or rough deposition at normal speed, is applied in order to investigate the ways of achieving designed thickness and satisfied surface finishes while keeping less heat affection on the substrate. Figure 4.2 [22] is a rough sketch of our ESD processing.

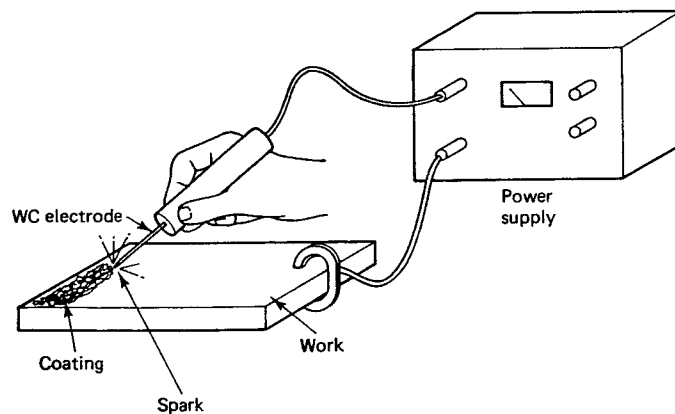


**Figure 4.2** Sketch of manually operated ESD.

### 4.2 Analysis of ESD Surface Coating

#### 4.2.1 Introduction

Surface quality including both the physical (microstructures, microhardness and etc.) and the geometrical (micro- and macro-) properties of the surface, largely determines its performance such as wear resistance, corrosion resistance, and fatigue limits. The physical quality of a surface is determined by the divergence of the physical properties (microstructures, microhardness, etc.) of the surface

coating material from the physical properties of the bulk material; while the geometrical quality of the surface is determined by the deviation of the actual surface from the conventional standard—an ideally smooth surface [25].

Surface coating analysis serving as a diagnostic technique to determine why the as-deposited surface does or does not possess those desired properties, is crucial in the understanding of the nature of the surface coating and thus many technologically important processes. Microstructure including structure-composition-properties, and surface geometrical quality of surface coating system are the closely related aspects of major emphases in study of surface coating technology.

Microanalysis is an effective approach for studying surface structure, processing mechanism, parameters and quality control. It involves investigation of microstructure and corresponding composition and properties on the micro-level in order to reveal the main characteristics of the surface coating system and provide the ways to realize the optimization of the process so as to achieve the best qualified surface coating. The main purpose of microanalysis is to determine the structural layers or phases, interface features, compositional and defect distribution which are depended on process parameters and techniques. By further analysis of these information, we can get a better understanding of the process mechanism including the relationships of microstructure-composition-process parameters-properties, based on which designing system can be established to produce the surface coatings of required properties through optimization of materials selection and process control.

Modern material analysis, based on the measurement of particles and radiation that emerges from a solid irradiated by photos, electrons or heavy particles, can give the further information of the image-composition-structure of an

microarea at high resolution far beyond that can be achieved by traditional techniques.

Up to now, the major techniques applied for microanalysis of ESD surface coating systems include traditional optical microscopic analysis, scanning electron microscopic analysis, electron probe x-ray microanalysis, x-ray diffraction analysis. Due to the objectives of this work as well as monetary problem and the availability of equipment, we focus on the microstructural analysis using optical microscope with image analysis system, scanning electron microscope (SEM) with energy dispersive spectrometer (EDS), surface topographical analysis is performed by using optical microscope and surfanalyzer, microhardness test, simple bending test and indentation test.

#### **4.2.2 Microscopic Analysis**

The primary purpose of microscopic analysis of ESD surface coating system is centered on distinguishing structural layers and measuring their thickness, studying interfaces, detecting composition of each layers or phases of special interest and distribution of composition along depth, examining defects and their distribution.

##### **4.2.2.1 Optical Metallographic Analysis**

Optical metallographic analysis entails examination of materials using visible light to provide a magnified image (no more than  $\times 1500$ ) of the microstructure. Based on the principle of light lensing action, it is used to characterize structure by revealing grain boundaries, phase boundaries, inclusion distribution, and evidence of mechanical deformation. In ESD surface coating system analysis, it is performed to:

- a. distinguish major structural layers and measure their thickness;
- b. determine phases and their distribution;

- c. study the interfaces of structural interfaces;
- d. examine defects and their distribution;
- e. make preparation for SEM & EDS analysis as well as microhardness test.

### 1. Sample Preparation

The first step in metallographic analysis is to select a sample truly representative of the material structure to be examined. In this research, metallographic samples are cross-sectioned or tape-sectioned from an as-deposited steel plate by ESD.

A typical procedure for preparation of metallographic samples as suggested by Leco [23] is applied as below, however with some special techniques adopted due to the feature of ESD samples.

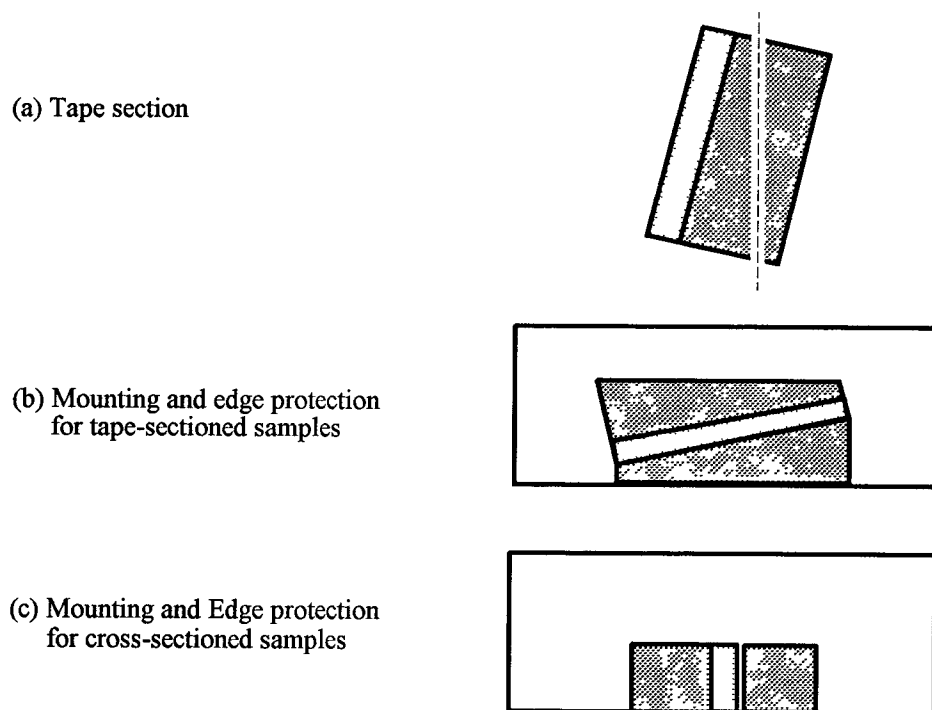


**Figure 4.3** Sketch of some techniques in metallographic sample preparation.

**Step 1—Sectioning:** A Leco diamond cutter is employed for low speed precision sectioning. One group of samples are cross-sectioned from the parent piece for microstructure analysis. The other group of samples are tape-sectioned about  $10^0$  from the parent piece for microhardness test as shown in the following Figure 4.3(a).

**Step 2—Coarse Grinding:** Slightly remove any of the deformation caused by sectioning and produce an initial flat surface. Clean the sample and measure the tape sectioned angle.

**Step 3—Mounting:** Embed the samples in thermoplastic materials by compression mounting for ease in manipulation and edge preservation. The special techniques for edge protection and mounting tape sectioned samples are shown in the following Figure 4.3(b) and (c).

**Step 4—Fine Grinding:** Wet grind to remove the deformed zone caused by the above steps and limit the depth of deformation during this step. The abrasive papers are selected as the following: SiC 320→SiC 400→SiC 600→SiC 800.

Special care should be taken as the big difference of coating materials and substrate. The reason of using SiC 800 Grit paper is due to lack of diamond paste for rough polishing.

**Step 5—Rough Polishing:** This step is to further limit the deformed zone produced by fine grinding.  $6\mu\text{m}$  diamond paste and Pan W cloth with water lubricant are used in this step.

**Step 6—Fine Polishing:** Fine polishing is to remove the localized deformed zone produced during rough polishing so as to get uniformly polished and scratch-free surface. However the inclusions and porosity, cracks and other second-phase particles may be visible.  $1\mu\text{m}$  diamond paste and Billiard Cloth are used in this step.

**Step 7—Etching:** Etching: is the process to reveal the microstructure details by preferential attack of a sample surface with etchants. Due to the restriction, we choose the convenient chemical etching technique for ESD samples with mainly 5% nital solution. Special results may require advanced methods such as electrochemical attack, thermal treatment or vacuum cathodic etching.

## **2. Optical Microscope and Image Analysis System**

Leco2001 Microanalysis Image System is employed for optical microstructure research. It consists mainly of a multipurpose Olympus optical microscope, a 386 computer system, image analysis processor and peripheral device, which combines the traditional metallographic techniques with computer, image processing and artificial intelligent technology. The image received from the microscope is processed by the image processor, qualitative and quantitative analysis of the microstructure are performed with data and image saved by the computer. Such kind of sophisticated techniques represents the trend of modern material analysis.

### **4.2.2.2 SEM and EDS Analysis**

#### **1. Introduction**

SEM combined with EDS analysis is a very popular and powerful tool in modern material analysis. It is applied to reveal further details about morphological, chemical and physical characteristics of coating structure on micron size level. In performed ESD sample analysis, it is employed for the following work:

- a. imaging of microstructure features at high magnification and resolution;
- b. compositional identification of features down to micron size in the surface layers;
- c. determination of compositional gradients along depth.



## 2. Principles

**A. Interaction of Electron Beam with Material:** When a beam of finely focused electrons strikes a specimen, it will either scatter elastically or cause an electronic transition in an atom, resulting in the release of a number of signals which contains the signature or are characteristic of the atom. Figure 4.4 shows the irradiated release of these characteristic signals which include secondary electrons, backscattering electrons, auger electron, characteristic x-rays and other types of radiation. The intensity of these signals will depend in some way on the shape, chemical composition and crystal orientation of the irradiated volume. Through collection and processing of these characteristic signals, both qualitative and quantitative details can be achieved.

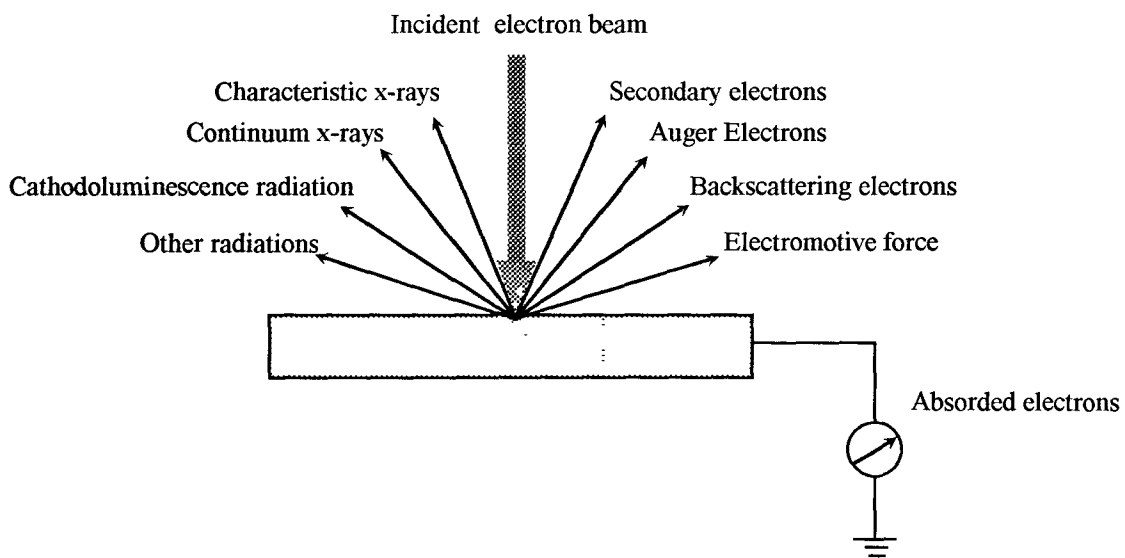


**Figure 4.4** Interaction between incident electron beam and solid sample

Different techniques of collecting and processing the signals result in different methods of materials analysis.

**B. Physical Base of SEM Analysis:** The second electrons of low energy is a conveniently collected signal for SEM to form the image since they are easily drawn to a positively biased detector system. The collected signal is eventually converted to an electronic signal which is imaged on a cathode ray tube (CRT). The scanning of the beam is synchronized with the scanning of the CRT, thus producing a one to one relation between points on the specimen and points on the CRT. The second electron image is very similar in appearance to a light optical image, except that it has no color and both the resolution and the depth of focus are greatly improved.

**C. Physical Base of EDS Analysis:** Once the incoming electron beam with enough energy knocks out intershell electrons (K, L, or M, depending on atomic number) from the atoms near the surface, vacancies are left in the inner shells which produce the excited state of the atoms. The excited state is so unstable that it will immediately be relaxed by filling the vacancies with electrons from an outer shell. Such kind of electron transition, at meanwhile, produces the x-rays specific to the excited atoms. These characteristic x-rays are detected, and their energies are measured by the semiconductor detector spectrometry which converts the energy of incident x-ray into a voltage pulse whose amplitude is proportional to that energy. A multichannel analysis is used to accumulate a histogram (such as shown in Figure 4.5) of the pulse amplitude spectrum.

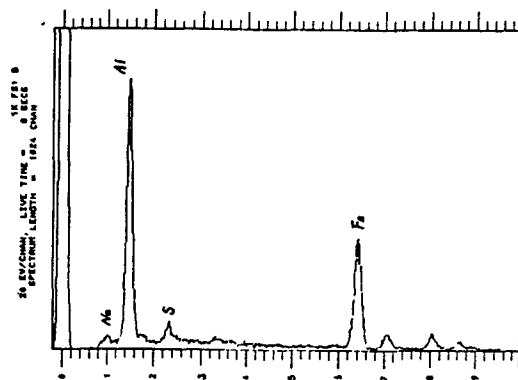


**Figure 4.5** Histogram of energy dispersive diagram.

The area of the individual characteristic x-ray peaks in the spectrum is proportional to the concentration of the respective elements in the tested sample. In this way, elements are identified according to their characteristic energy spectra (qualitative analysis), and after some corrective computation, the intensities of the energy lines allow determination of the concentration of the tested sample (quantitative analysis).

EDS is usually attached with SEM so that it allows to combine the image analysis with the compositional detection. Thus direct information of microstructure-composition can be easily obtained.

However, the detection limits of EDS make it difficult to measure the light elements of atomic number less than 11. Further analysis of these light elements should use wavelength dispersive spectrometry or other kind of methods.

### **3. Equipment**

**A. Scanning Electron Microscope:** JEOL840 (30A Resolution) with Tracor Northern TN5500 is employed in this research. Figure 4.6 shows the basic components of SEM which can be categorized as:

- 1) Electron column;
- 2) Specimen chamber;
- 3) Vacuum pumping system;
- 4) Electronic control and imaging system.

**B. Energy Dispersive Spectrometer:** A EDS attached with the SEM is manipulated by a computerized analysis system to perform qualitative and semi-quantitative compositional analysis.

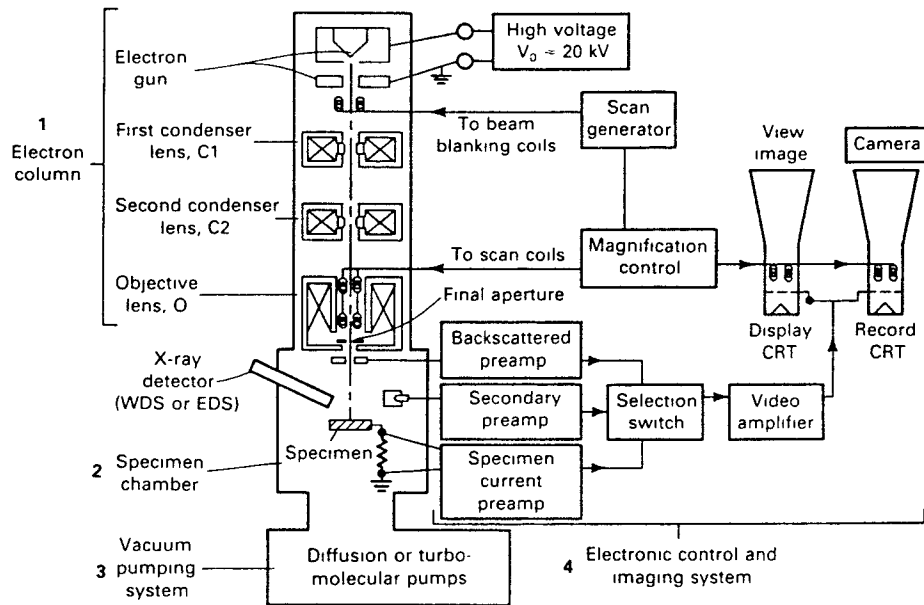


**Figure 4.6** Basic component of SEM [21].

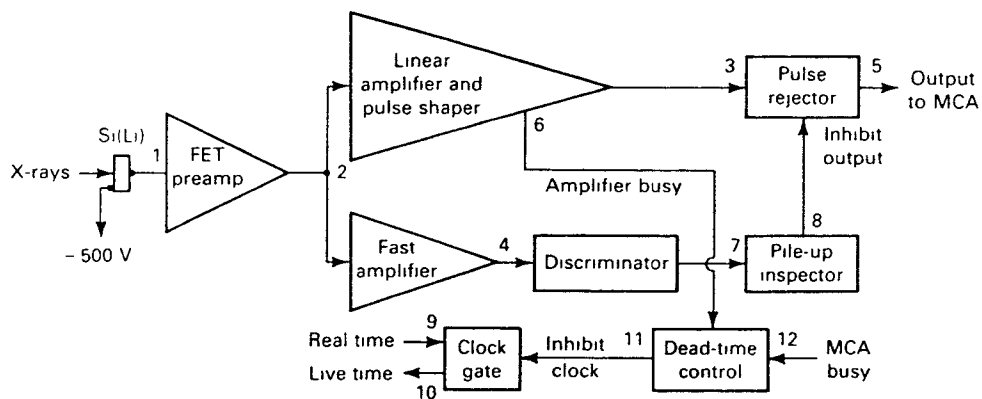


**Figure 4.7** Schematic diagram of the detector of EDS [21].

#### **4. Sample Preparation**

Cross-sectioned samples preparation follows the standard metallographic procedure of sample preparation as mentioned before. However, some special techniques are adopted as below:

- a. avoid mounting materials of high vapor pressure;
- b. slightly etch samples for optimum analysis;
- c. make samples fresh and extremely clean;
- d. apply silver paint to mounted samples to establish electrically conducting path and let the paint thoroughly dry;
- e. sputter the painted sample to achieve good electric conductivity and clean surface.

#### **5. Procedure of Analysis**

- a. Insert the sputtered sample into the sample chamber of SEM and vacuum the Chamber;
- b. Select the accelerated voltage at 15KV and regulate the current to achieve the best SEM micrograph at proper magnification;
- c. Select the typical characteristic area to study its microstructure;
- d. Set cross line at the surface and take micrograph at certain magnification;
- e. Do spot analysis along the set line from the surface into the substrate while detect some specific characteristic areas in the micrograph as well. The interval of the spots is set according to the selection of the spots of special interest. The distance between any two spots is determined according to standard length shown on the SEM micrograph.

The following Figure 4.8 is a sketch of doing spot analysis along the depth.

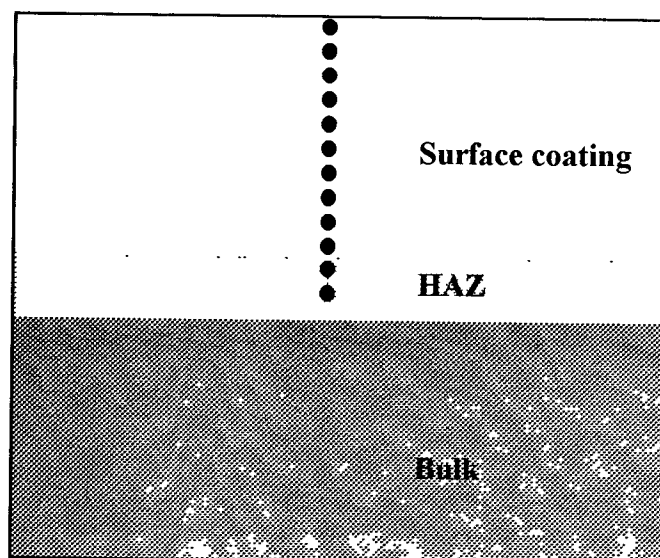


**Figure 4.8** Sketch of doing spot analysis using SEM and EDS.

### **4.2.3 Surface Topography**

#### **4.2.3.1 Introduction**

Every kind of processing will produce the surface with its special characteristics which will largely affects the surface performance. The finish and structure are usually considered the most important qualities of the surface. The investigation of the macrostructures and microstructures of ESD surfaces is a matter of particular interest, because no other kind of surface deposition techniques can produce a surface similar in appearance to the surface produced by ESD. Besides, through the study of surface morphology and topography, the typical surface characteristics of ESD can be revealed so as to help realize the optimization of the process parameters and control which will lead to produce the best surface qualities.

In performed work, we limit our attention to study the surface morphology by using optical microscope and the surface roughness by a stylus surfalyzer.

### **4.2.3.2 Methodology**

#### **1. Investigation of Surface Morphology**

Through using optical microscopy, the overall views of the ESD surfaces at small magnifications can be obtained to reveal the general features that are lost at high magnification. However the observation at high magnifications is still useful in examining microscopic details such as surface defects like microcracks, pores, pits and etc. By utilizing the dark field observation, polarizing observation or Nomarski differential interference contrast observation, little bit three-dimensional effect can be obtained. However further study of three-dimensional morphology should employ SEM. Usually the comparison with the surface morphology after wear test can provide more information about the surface properties achieved by ESD. Due to the monetary problem and our initial objective, we do not go further to these two stages.

#### **2. Analysis of Surface Profile and Surface Topography**

The contour of ESD surfaces were measured for quantitative analysis of surface topography and build-up on the surface as well as rough estimation of as-deposited thickness (and melting depth). A computer-assisted stylus surfanalyzer was employed for the work.

**A. Surface Profile Recording:** In this work, a stylus follows the fine surface details while drawing from original surface to and across the ESD surface so as to record the build-up on the surface by ESD. After amplification of the movement of the stylus, a graphical trace of the amplified profile is produced, from which direct measurement can be made. However such profiles are usually distorted with a large gain on the vertical axis to the slope of reference surface to the ideal horizontal level on the micro-scale. Therefore manipulation of computer is applied for error extraction using least square method as well as the following quantitative analysis of surface roughness.

## B. Quantitative Analysis of ESD Surface Topography

Quantitative analysis of ESD surface topography involves in computer assisted numerical analysis of the recorded surface profile which defines a number of parameters that characterize the surface (illustrated in Figure 4.9 [21]).

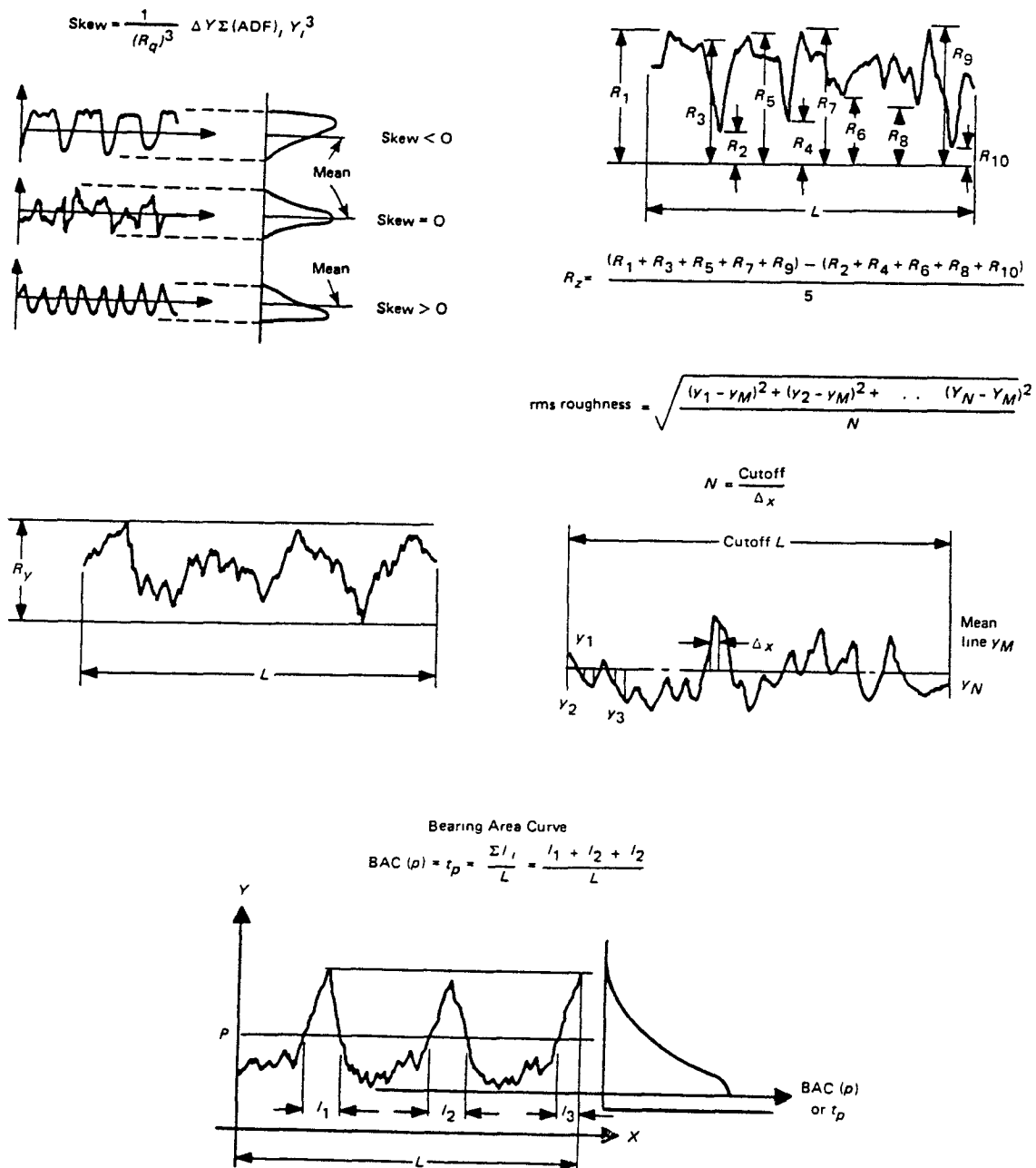


Figure 4.9 Illustration of some surface roughness parameters [21].



- a.  $R_a$ : the average deviation from the mean surface, which is the most common parameter referring to the surface roughness.

$$R_a = \frac{1}{l} \int_0^l |y| dl \quad (4.3)$$

- b.  $R_q$ : the root mean square.

$$R_q = \left[ \frac{1}{l} \int_0^l y^2 dl \right]^{1/2} \quad (4.4)$$

- c.  $R_y$ : the maximum peak-to-valley height measured parallel to the mean line ( $R_y$  is an ISO parameter).
- d.  $R_z$ : the average distance between the five highest peaks and the five deepest valleys within the sampling length, measured from a line parallel to the mean line and not crossing the roughness profile ( $R_z$  is an ISO parameter).
- e.  $R_{sk}$ : the symmetry of the profile about a mean line, called skewness. It does not encompass waviness in contrast to fullness of bearing ratio curve.

$$R_{sk} = \frac{1}{R_q^3} \frac{1}{n} \sum y^3 \quad (4.3)$$

where  $n$  is the number of coordinates ( $y$  values) chosen in the record length.

- f. **Bearing Ratio Curve**: The bearing ratio curve is plotted by the variation of bearing area (%) vs the distance (%) from the reference plane. It illustrates the influence of asperity radius and slope and of roughness width. The fullness of the profile is extremely useful in that it gives direct information on the ability of the surface to entrap lubricants or accommodate wear particles. A profile of greater fullness provides less entrapment volume.

Although the above analysis can never be sufficient due to lack of very effective methods for surface description, these parameters combined with surface morphological analysis can give a fairly good description of the general characteristics of ESD surface.

### 3. Estimation of Build-up on Surface and Coating Thickness

Since the performances of all metal coatings depend upon the coverage of the substrate with a complete coating of adequate thickness, and furthermore the life of the coating maybe dependent upon its thickness. Therefore determination of coating thickness is one of the most important tests in surface coating analysis. Table 4.3 shows various methods of determining coating thickness and their general applicability.

**Table 4.3** Methods of thickness test[22]

Test Methods	General Applicability
Magnetic	All coatings on ferrous substrates and some nickel coatings
Eddy current	Metal coatings on non-metallic substrates
X-ray spectrometry	All system
back-scatter	Almost all systems provided that the difference in atomic number between coating and substrate exceeds 5
Light section microscope	All systems
Interferometry	All systems
Profilometry	All systems
Chemical solution	All systems
Coulometric	Almost all systems except coatings of precious metals
Microscope cross-section	All systems

In cases where coating is of sufficient thickness and the dimension of the uncoated component are accurately known, it is obviously possible to determine

the coating thickness directly by use of conventional measuring instruments. However, since with lots of coatings, their thickness is small in relation to the dimensions of the uncoated article and so insufficient accuracy can be achieved even if direct measurement is feasible.

In the case of ESD coatings, the as-deposited thickness is usually achieved below  $100\mu\text{m}$  (mostly from 10 to  $50\mu\text{m}$ ) by alloying with the substrate. In particular the height variation of ESD surface is on almost the same scale as its thickness. Thus only insufficient accuracy can be obtained, especially with the surfaces manually deposited. However such measurements still provide the information of mean thickness or build-up on surface. The methods used in our work are summarized as below:

**A. Cross-Section Microscopic Method:** This is a universally applicable method that provide direct measurement of local thickness by means of examination under a microscope of a cross-sectioned metallographic sample. It is irrespective of the materials concerned and of the shape of the coated article. By using this method it is also possible to determine accurately the extent of alloying between coating and substrate.

Normal metallographic cross-sectioned samples with optical microscope and image analysis system are always used to get the measurement with good accuracy. Further extension of the method can be made by using electron microscopic techniques in order to measure even thinner deposits or each distinguished layers in the surface structure.

In our work both techniques are used to get the measurements at different microscopic level. The disadvantage of such method lies in its locality which can not reflect the macro-scale situation, especially in the case of ESD surface due to its non-uniform and very rough nature. Therefore the following techniques are used to estimate the general build-up on the surface produced by ESD.

**B. Surface Profilometry Method:** The measurement using this method is achieved by recording the extent of movement of a stylus that follows the profile of the step between coating and substrate as it is drawn across the surface. Therefore it is done at the same time when recording surface profile. The numerical processing by computer is very important in the final result. As mentioned above, the height variation of ESD surface is on the same scale as the build-up or thickness dimension, the quantitative results have only limited accuracy but with good qualitative information.

### 4.3 Performance Evaluation

Evaluation of surface performance is a very important stage in study of the surface coating process. The service requirements will determine the mainly concerned properties of the achieved surface. Up to know, the ESD surfaces are mainly applied for wear environments and are gaining favor for corrosive environments as well. Therefore the main efforts are put on the study of wear resistance and corrosive resistance. A lots of work done by some researchers have demonstrated the great improvement of wear resistance achieved by ESD coatings while the corrosive resistance is more complicated due to lack of further work. Anyway the most important nature of ESD coating is always lack of study. By considering the restriction, we put our main effort on study of the microstructure of ESD surface coating and its related mechanical properties in order to reveal some of the nature of ESD surface coating system, based on which surface performance can be predicted.

Three types of convenient mechanical property tests with aid of optical microscope are employed as below.

### 4.3.1 Microhardness Test

Microhardness test is one of the most convenient and useful tool for surface coating analysis. It tests material resistance to plastic deformation caused by the impression of external load on the microsurface area. The impressive load of no more than 1000g is applied on a polished metallographic sample by a diamond brale of certain geometric configure, which results in a micro-indentation on the micrometer scale. In this way it can be utilized to measure the microstructural phases, various components of an alloying coating or a multilayer coating system, which provides the information for the analysis of materials structure and properties. By combination with the microstructure examination, it serves as an effective and convenient way in estimating the mechanical properties of a microareas.

Due to the rough nature of the exterior surface and the achieved thinness of the ESD samples, tape-sectioned samples which magnify the details on the cross-sectioned samples were selected to measure the hardness of distinguished thin layers or microareas of special interest as well as the hardness gradients along the depth of the coating system.

Leco Microhardness Tester System is employed in the testing. It consists of an M-400 Microhardness Tester, a microscope with a monitor, a DME digital micrometer and a TR 6193 digital printer. The Knoop brale with 10g load is chosen for the testing.

The taped-sectioned metallographic sample preparation has been stated before. Only two specific points should be emphasized as below.

- a. The samples should be made fresh, clean and less-etched.
- b. The brale should be perpendicular to the testing areas.

The testing conditions were set as following:

- a. The areas of interest were selected at the regions where good coating quality with typical characteristics and usually bigger thickness were achieved.
- b. Small load of 10g and the smallest interval of 5 $\mu$ m between two indentation were applied for all gradient tests in order to examine the structure as fine as possible.
- c. The variation of hardness along width at rather non-uniform regions was also recorded.

#### **4.3.2 Bonding and Strength Evaluation**

The bonding between surface coating and its substrate is of extreme importance to the performance of surface coating. A surface coating of good bonding will remain adherence whereas coatings lacking in adherence or ductility will generally break and delaminate from the substrate. Therefore bonding and strength tests can serve as an effective way for evaluation of surface quality and performance.

Due to the metallurgical bonding nature, ESD coating should be of such high bonding strength with the substrate that lack of adhesion in service is unlikely to occur. However, the bonding strength of ESD coating is determined not only by the strength of its adhesion to the substrate but also by the ductility and uniformity of the coating itself. Moreover even all these three properties of the ESD surface coating cannot be characterized by a common aspect, since they depend on the condition in which the coating was formed. Therefore, some simple and empirical testing methods are usually applied for practical evaluation of the bonding and strength of the surface coating.

For ESD surface coatings, two simple testing methods were performed as below.

#### **4.3.2.1 Simple Bending Test**

This is a simple and useful method which is used as a measure of both adhesion strength and the ductility of the coating to accommodate residual stresses. It involves deforming a test sample round a mandrel of specified curvature until certain degree which is set as the criteria for assessing failure. When testing mainly for ductility cracking in the cross-section of the coating is required, adhesion testing failure is indicated by lifting of the coating from the substrate.

The performed testing of the ESD samples adopted the following procedure and the corresponding criteria.

- a. simply bending the test sample of 90° with curvature of about 4mm.
- b. visually checking if there is any delamination or spalling of the coating from the substrate.
- c. applying optical microscope to further examine the micrograph of bent samples after being cross-sectioned and metallographically prepared.

#### **4.3.2.2 Indentation Test**

This test involves making hardness indentations at the interface between ESD coating and substrate to check if any separations or cracks occur at the interface. It is an easily doing way to provide additional verification of bonding between coating and substrate. The procedure of test is performed as the following:

- a. preparing cross-sectioned metallographic samples;
- b. making indentation at the interface by use of a diamond brale under 60kg load;
- c. using optical microscope to check if there are any separations or cracks produced along the interface.

## **CHAPTER 5**

### **RESULTS**

#### **5.1 Microstructure of ESD Surface Coating**

##### **5.1.1 General Structure**

The main efforts in this research are put on the study of microstructures in order to obtain better understanding of the nature of ESD coating systems. Under our available conditions, the examination of microstructures is performed by use of optical metallographic analysis and SEM analysis combined with EDS detection.

As shown in the optical micrographs (Figure 5.1—5.4), the general feature of ESD coating systems is a two-zone structure, i.e. a fusion zone followed by a heat affected zone (HAZ) over the bulk materials. It is easily to distinguish this structure using optical microscopy due to the contrasting resistance to etching solution. The fusion zone of high etching resistance usually appears white and featureless while the HAZ appears dark or slightly etched showing modified structures with respect to bulk material. However, further examination of the structure should be performed using electron microscopic analysis including the combined micro-area compositional analysis.

As a matter of fact, the characteristics of the microstructures of each ESD coating system are different, depending largely upon the materials systems, environment media, manipulating methods, process parameters and control. Four kinds of electrode materials are applied to get achieve the following results.

##### **5.1.2 Microstructure of Specimen 1**

As shown in Figure 5.1, the structure of this ESD specimen consists of a fusion zone created by surface alloying , a heat affected zone and the substrate.



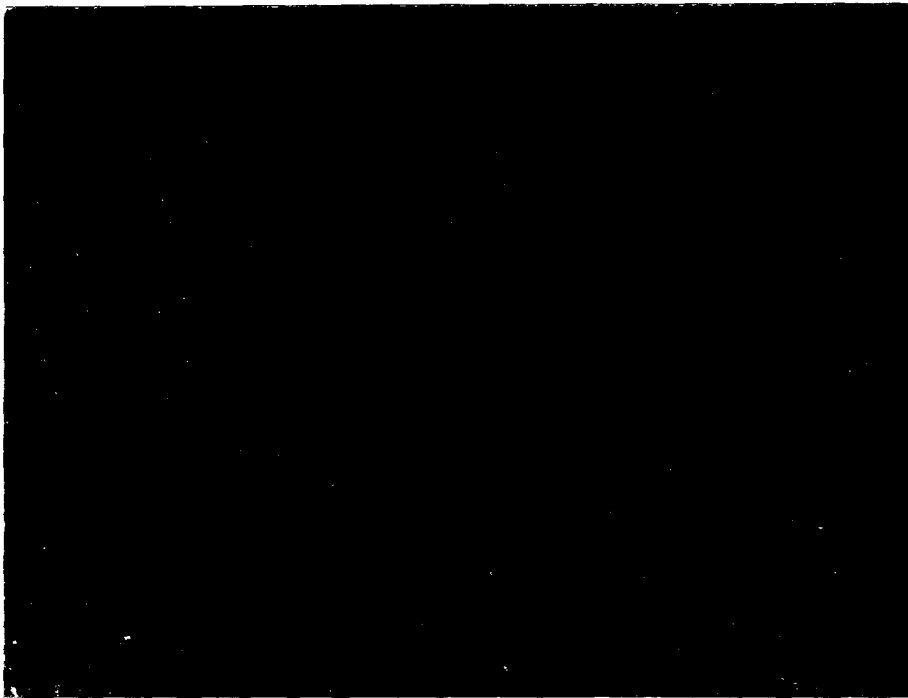


**Figure 5.1** Optical micrograph of Specimen 1 deposited with Eltd1 ( $\times 1200$ ).

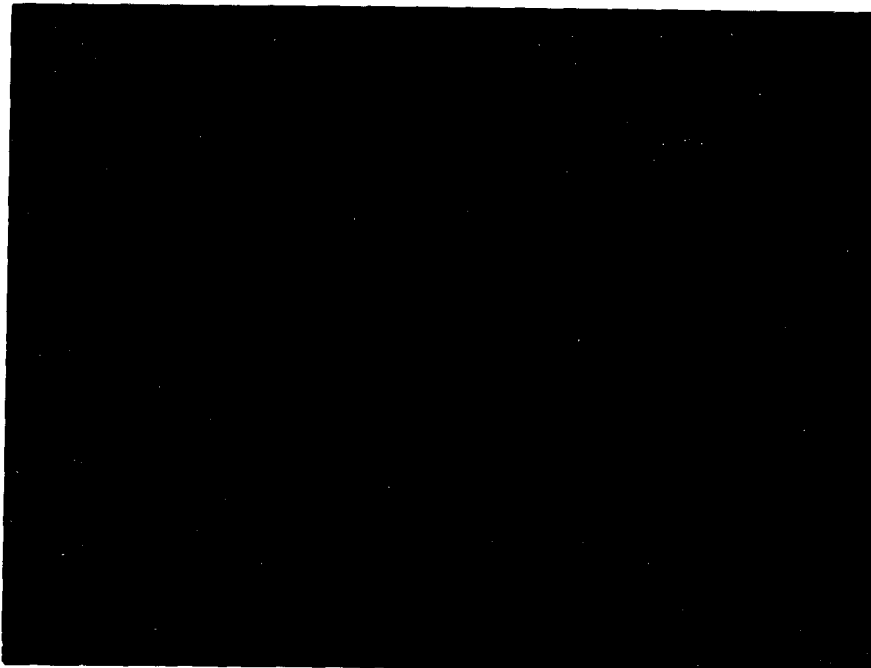


**Figure 5.2** Optical micrograph of Specimen 2 deposited with Eltd2 ( $\times 1000$ ).

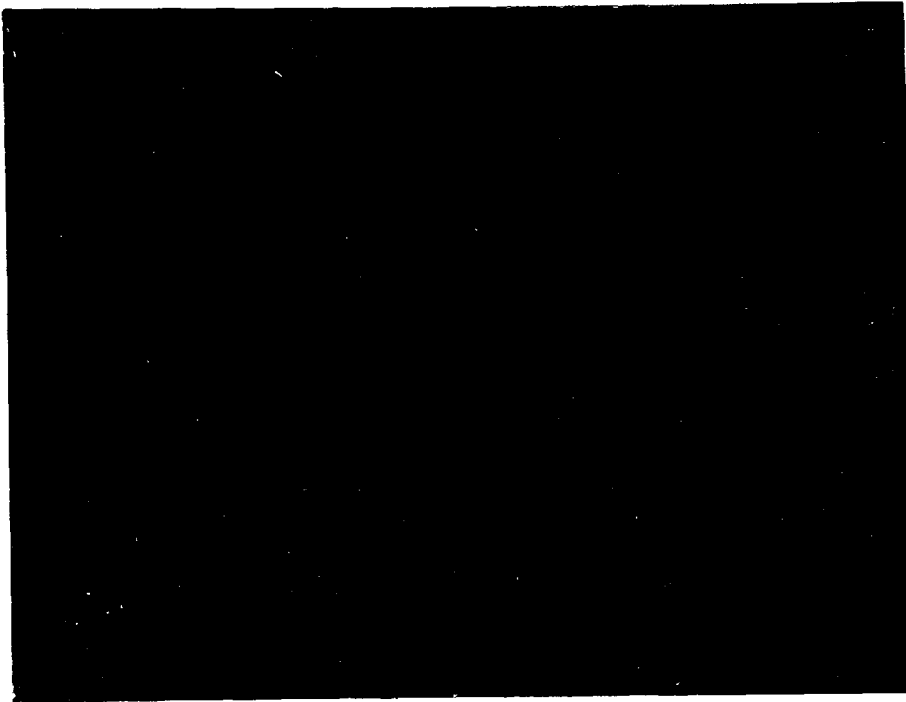


**Figure 5.3** Optical micrograph of Specimen 3 deposited with Eltd3 ( $\times 1200$ ).

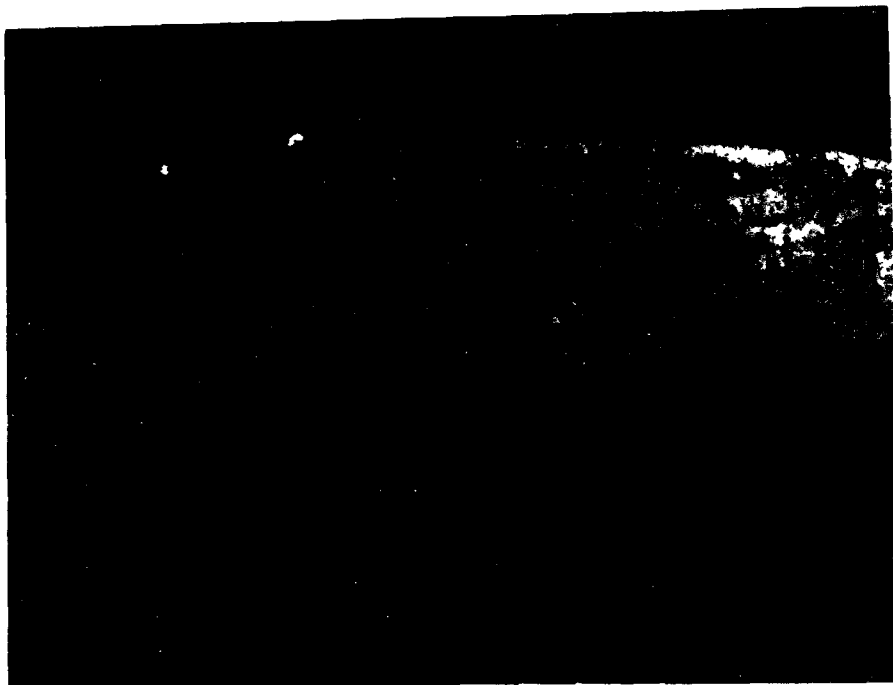


**Figure 5.4** Optical micrograph of Specimen 4 deposited with Eltd4 ( $\times 1200$ ).

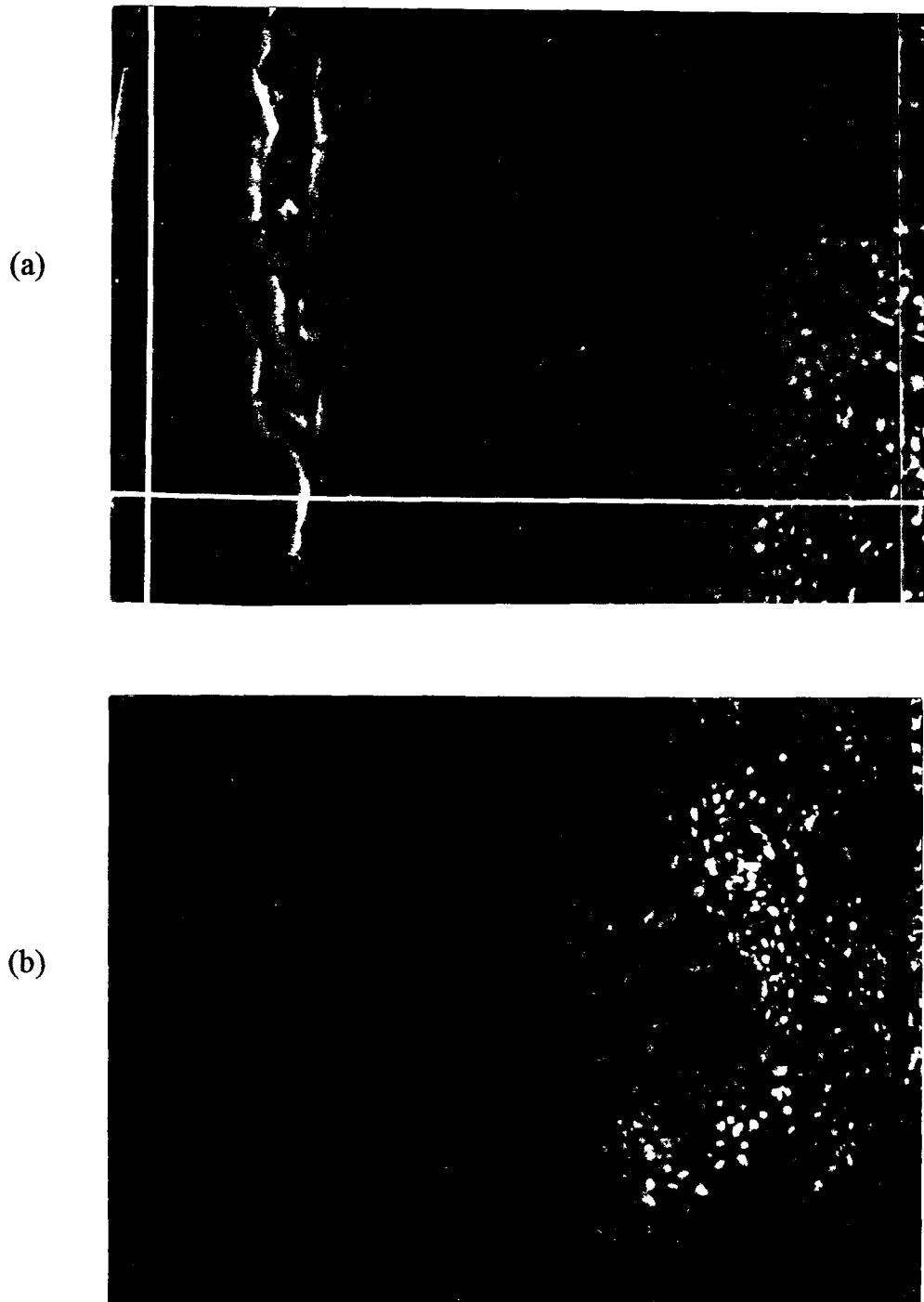


**Figure 5.5** SEM micrograph of Specimen 1 deposited Eltd1 ( $\times 3500$ ).  
(a) Fusion zone; (b) Transitional region from fusion zone to HAZ.

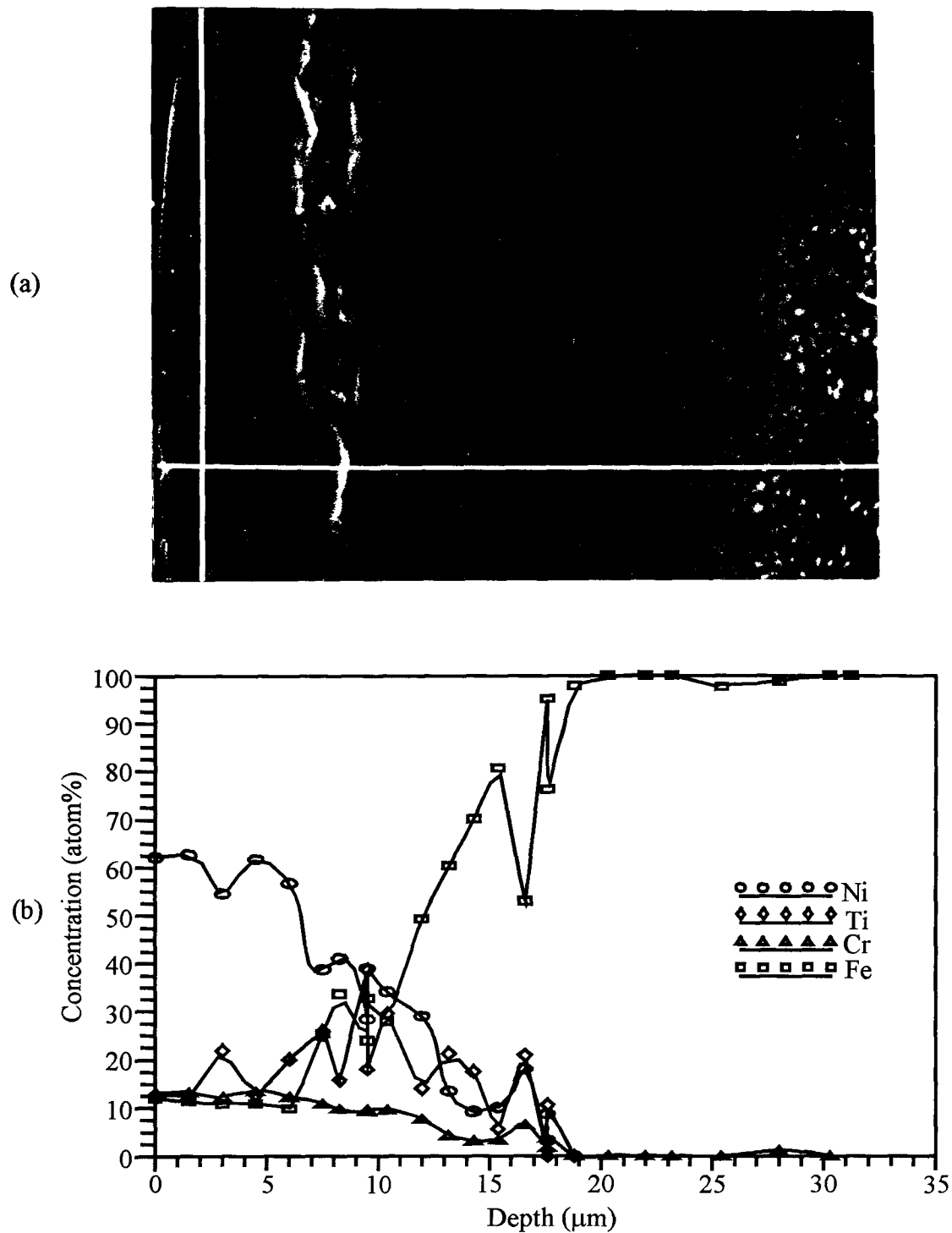


**Figure 5.6** Variation in concentration with respect to micrograph of Specimen 1.

(a) SEM micrograph of EDS detecting area and line; (b) EDS profile.

### **5.1.2.1 Fusion Zone**

Figure 5.1 is the optical micrograph. It is quite noticeable that the "white" fusion zone is divided into three main layers by two lamella-like "lines" which seems to be like some new phases or compounds or separation interfaces. The second "line" has some "sublines" penetrating mostly into the second layer while few into the bottom layer. In SEM micrograph (Figure 5.5), it is quite obvious that a big cracking exist along the first "line". Whereas, there are only microcracks or new phases (or compounds) along the second "line" or penetrating into the second layer. Still there is a visible pore adjoining the second "line". Each layer is still featureless except the visible cracks and porosity. It is worth noticing that there is an unwelcome pore at the second lamella-like "line".

#### **1. Outmost Layer**

This layer is made of materials approximating to the composition of the electrode, but not the same due to the participation of air as the environment medium as well as the extent of alloying. From the SEM micrograph (Figure 5.5), it has the thickness of about  $8\mu\text{m}$ .

Moreover, in the layer, there seems to be a horizontal crack while a small separation is shown at the right side of the micrograph.

#### **2. Middle Layer**

The middle layer separated from the first layer by a big cracking, has some penetrating "sublines" from the second "line".

As shown in EDS profiles (Figure 5.6(b)), the concentration of each element in this layer follows an obvious gradient, serving as a "bridge" linking upper and lower layer. By associated with its micrograph, this layer is most non-uniform in the fusion zone. The thickness of the layer is about  $10\mu\text{m}$ .

#### **3. Bottom Layer**

This layer is almost featureless except an occasional pore adjoining the second

"line". As shown in EDS profile, this layer of about  $6\mu\text{m}$  in thickness does not contain any detectable amount of major alloying elements—Ni, Ti and Cr. Instead, it has nearly the same composition as the bulk materials. This phenomenon is quite beyond expectation, since we have not ever seen such result in any relative literature. As an imprudent assumption, this layer is produced by melted or incompletely melted bulk material which does not get chances to participate in the alloying with electrode materials due to exceptionally rapid solidification, short duration of pulsed sparking and extremely low heat input. Its high resistance to etching solution seems to indicate extremely fine or even amorphous structure. More work should be done to reveal this phenomenon.

As should be pointed out, the optical micrograph is taken of the metallographic sample which is finely re-polished and re-etched after SEM and EDS analysis. Besides, the SEM analysis examines the microarea at much higher magnification than optical microscopic analysis. Therefore less details are shown in the optical micrograph, especially that of the cracking along the first "line".

In general, the EDS profile shows the gradient of Ni from high concentration in the outmost layer to zero at the second "line". However there is a quick drop across the big cracking and a small peak between the second "line" and one of its "sublines". Both of these two characteristic variations are accompanied by the corresponding variation of Ti and Fe, whereas the Cr keeps a smooth gradient from the outmost layer till the second "line" except a little increase corresponding to the small peak of Ni. Therefore, it is more reasonable to make assumption that new phases or compounds formed at those "lines", which result in cracking when they are very brittle. Further information can be obtained by x-ray diffraction analysis.

Anyway, the profiles of concentration along the depth demonstrate much smoother gradients than expected, from the outmost surface towards the fusion

line. This phenomena leads to our thinking of diffusion which used to be considered almost negligible in ESD processes.

#### **5.1.2.2 HAZ**

Both SEM and optical micrographs can be used to distinguish the HAZ. The grain boundaries in HAZ are not so clear that this zone seems to bear the transitional microstrutural feature between the fusion zone and the substrate. On scrutiny, the HAZ can be divided into a less etched thick layer and a deeply etched thin layer because of two-stage deposition or overlapping deposition.

Due to limited heat affection, the average thickness is only about  $7\mu\text{m}$  By the examination through the sample, the thickness of HAZ is not so uniform due to the non-uniformity or waviness of fusion line which reflects the inherent feature of ESD and manual operation.

#### **5.1.2.3 Fusion Line**

The excellent fusion line or the interface between fusion zone and HAZ, which is made of merging co-grains indicates good bonding effect. The compositional homogeneity of both side contribute a lot to the good bonding.

### **5.1.3 Microstructure of Specimen 2**

As shown in its optical micrograph (Figure 5.2), it is clear that the general structure is similar to the above specimen, consisting of a fusion zone and a HAZ adjoining the bulk material. However, its specific features make it different from the other specimens.

#### **5.1.3.1 Fusion Zone**

In its optical micrograph, a thin layer made of tiny protruding particles can be seen



**Figure 5.7** SEM micrograph of Specimen 2 deposited with Eltd2 ( $\times 2000$ ). The marked dots in sequence from the outface into the substrate within marked areas are the detected spots.



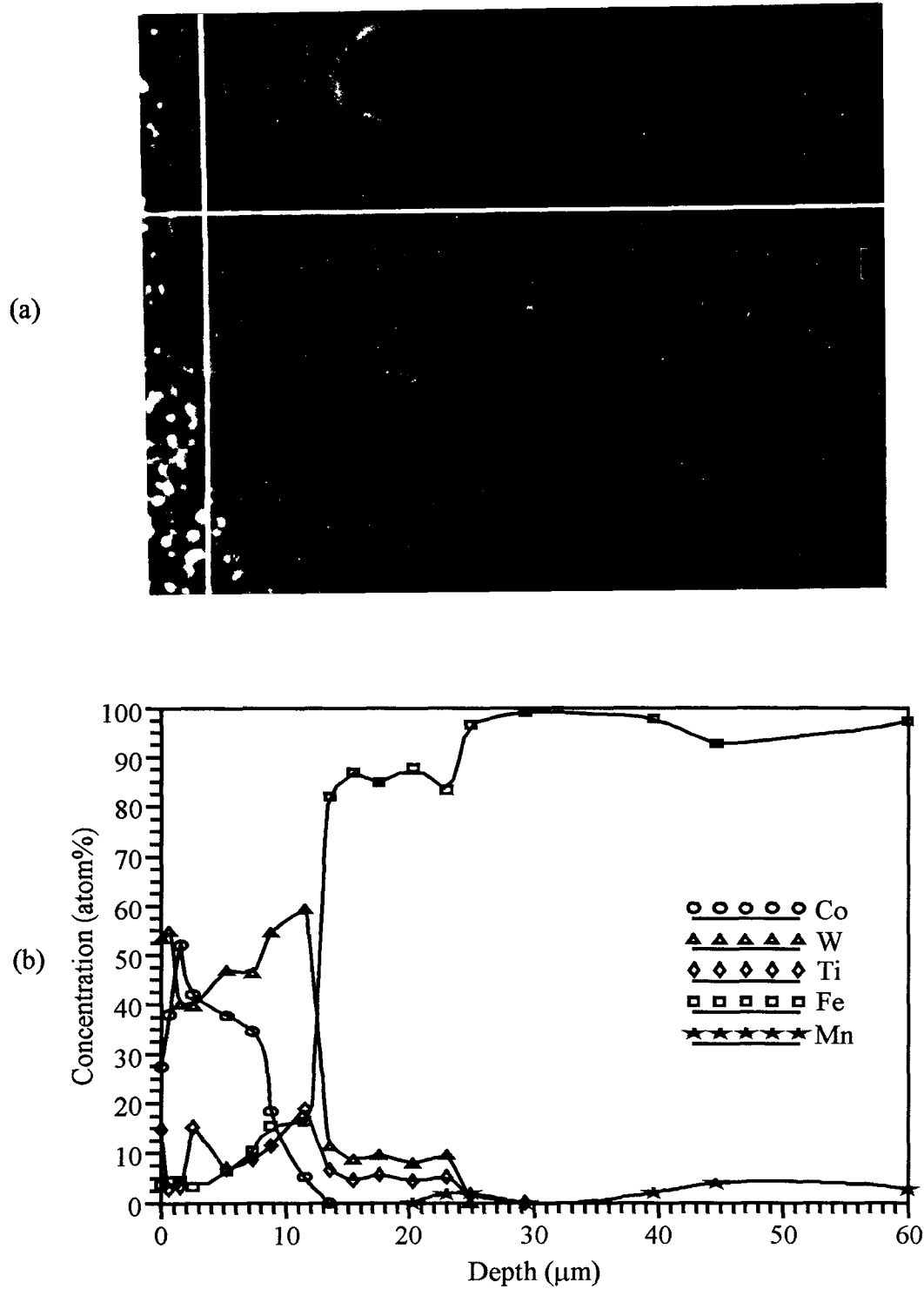


**Figure 5.8** Variation in concentration with respect to micrograph of Specimen 2.

(a) SEM micrograph of EDS detecting area and line; (b) EDS profile.

somewhere at the top of the fusion zone. In SEM micrograph (Figure 5.7), it is clear that fusion zone can be divided into three characteristic layers as below.

### **1. Outmost Layer**

This layer is made of small block particles in certain matrix. By EDS detection (Figure 5.8) the small white particles have high concentration of Co and W while the matrix is contains of W, Co and Ti. The concentration of Fe in this layer is quite low, indicating that the layer approximate the composition of electrode material. Porosity is visible in the matrix. Moreover, the layer is not so continuously distributed on the surface. The average thickness can be roughly estimated from the SEM micrograph as about  $7\mu\text{m}$ .

### **2. Middle Layer**

This layer appears white and almost featureless. It is neither continuously nor horizontally distributed as shown in the SEM micrograph. A discernable "line" like a microcrack, on scrutiny, divides the layer into two sublayers. The upper one has increasingly high concentration of W and correspondingly sharp drop of Co, whereas Ti and Fe show smooth increase. By contrast, the lower sublayer, has extremely high concentration of Fe and no detectable amount of Co (this is due to the detection limit of the employed EDS.). It is quite noticeable that the "line" serves as an interface, across which there exist two sublayer of extremely different composition, though both of them appear similar on the micrograph. Besides, there are some small pores along the upper extension part of the "line". Moreover, an extra-large pore is visible through the layer. Therefore, the top two layers do not seem to have good bonding with the beneath layers. The thickness of the layer is roughly about  $4\mu\text{m}$ .

### **3. Bottom Layer**

This featureless layer of about  $23\mu\text{m}$  in thickness looking just a little bit darker than the matrix of outmost layer, seems quite homogeneous and continuously

distributes over the substrate. Its EDS profiles show 8 $\mu\text{m}$  long steps of concentration of Fe, Ti and W followed by roughly 2 $\mu\text{m}$  long gradients to reach the composition of the bulk material, which seems to relate with formation of compounds or solid solutions, and diffusion. Further work is necessary to reveal its nature.

Anyway, this layer shows quite desirable features that the above two specimen do not possess. Its homogeneous appearance, comparatively quite large thickness and the specific transition of composition indicate good surface performance.

#### **5.1.3.2 HAZ and Fusion Line**

Except for the much small thickness of about 5 $\mu\text{m}$ , the HAZ of this specimen still has the other similar features to the above specimen. The fusion line also shows good bonding between fusion zone and HAZ.

#### **5.1.4 Specimen 3**

As shown in Figure 5.3, the specimen also has the general two-zone structure while it presents quite specific features.

**5.1.4.1 Fusion Zone:** The SEM micrograph (Figure 5.9) shows only two structural layers of specific features which are distinguished by a crack-like interface. Microcracks, porosity and non-homogeneity are visible.

##### **1. Outmost Layer**

The specific feature of this layer is its non-uniformity with white particles of various figures and sizes dispersing in the matrix of the layer. In particular, at the lower region of this layer, there is a wide strip transversing horizontally across the layer while some microcracks exist in the strip. According to EDS analysis, this

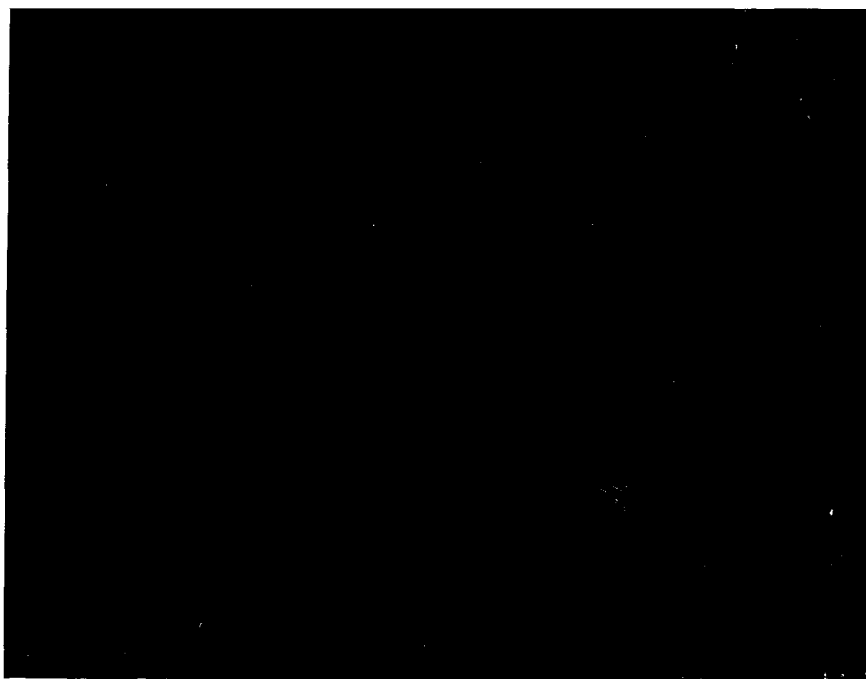


**Figure 5.9** SEM micrograph of Specimen 3 deposited with Eltd3 ( $\times 2000$ ). The marked dots in sequence from the outface into the substrate within marked areas are the detected spots.

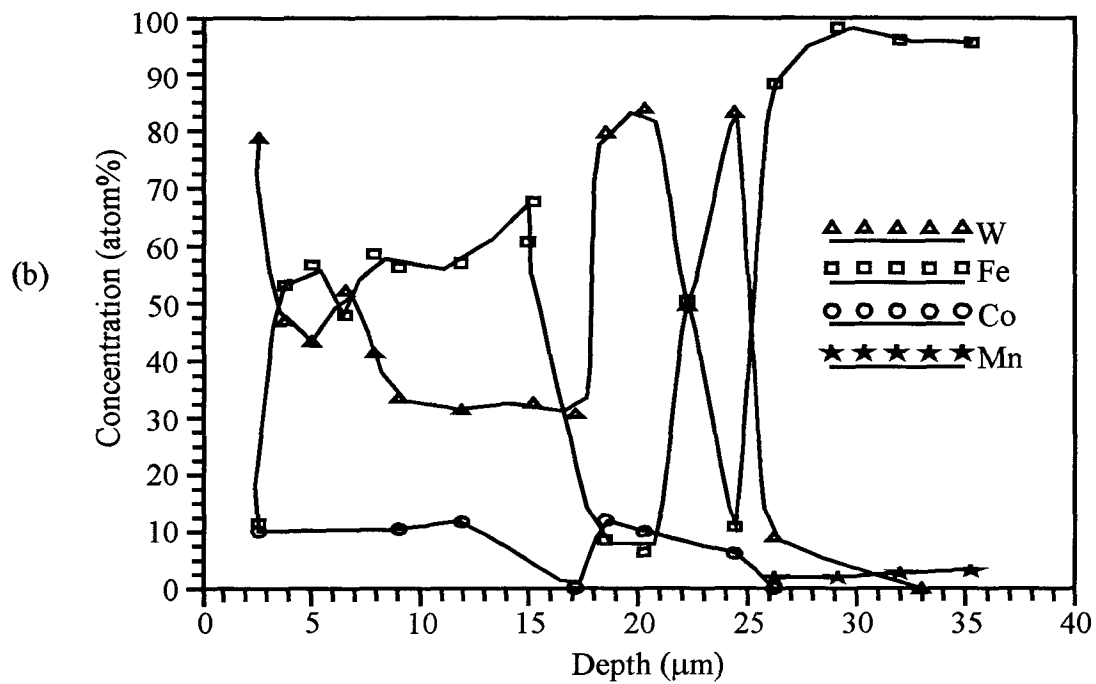
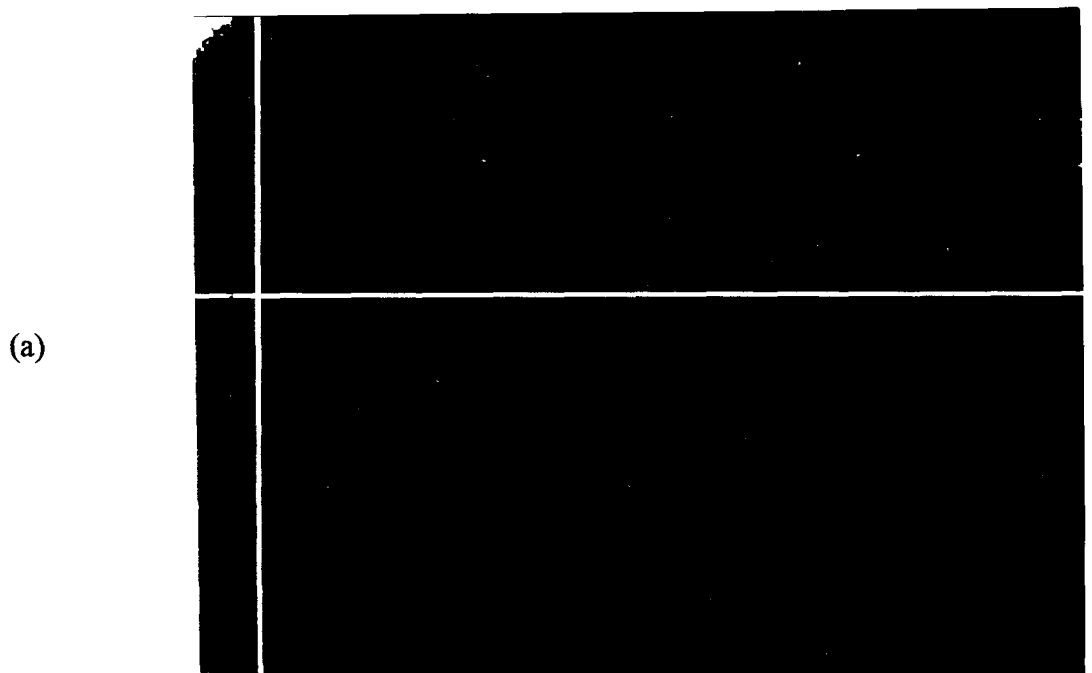


**Figure 5.10** Variation in concentration with respect to micrograph of Specimen 3.

(a) SEM micrograph of EDS detecting area and line; (b) EDS profile.

wide strip has extremely high concentration of W and some amount of Co, which approximates to the composition of electrode material.

However, in the upper part of the layer, the white particles are small and widely dispersive so as to give a welcome appearance. The EDS analysis (Figure 5.10) also shows that these white particles are concentrated of W and small amount of Co, approximating to the composition of electrode materials. Whereas the matrix contains Fe in addition to W. These are the results of surface alloying during ESD processes. On scrutiny, the matrix shows some loose regions in middle of the upper part of the layer, which needs further examination.

Between the transversing strip and the second featureless layer, there also exist some small white strips of similar composition as that of the wide strip. However, microcracks and porosity are quite noticeable in this region. In particle, microcracks and occasional pores are visible along the layer interface, which seems similar to that of the above specimen. Therefore, this region appears most undesirable and may result in separation from the next layer.

In general, the EDS profiles of this specimen demonstrates much greater variation than the above specimen while having some compositional steps. The EDS profile of W shows extremely high concentration at white particles in the outmost region followed by a drop to a short step, then another drop to a little longer step followed by a sharp increase and drop and another increase. These rapid variations correspond to the serious non-uniformity of the layer as well as likely formation of some compounds. The Co in the layer seems to only accompany with the white particles or white strips. The concentration of Fe varies with those of W and Co. The thickness of this layer is estimated from the SEM micrograph to be about 24 $\mu\text{m}$ .

## **2. Second Layer**

This layer in fusion zone is featureless, and also similar to that of the above sample. However, its EDS profile does present some penetration of W from the upper layer which seems reasonable to be explained as the result of diffusion. The thickness of this layer is only  $5\mu\text{m}$ . Therefore the diffusion is extremely limited.

## **3. Interface between Two Layers**

As mentioned above, microcracks are visible along the interface, indicating not so good bonding effect. As we can see from the micrograph, some long strips are formed near the interface or even along the interface, which may not result in the microcracking but only micro-height steps due to the difference of etching effects. The occasional porosity is still visible along the interface.

### **5.1.4.2 HAZ and Fusion Line**

The HAZ has the thickness of about  $8\mu\text{m}$ . Its microstructure features are similar to those of the above specimen. So it is with the fusion line.

### **5.1.5 Specimen 4**

In its optical micrograph (Figure 5.4), the overlapped fusion zone and HAZ are easily distinguished, whereas the SEM micrograph (Figure 5.11) taken at another region of the same specimen does not show the overlapping phenomenon. The specific features of the specimen described below are based on the SEM micrograph and EDS detection.

#### **5.1.5.1 Fusion Zone**

As shown in SEM micrograph, in the case of no overlapping layer, the fusion zone is divided into two layer by a visible "line" which seems to correspond to the "second horizontal line" in the optical micrograph.

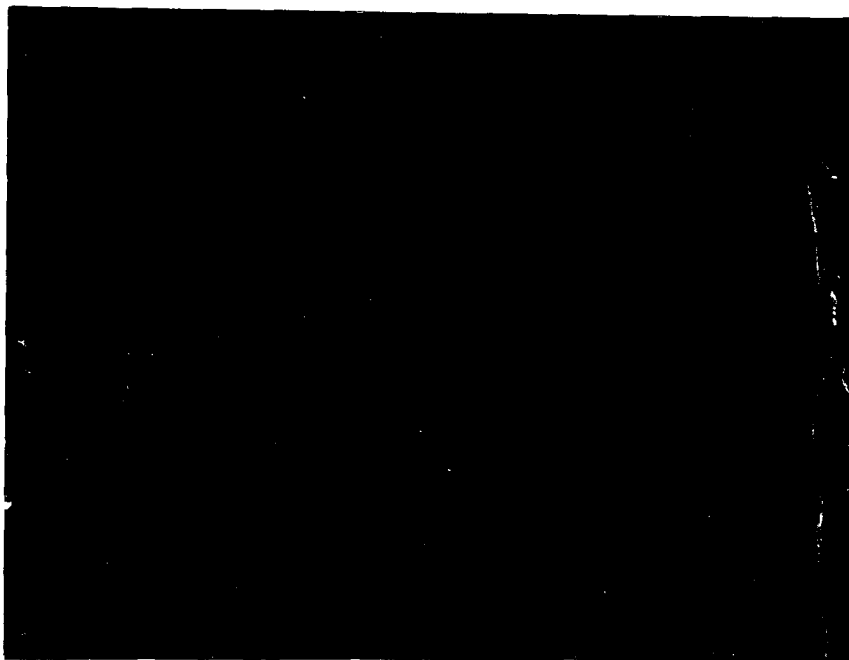


**Figure 5.11** SEM micrograph of Specimen 4 deposited with Eltd4 ( $\times 1600$ ). The marked dots in sequence from the outface into the substrate within marked areas are the detected spots.



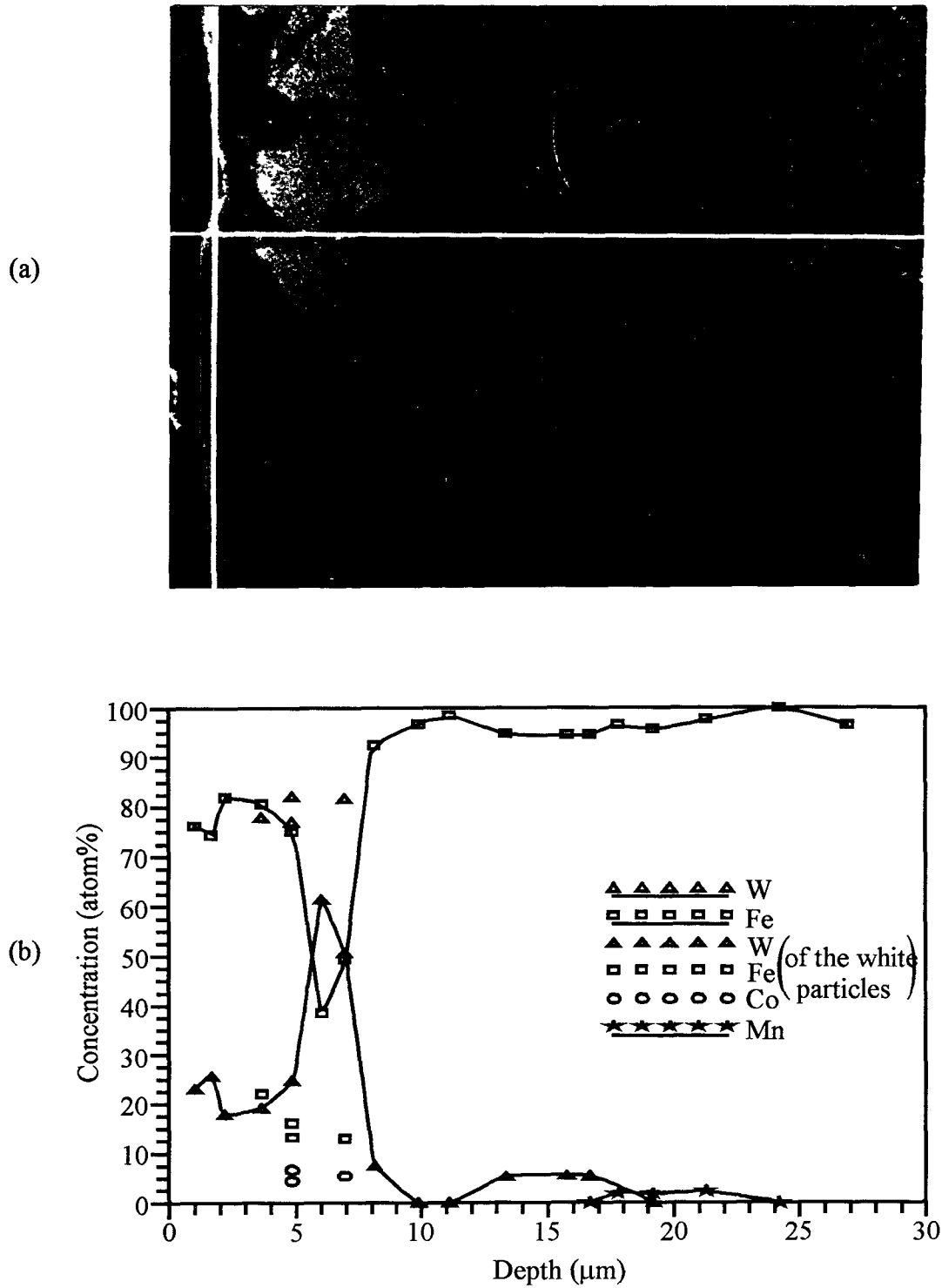


**Figure 5.12** Variation in concentration with respect to micrograph of Specimen 4.  
 (a) SEM micrograph of EDS detecting area and line; (b) EDS profile.

### **1. Outmost Layer**

This layer of about  $7\mu\text{m}$  has several white particles agglomerating near or even along the interface "line". The EDS detection (Figure 5.12) shows their composition of highly concentrated W with some Co, which is similar to that of electrode. The matrix, however, has quite high concentration of Fe versus low concentration of W and no detectable amount of Co. The high concentration of Fe in the matrix can be assumed as below:

- a. the electrode material containing quite amount of Fe-base matrix;
- b. sufficient surface alloying;
- c. the real outmost layer of the composition similar to that of the electrode having been separated off.

Detail information about the electrode materials or further detection of the overlapping layer is necessary to draw a final conclusion.

### **2. Second Layer**

This layer is featureless except few occasional particles or pits which may be produced during sample preparation. By EDS analysis, a concentration step of W and its corresponding step of Fe have been presented on the EDS profiles. The length of the steps can be roughly estimated as about  $8\mu\text{m}$ . Following the steps are the smooth gradients to the composition approximating to that of the bulk materials. The thickness of this layer is about  $20\mu\text{m}$ .

### **3. "Line"**

The "line" in SEM micrograph looks more like structure looseness than a crack in the optical micrograph. The sharp gradients of composition still occur across the "line", though not so severely at the regions that are lack of the white particles due to the high concentration of Fe in the matrix of the upper layer. Anyway, such phenomenon are quite similar to that of Specimen 2, and may be explained in the same way.

#### **4. The Overlapping Layer**

Although no overlapping layer is shown in the SEM micrograph, it is still worth considering the case when the overlapping layer exists as shown in the optical micrograph. It can be assumed that the overlapping layer should be closely dispersed with white particles of the composition similar to that of the electrode. In our cases its non-uniformity, non-continuity and lack of good bonding with the beneath layer can also be expected, which actually have been shown in the optical micrograph. The microhardness test result will give more information about it.

#### **5. Defects**

As shown in the optical micrograph, besides the crack between the overlapping layer and the layer below, there is vertical microcracking in both two layers below. Fortunately, the vertical microcrack in the upper layer has not yet merged into the vertical microcrack in the lower layer.

Besides, the porosity is still visible. These two kinds of defects seem inherent to the ESD processes. Anyway more work should be done to reveal the mechanisms.

**5.1.5.2 HAZ and Fusion Line:** The thickness of HAZ measured from SEM micrograph is about 4 $\mu$ m. All the other features of HAZ and fusion line are similar to those of the other specimen described above.

Overall, ESD coatings achieve a two-zone structure. One identified as fusion zone resulting from alloying can be further distinguished as two or three layers. The outmost layer usually approaches the composition of electrode materials, whereas the beneath one or two layers show the compositional transition from surface to the bulk substrate with some information about alloyed phases or diffusion. The other zone is identified as heat affected zone which experiences no compositional changes but some structure changes below melting temperature.

However, the specific features of each specimen vary a lot with the materials system involved as well as other factors. More work should be done on this aspect in order to get a thorough understanding.

## **5.2 Surface Topography**

The geometrical features of ESD surfaces are of great importance to surface quality. The ESD surface morphology usually present a matte appearance which can range from a very fine "pebbly" texture to a quite rough patchy texture. The wide range of ESD surface roughness depends largely upon the materials system involved, manipulating method, process parameters and control. For most materials, these range from the very rough deposits to relatively smooth deposits of 2 to 2.5 $\mu\text{m}$  AA (80 to 100 $\mu\text{in}$  AA). In some special cases such as carburizing surfaces using carbon electrodes, smoother deposits of less than 1.5 $\mu\text{m}$  have been obtained. However, surfaces are extremely complicated, the following results obtained under our conditions can not reveal all the features of ESD surfaces but do present some general features of ESD surfaces.

### **5.2.1 Surface Morphology**

Due to the local roughing produced by individual spark, the ESD surface usually achieves a matte appearance. Many factors such as materials system, process parameters, manipulating methods and environment medium, will determine the feature of mass transfer and deposition rate so as to produce the distinct surface appearance. The wide range and complexity of these factors result in the wide range of ESD surface finishes that can be achieved. In certain condition, the localized form of surface roughing may became so particular that slight protuberances at random points are formed shielding the intervening metal from the influence of the sparks and results in a patchy appearance which is not

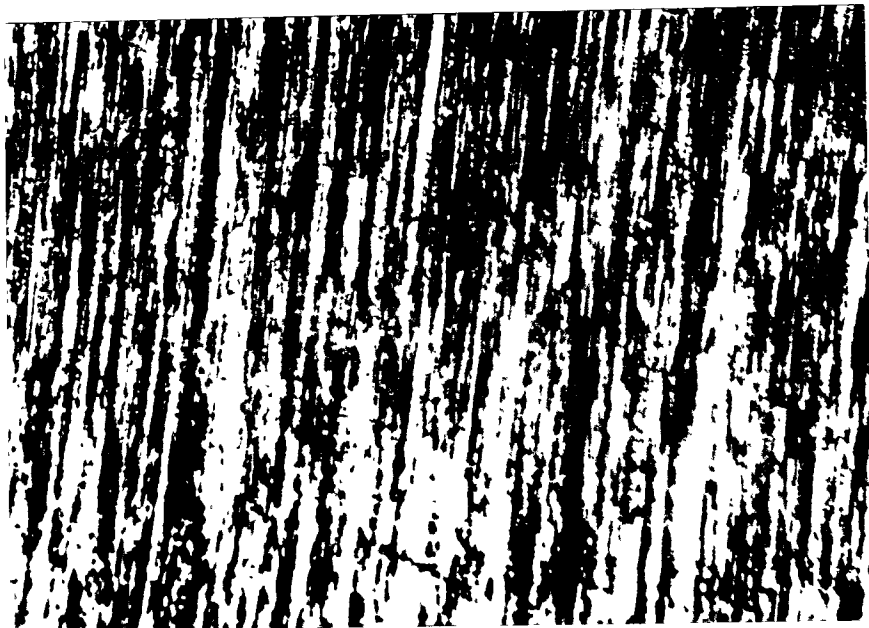


**Figure 5.13(a)** Surface micrograph of original surface.

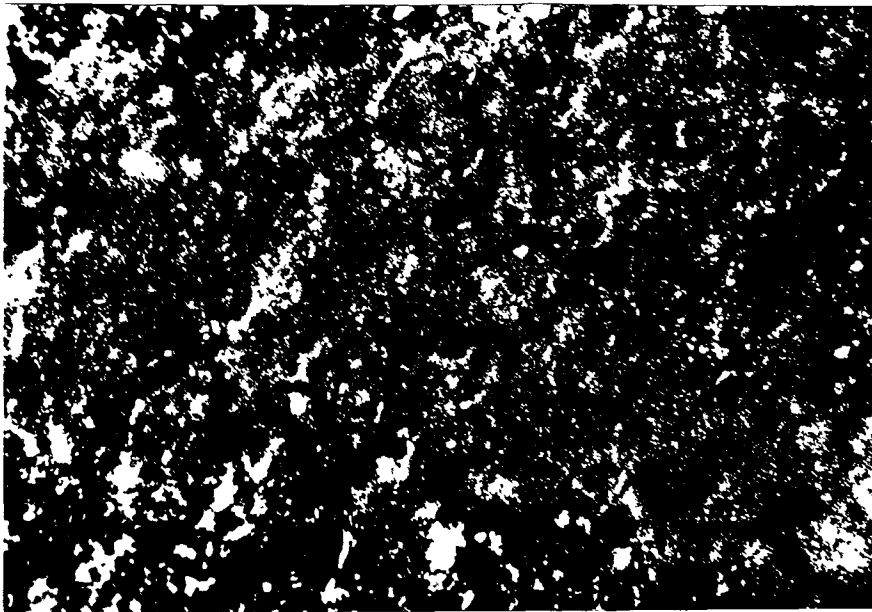


**Figure 5.13(b)** Surface micrograph of Specimen 1 deposited with Eltd1.

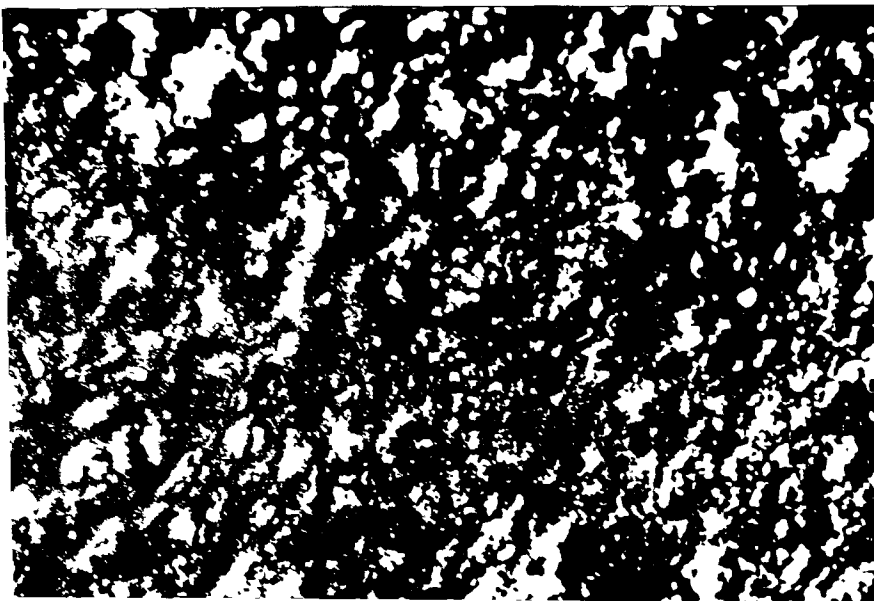


**Figure 5.13(c)** Surface micrograph of Specimen 2 deposited with Eltd2.

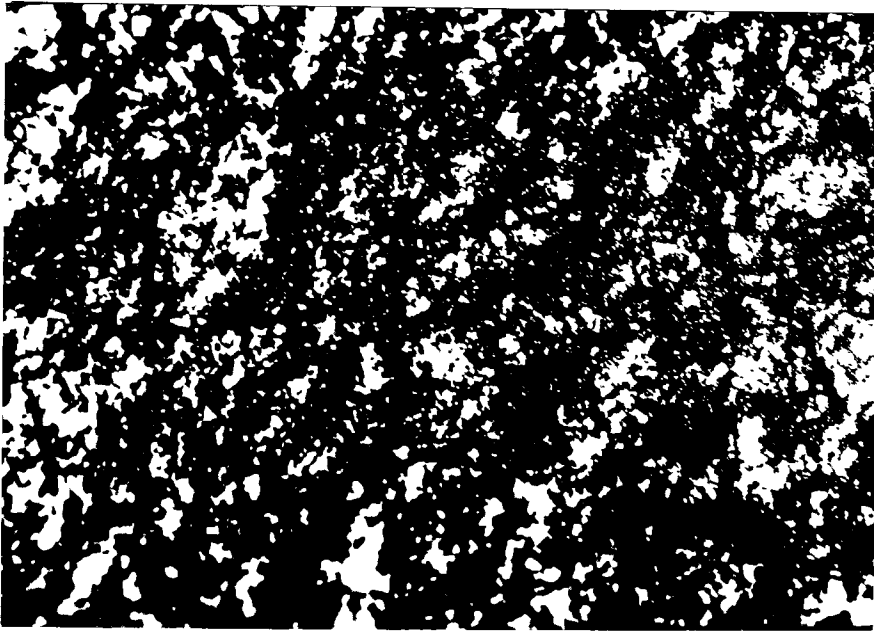


Figure 5.13(d) Surface micrograph of Specimen 3 deposited with Eltd3.

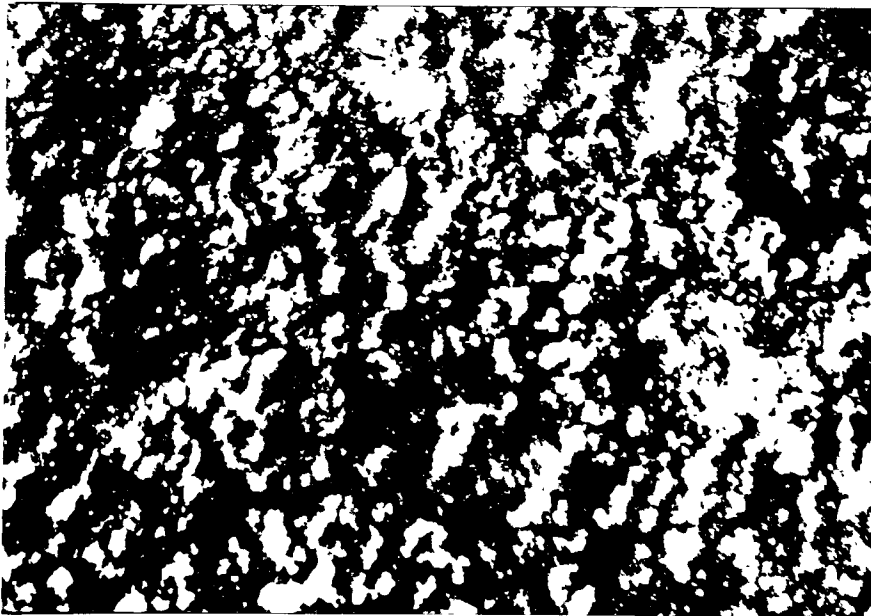


Figure 5.13(e) Surface micrograph of Specimen 4 deposited with Eltd4.

desirable. Figure 5.13 (a) shows the surface morphology of original surface of the substrate which is the typical texture of ground surface. Figure 5.13 (b)–(d) are the respective surface micrographs of performed ESD samples. It is obvious that those surfaces demonstrate mainly the feature of the matte appearance while combined with slightly patchy appearance.

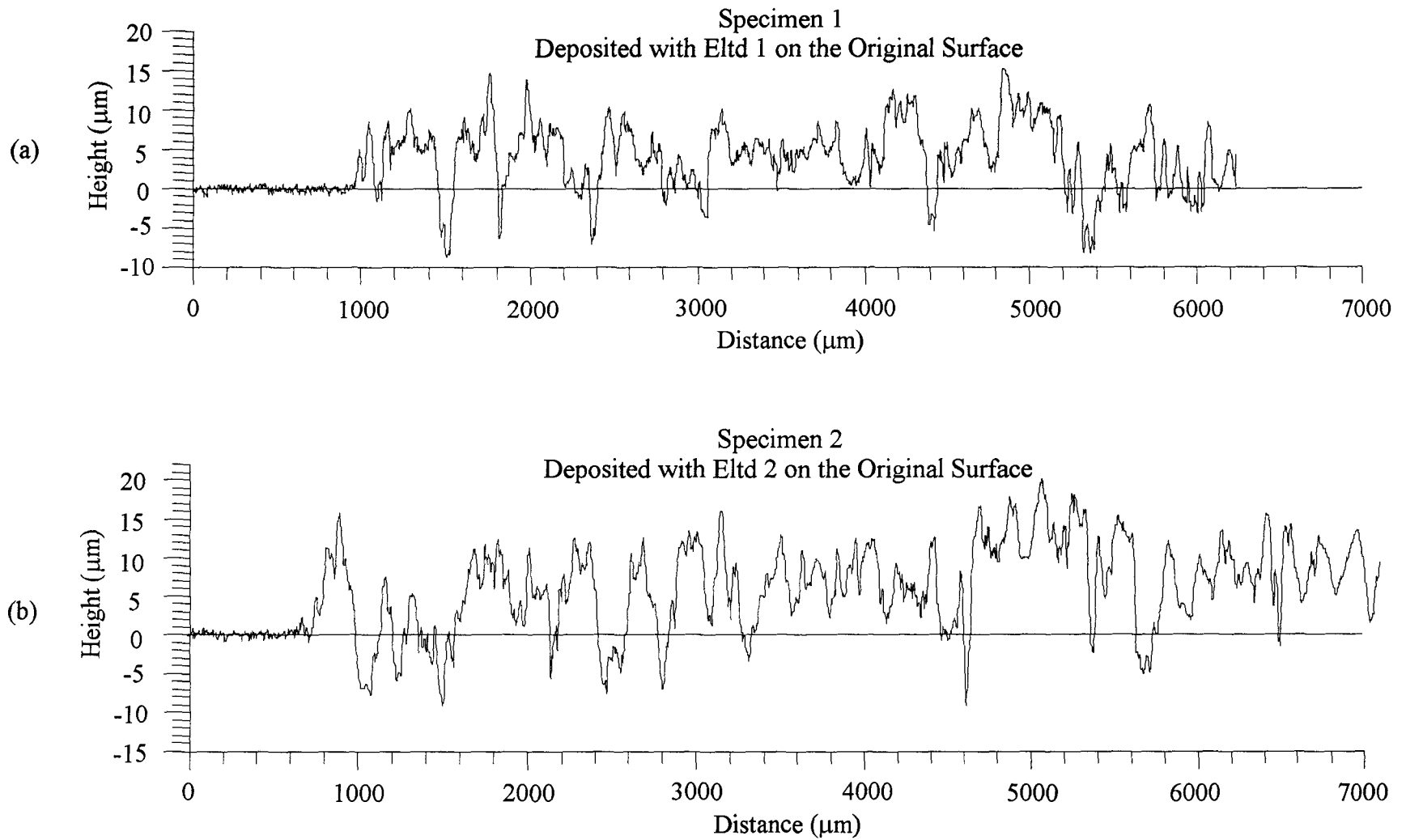
A noticeable feature is the pores and occasional erosion pits on the surfaces, especially in the case of Specimen 1 deposited using Eltd1. Besides, the outline of the "crater" indicates the superficial roughing produced by single spark or "overlapping" of spark-affected regions. In surface micrographs under higher magnification the pores and even some microcracks can be clearly presented. By comparison, the surface features of Specimen 1 is quite different from that of the others. This is the obvious result due to the quite different electrode materials applied. By visual inspection, its dark colored surface is lack of metallic shining feature, indicating the formation of special compounds. The others looks a little bit similar and do have some metallic shining feature, although to the much less extent that can be achieved by the real metals. On scrutiny, the surface of Specimen 3 seems to be the roughest whereas Specimen 4 achieves the surface of the least density.

In general, all the ESD surfaces we achieved are not so rough that no typically patchy texture is distinguishable. All the specimen show the deposits where both globular and spray transfer have occurred. Anyway it is rather difficult to give the exact description about these ESD surface appearance.

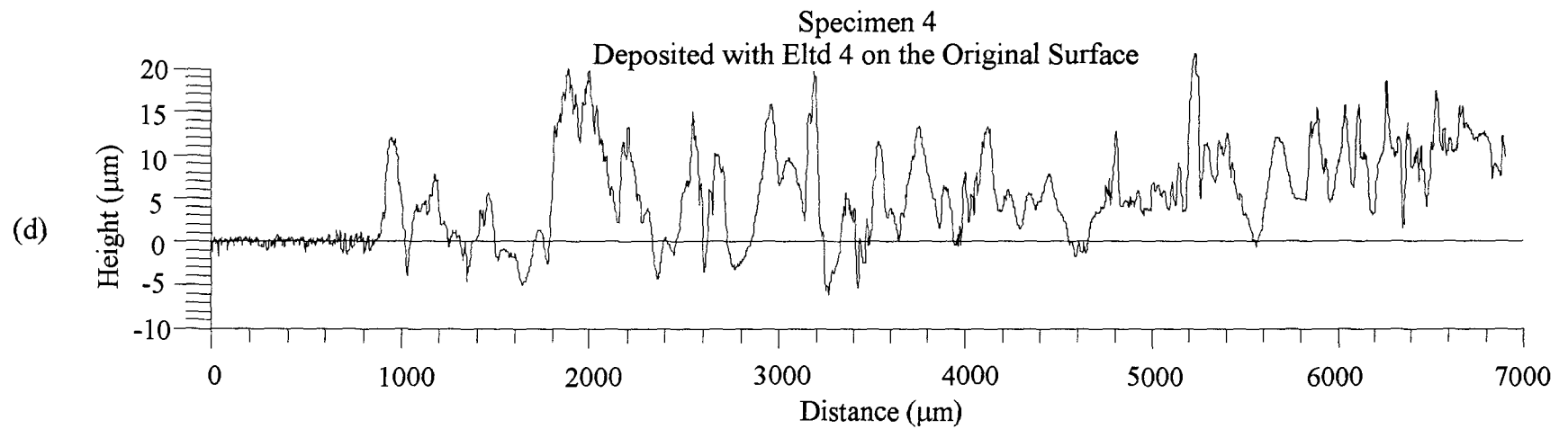
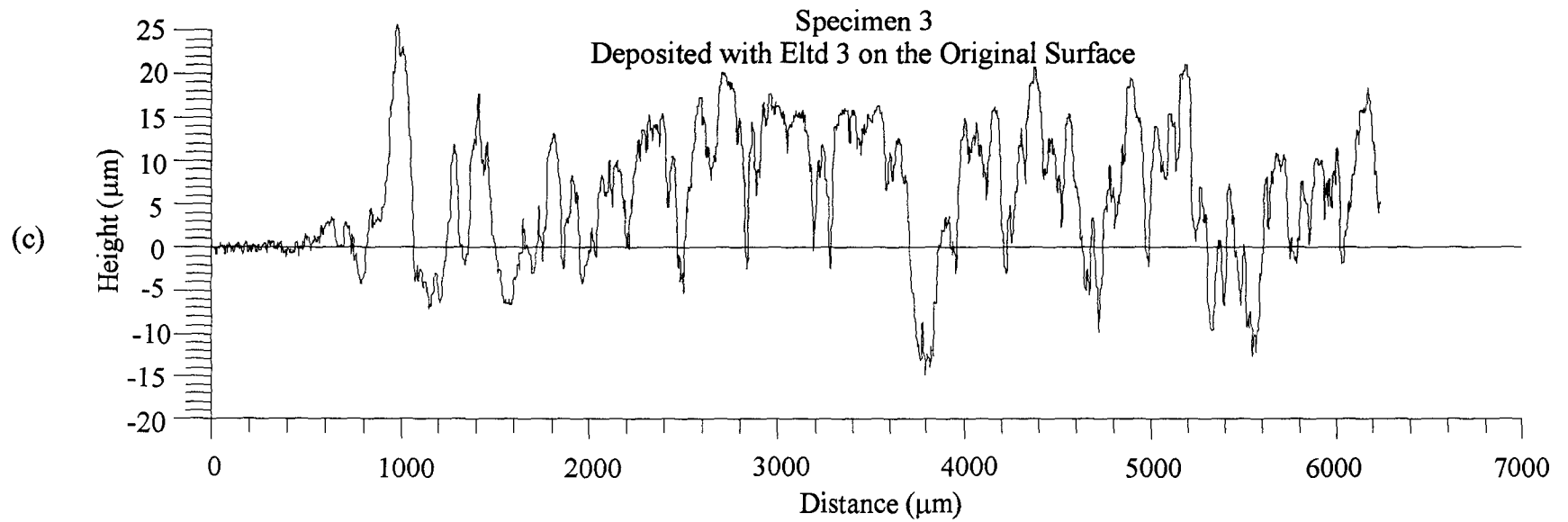
### 5.2.2 Surface Roughness

Surfanalyzer<sup>®</sup> 400 records the surface profiles of all the specimen as shown in Figure 5.14. These surface profiles combined with the corresponding surface roughness parameters (Table 5.1) by computer analysis, reveal the features of





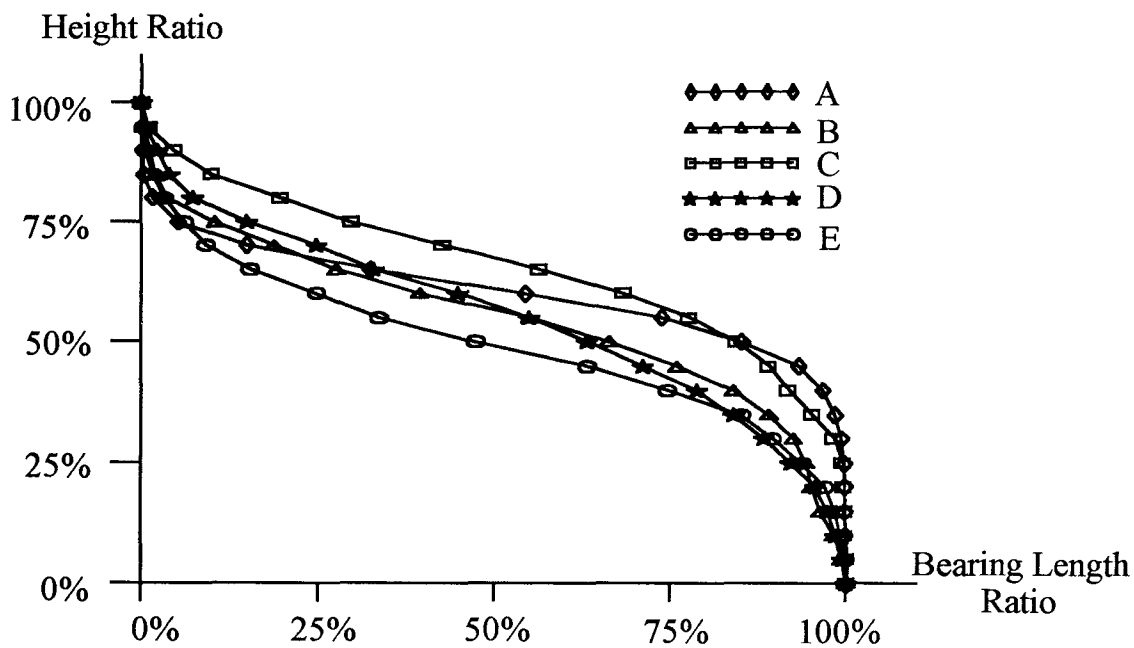
**Figure 5.14** Surface Profiles of Electro-Spark Deposited Specimen : (a) Specimen 1; (b) Specimen 2.



**Figure 5.14** Surface Profiles of Electro-Spark Deposited Specimen : (c) Specimen 3; (d) Specimen 4.

**Table 5.1** Surface roughness parameters

	Ra ( $\mu\text{m}$ )	Rq ( $\mu\text{m}$ )	Rz ( $\mu\text{m}$ )	Ry ( $\mu\text{m}$ )	Rsk (Skewness)	Bearing Area Curves
Original surface	0.25	0.32	2.82	3.20	-0.61	A
Specimen 1	3.11	4.07	23.84	23.99	-0.61	B
Specimen 2	3.90	4.92	30.35	30.88	-0.54	C
Specimen 3	5.73	7.04	36.22	36.75	-0.36	D
Specimen 4	3.59	4.64	29.33	29.59	0.048	E

**Figure 5.15** Bearing area curves.

surface roughening produced by ESD, and illustrate the achieved buildup on the surface as well as some information about melting depth of the substrate during ESD processes.

The results demonstrate that the roughening produced by sparking is quite obvious and seems to be not so welcome, since the typical surface roughness parameters such as Ra and Rz have been increased more than 10 times as big as that of the original surface. By comparison with the bearing area ratio curves as shown in Figure 5.15, materials system, manipulation method, process parameters and control are the main factors of determining the surface features. Here we just can see the obvious effects of the applied materials systems in our condition. Further comparison can be performed by choosing different process parameters, manipulation methods and setting more conditions.

In our cases, the ESD is performed by manual operation with the manipulator's empirical experience. Therefore only rough and general comparisons can be made as the following.

#### **5.2.2.1 Specimen 1**

Specimen 3 achieved the least roughening surface with the smallest value of Ra, Rz and Ry. Its bearing area ratio curve shows next to the best of fullness; and the skewness is the best of all. However its bearing ratio curve also indicates its sharp and short asperities on the top contour. This may be one of the major reasons why the top layers of the specimen are easily separated as shown in the microstructure.

The mean increase of build-up on the surface achieved the least of the four specimen. Its surface profile indicates the maximum melting depths to be more than 10 $\mu$ m.

#### **5.2.2.2 Specimen 2**

Specimen 2 has the second most roughening surface. However, its bearing area ratio curve shows the best of fullness while its skewness also presents the second best value of all. In general these two parameters achieve the values most approximating to those of original ground surface, which indicate the good load carrying capacity and less entrapment volume. In this way comparatively good wear resistance maybe expected. Wear test should be performed to support this saying.

The mean increase of build-up on the surface is about  $6.36\mu\text{m}$ . The maximum melting depth seems to be bigger than  $10\mu\text{m}$ .

#### **5.2.2.3 Specimen 3**

Specimen 3 achieved the most roughening surface with the biggest values of  $R_a$ ,  $R_z$ ,  $R_y$ . Whereas its bearing area ratio curve shows next to the least fullness; and the skewness is at the middle level of all the four specimen.

The mean increase of build-up on the surface is about  $7\mu\text{m}$ , which is on the same scale as the value of  $R_a$ . From the surface profile, its maximum melting depth can be roughly estimated to be  $15\mu\text{m}$ .

#### **5.2.2.4 Specimen 4**

Specimen 4 achieved the less roughening surface than Specimen 2. The skewness is nearly zero, indicating very good symmetry of amplitude distribution about mean line. Whereas its bearing area curve has the least fullness. Moreover the bearing area curve also indicates the sharp asperities on the top part of the surface contour. By comparison with other specimen, sharpness of the top asperities seems to be more serious than all the other samples. In general this specimen seems to have the less load carrying capacity and bigger entrapment.

The average build-up on the surface is about  $7.69\mu\text{m}$  and the maximum melting depths seems to be not less than  $10\mu\text{m}$ .

In general, all our ESD surfaces achieve negative skewness except one with nearly zero skewness. All the bearing area curves, though having different fullness, show the sharp asperities on the top part of surface contours, which corresponds to "pips" on matte appearance of ESD coating. Such "pips" approximating to the composition of the involved electrode materials, are easily separated, which can be assumed as due to the non-sufficient alloying and too rapid solidification during the last period of each sparking pulse as well as its weak appearance.

### **5.3 Microhardness Test**

Knoop microhardness tests are employed in examining the properties of ESD surface coatings. The microhardness gradient profiles along the depth from top surface to the bulk material provide important information about the structure and properties of the coatings, which include the microhardness identification of each layers and the microhardness gradient across the interfaces.

As the ESD coating thickness is usually not big enough to entail general microhardness distribution along depth, the tape-sectioned samples at about  $10^\circ$  are used to enlarge the details of surface structures. All the following microhardness profile are made by using Leco microhardness test system with Knoop indenter at the load of 10g.

#### **5.3.1 Specimen 1**

Figure 5.16 is the microhardness distribution profile and its corresponding optical micrograph at  $10^\circ$  tape-section of specimen 1.

As mentioned before, the fusion zone of the specimen 1 consists of three layers, of which the top two layer are easily separated from the surface due to the

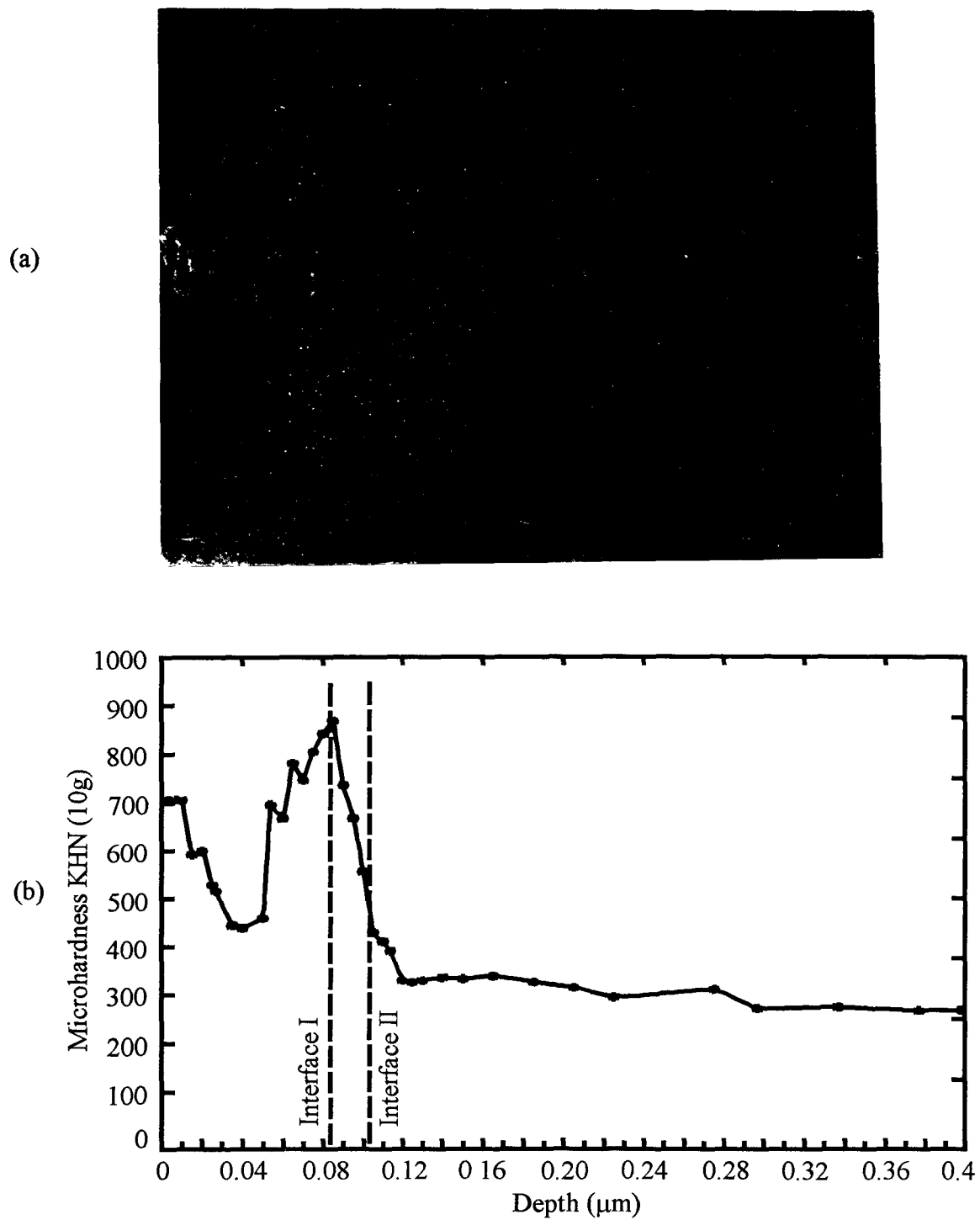


**Figure 5.16** Variation in microhardness with respect to tape-sectioned micrograph of Specimen 1.

(a) Optical micrograph of detecting area; (b) Microhardness profile.

brittle phases produced at the interfaces resulting in less bonding strength. As shown in the micrograph, only a little bit part of the second layer is left. Therefore the microhardness distribution profile of specimen 3 only reveal the feature from this part to the bulk materials.

It is obvious that there is a soft region in the bottom layer of the fusion zone due to less alloying while a big increase is achieved across the interface between fusion zone and heat-affected zone which of no doubt can be attributed to the spark induced hardening by thermal effect. Moreover, the measured hardness values of the superficial surface are even lower than those across the interface between fusion zone and HAZ. Since all the ESD specimen in the work are deposited by a two-stage deposition process, the softening effect can be attributed to the least alloying near the fusion line (the interface between fusion zone and HAZ) followed by rapid quenching and then the reheat affection during the second-stage deposition. This saying is well confirmed by the microstructure examination mentioned before which shows that the electrode material does not disperse deeply into the bottom layer of the fusion zone. Therefore, the rapid quenching followed by reheating and re-quenching results in the softening of this layers. An extremely narrow region of nearly 100% Fe (detected by EDS) near the fusion line can be another support to such saying.

Besides, there is a narrow microhardness gradient near the interface between HAZ and bulk material, which can be included in the HAZ and seems to correspond to the dark etched thin sublayer as shown in Figure 5.1 However this layer is not so uniformly distributed due to the manual operation of ESD processing. It can be assumed as the result of reheat-affection because of the two-stage processing. Further efforts are necessary to investigate the thermal effort of multi-stage ESD processing.



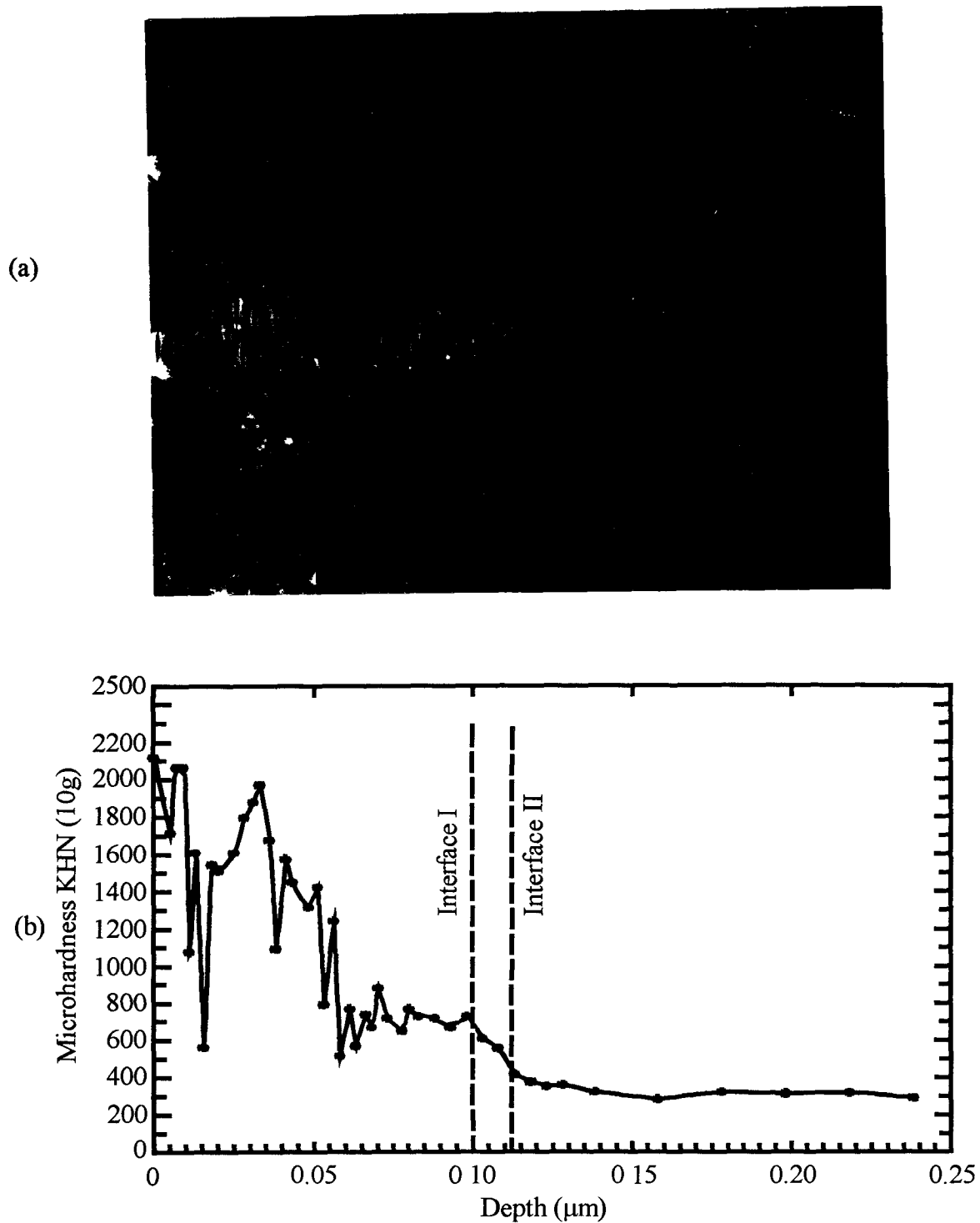


**Figure 5.17** Variation in microhardness with respect to tape-sectioned micrograph of Specimen 2.

(a) Optical micrograph of detecting area; (b) Microhardness profile.

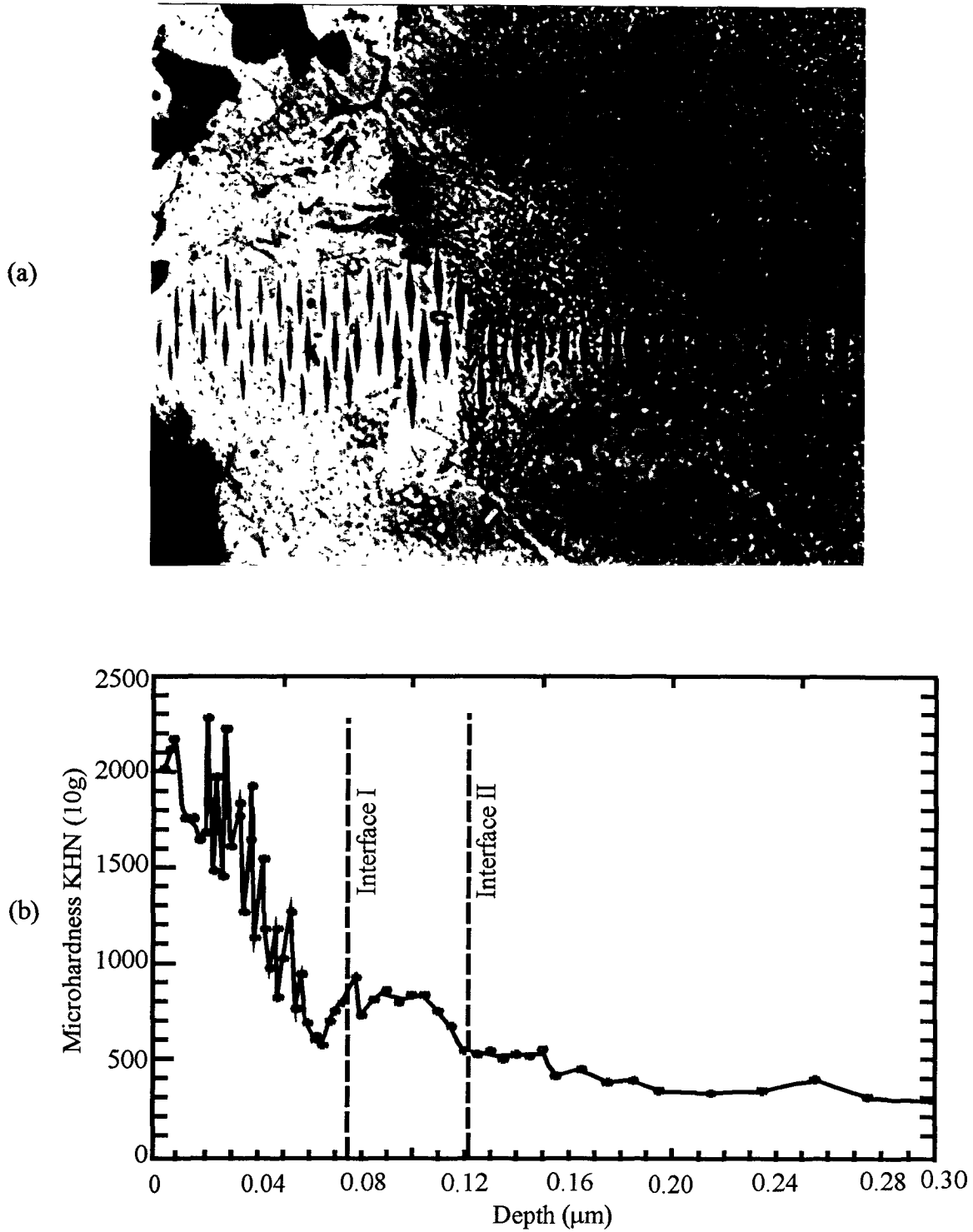


**Figure 5.18** Variation in microhardness with respect to tape-sectioned micrograph of Specimen 3.

(a) Optical micrograph of detecting area; (b) Microhardness profile.

### 5.3.2 Specimen 2

Figure 5.17 shows the microhardness profile and the optical micrograph at 15° tape-section.

It is quite noticeable in the micrograph that the thermal cracks exist due to rapid solidification. These microcracks result in the lowering of measured hardness values. The gradient of microhardness shows gradual transition from outmost surface to the bulk materials. The hardness variation in the outmost layer still reveals the compositional non-uniformity and the existence of microcracks as well. The highest hardness value is over 2000KHN, approximating to the hardness of electrode materials.

By comparison with Specimen 1 and Specimen 3, both the softening and hardening effect near the interface between fusion zone and bulk material are achieved to a mild extent so that better bonding can be expected. Besides, the HAZ of this specimen is rather narrow, indicating less heat affection. Similarly, the gradient of microhardness from major HAZ to the bulk materials is so smooth that the sublayer as mentioned in the other sample is hardly distinguishable.

Moreover, the microhardness values before the fusion line present less variation, which seems correspondent to the step of concentration in the EDS compositional distribution profile along depth (shown in Figure 5.8). Therefore, some kind of solid solution or compound may be formed or diffusion is effective. Further work should be done to support this assumption.

### 5.3.3 Specimen 3

Figure 5.18 is the microhardness profile and its correspond optical micrograph at 11° tape-section of Specimen 3.

The microhardness profile shows the superficial hardness values are over 2000 KHN, which approximate to the hardness of electrode materials .Except the

variation of measured values in fusion zone which corresponds to the non-uniformity, gradient of microhardness is still obvious along the depth. Similar to the case of Specimen 1, a softening region exists near the fusion line, which also corresponds to the least alloying region in the bottom layer of the fusion zone. However, the result of EDS analysis shows that the bottom layer of fusion zone has such a little bit penetration of tungsten that less softening effect is resulted in as compared with Specimen 1.

The thicker HAZ than that of Specimen 1 indicates more heat input during the processes. This may be one of the major reasons why tungsten presents a little bit penetration into the bottom layer of the fusion zone so as to reduce the softening effort.

Moreover, the microhardness profile presents a thicker HAZ than that can be distinguished from the micrograph of this less etched sample. This indicates that there exists a less heat-affected sublayer serving as a "bridge" between the major HAZ and substrate, which may be similar to the dark etched sublayer beneath the major HAZ in Specimen 1. Anyway this sublayer seems to be a good "bridge" in offering a smooth gradient of properties between HAZ and bulk materials.

#### **5.3.4 Specimen 4**

Figure 5.19 is the microhardness profile and the optical micrograph at 18° tape-section.

Similar to Specimen 2, solidification induced microcracks are visible in the fusion zone and cause the drop of microhardness. Comparatively, the microhardness profile of Specimen 4 presents the similar general feature of gradient to that of Specimen 2. However, the hardening effect in fusion zone achieved by Specimen 4 is much stronger, resulting in no distinguishable softening region near the interface between fusion zone and bulk materials. As shown in

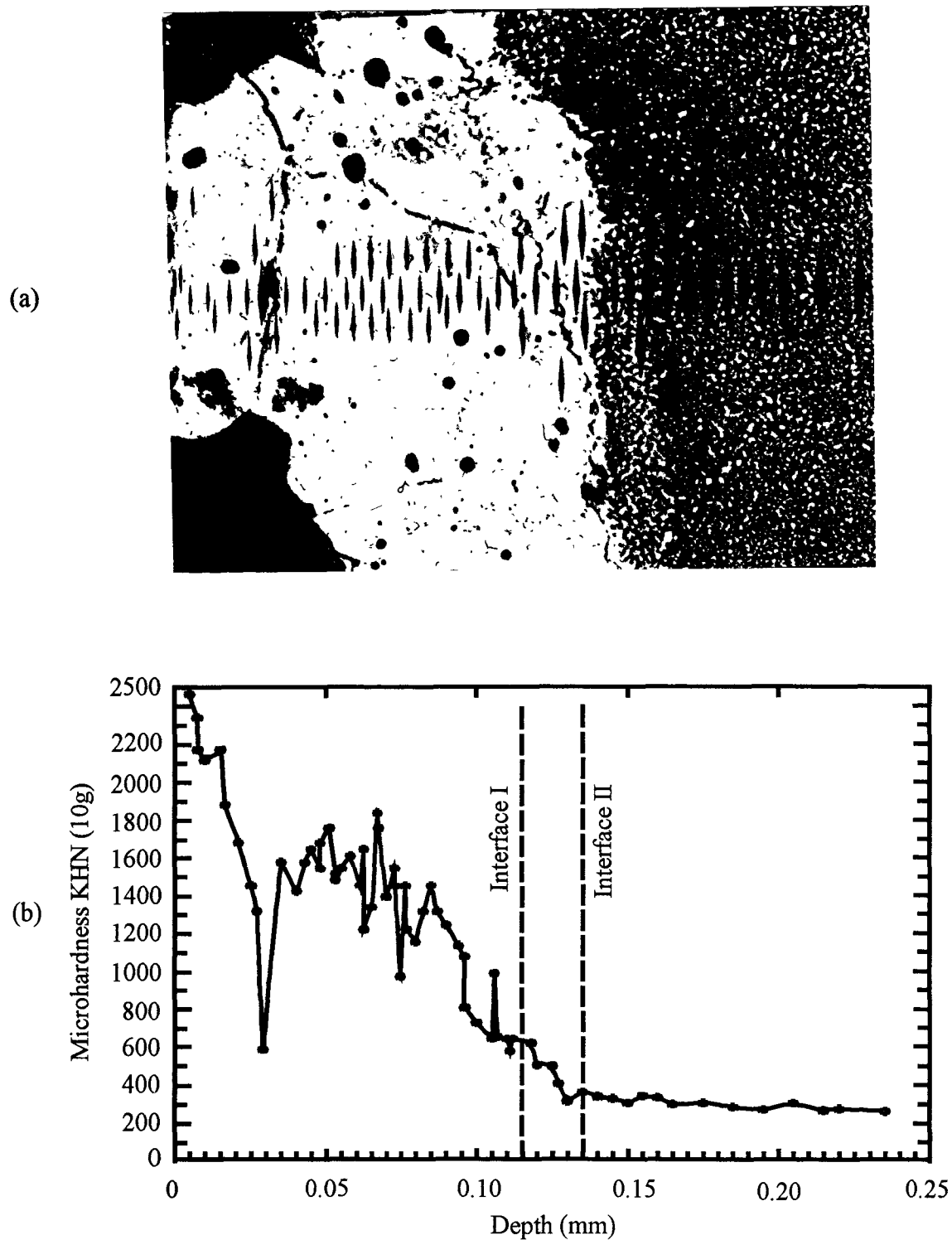


**Figure 5.19** Variation in microhardness with respect to tape-sectioned micrograph of Specimen 4.

(a) Optical micrograph of detecting area; (b) Microhardness profile.

SEM micrograph (Figure 5.12), some white particles in high concentration of tungsten exist in the fusion zone and largely contribute to the hardening effect. The highest value of microhardness is over 2000 KHN.

The smooth gradient of microhardness across the fusion line indicates the gradual transition of properties from the fusion zone to HAZ, upon which good bonding can be predicted.

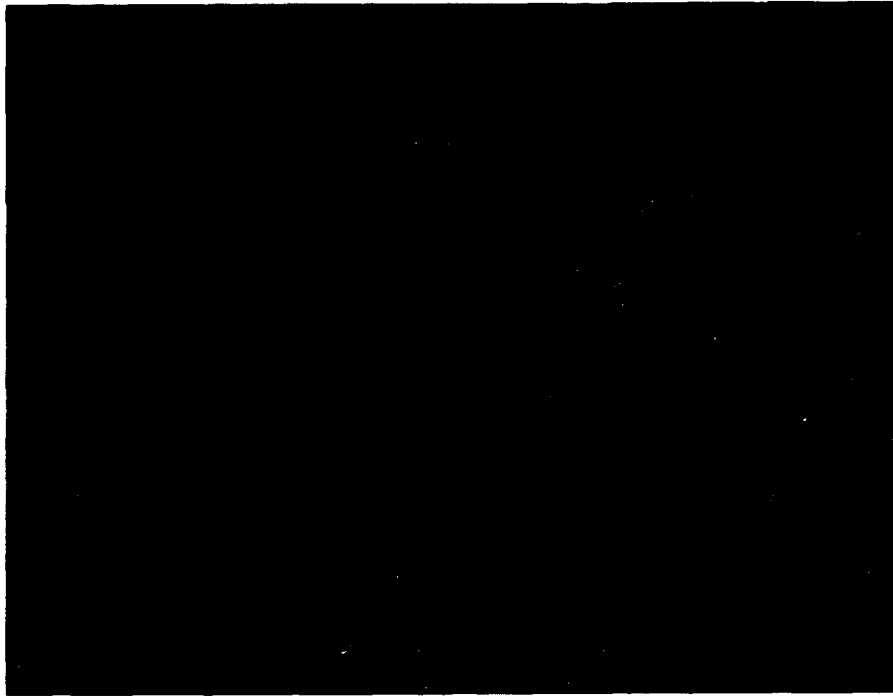
Similarly, the HAZ is narrow and non distinguishable sublayer beneath major HAZ exists.

#### 5.4 Simple Bend Test

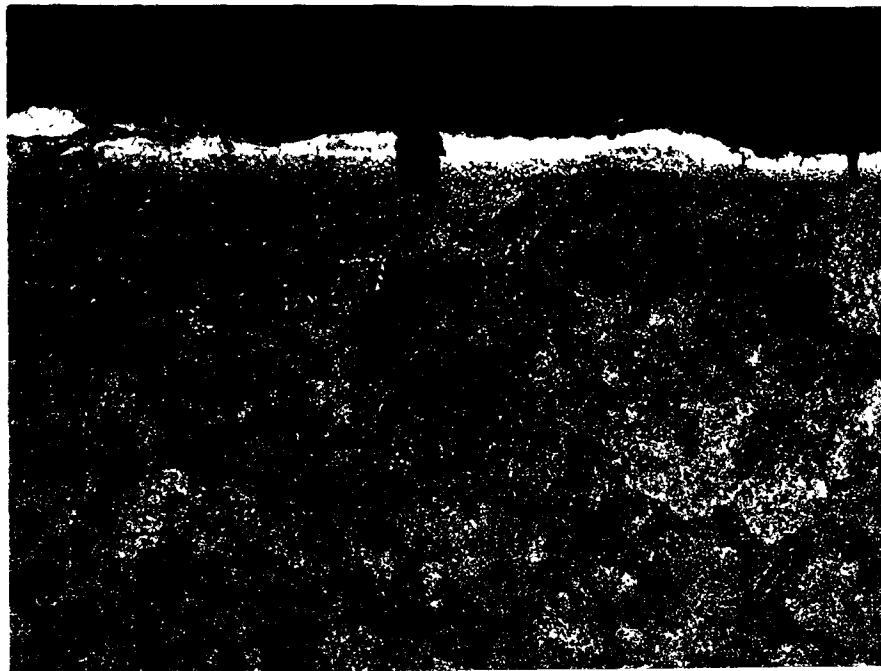
Simple bend test is an easy and effective way to evaluate both adhesion strength and ductility of the coating to accommodate residual stresses. Some researchers have reported the high spalling resistance of ESD coatings by showing no detectable material loss or spalling in even a severe 180° bend. However, no microstructure examinations of such bent samples have been performed. Therefore, in our work, simple bend tests in 90° (at curvature of about 4 mm) are performed with microstructure examination to check the spalling resistance and the bonding effect.

Figure 5.20 is the cross-sectioned micrographs of bent specimen. It is shown that cracks occur and propagate toward or into the bulk materials. But most of the cracks are perpendicular to the surface or fusion line. In Specimen 1, 2 and 4, no visible cracking occurs along interface between fusion zone and HAZ. Only in Specimen 3, cracking is visible somewhere at the interface, which seems to correspond to the original microcrack as shown in the SEM micrograph (Figure 5.9). The horizontal cracking in the fusion zone away from the fusion line (i.e. the interface between fusion zone and HAZ) further confirm the fact that the topmost layers are easy to be separated from the surface due to the following reasons:

(a)



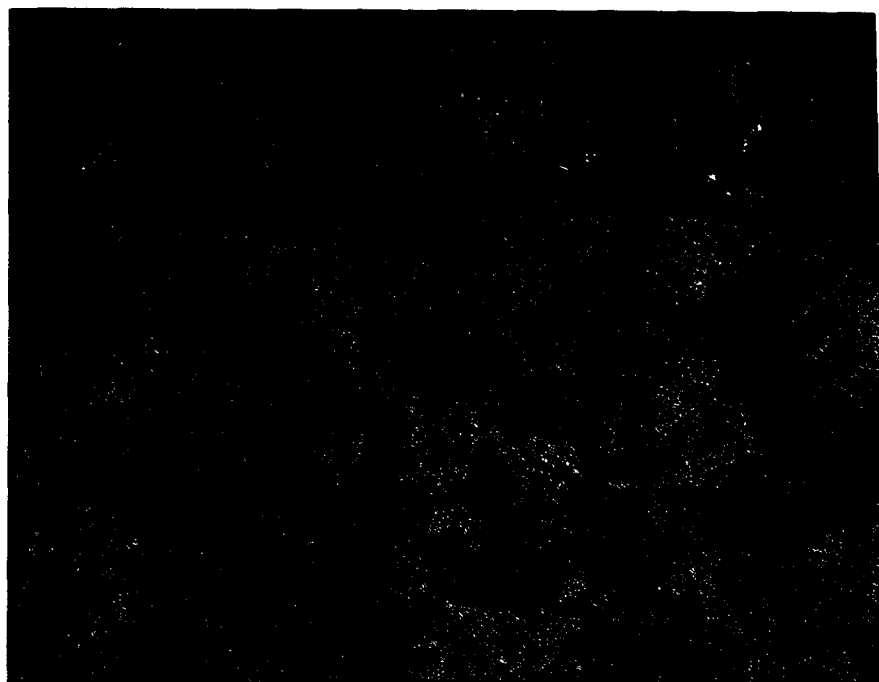
(b)



**Figure 5.20(I)** Optical micrographs of cross-sectioned specimens after 90° simple bend tests.

(a) Specimen 1 ( $\times 375$ ); (b) Specimen 2 ( $\times 375$ ).

(a)



(b)



**Figure 5.20(II)** Optical micrographs of cross-sectioned specimens after 90° simple bend tests.  
(a) Specimen 3 ( $\times 375$ ); (b) Specimen 4 ( $\times 375$ ).



- a. non-sufficient alloying and the consequent superficial composition approximating to the electrode materials which is originally brittle and probably becomes more brittle as the structure changes in the case of ESD;
- b. formation of brittle phases or compounds during alloying;
- c. non-uniformity and big difference of involved materials properties;
- d. rapid solidification

The vertical cracking originates from the tension induced propagation of the original vertical microcracks produced during ESD processes. Therefore, in such cases, the good spalling resistance are partially attributed to the stress release by vertical cracking. Therefore the simple bending test can be used as a good way to examine the original microcracking structures of the ESD coatings as well as the ductility. Whereas it can not provide the real bonding information about coating and substrate.

As has been reported by some researchers, ESD coatings of the vertical microcrack structure when in condition that microcracks do not propagate either parallel to the fusion line or into the bulk material, perform better in wear rate, galling resistance, and friction coefficients in high-temperature sodium than even the crack-free deposits. Our ESD coatings seem to have such vertical microcrack structure. Therefore no materials loss or spalling is distinguished by visual inspection.

### **5.5 Indentation Test**

This simple test on the microscopic scale is quite effective for evaluating the bonding between fusion zone and substrate by making a deep indentation on their interface using a Rockwell diamond brale with the load of 60kgf.

The results are presented in Figure 5.21. It is obvious that no cracking is

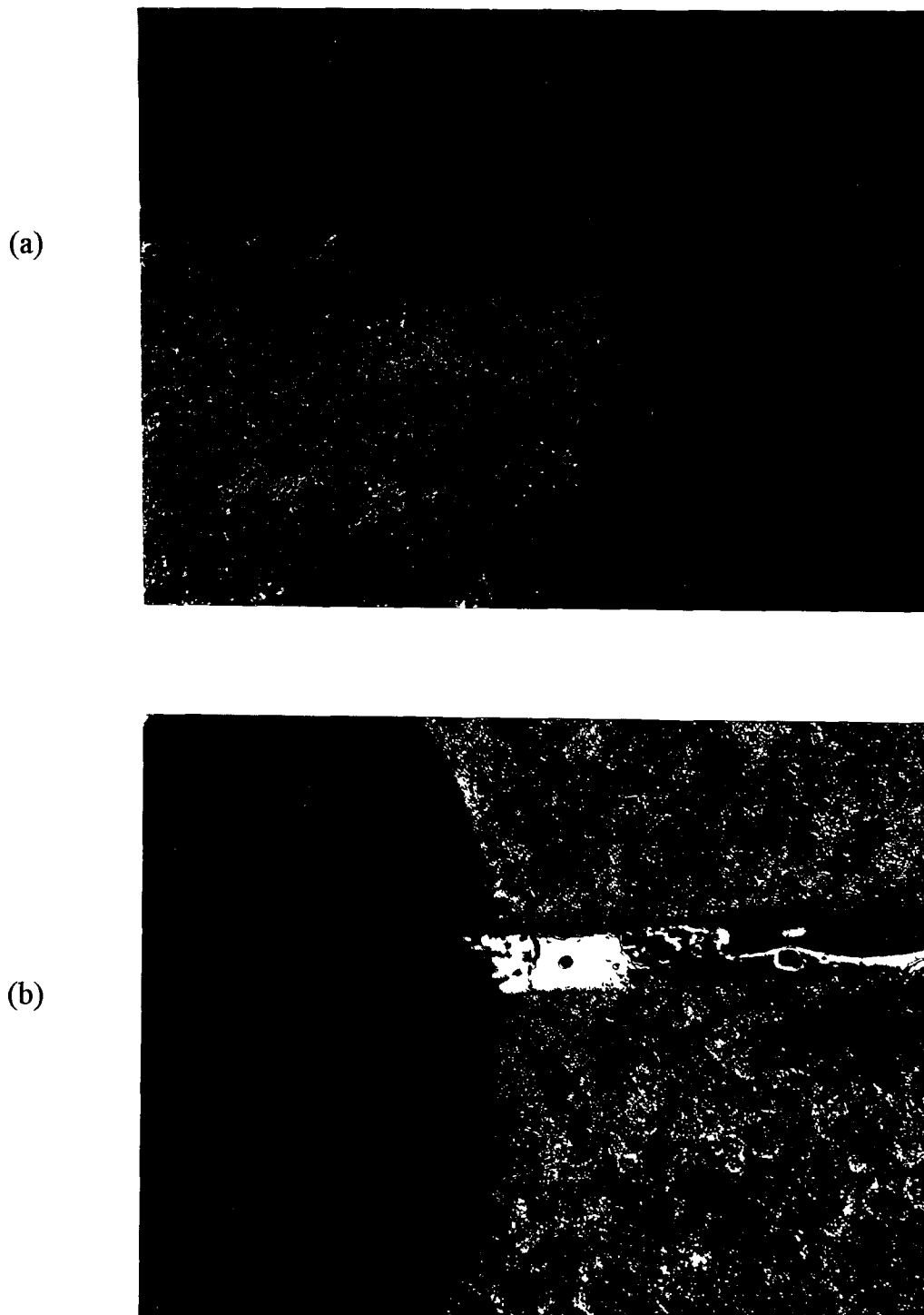


**Figure 5.21(I)** Optical micrographs of specimens after indentation tests using diamond brale with load of 60kgf.  
(a) Specimen 1 ( $\times 375$ ); (b) Specimen 2 ( $\times 300$ ).

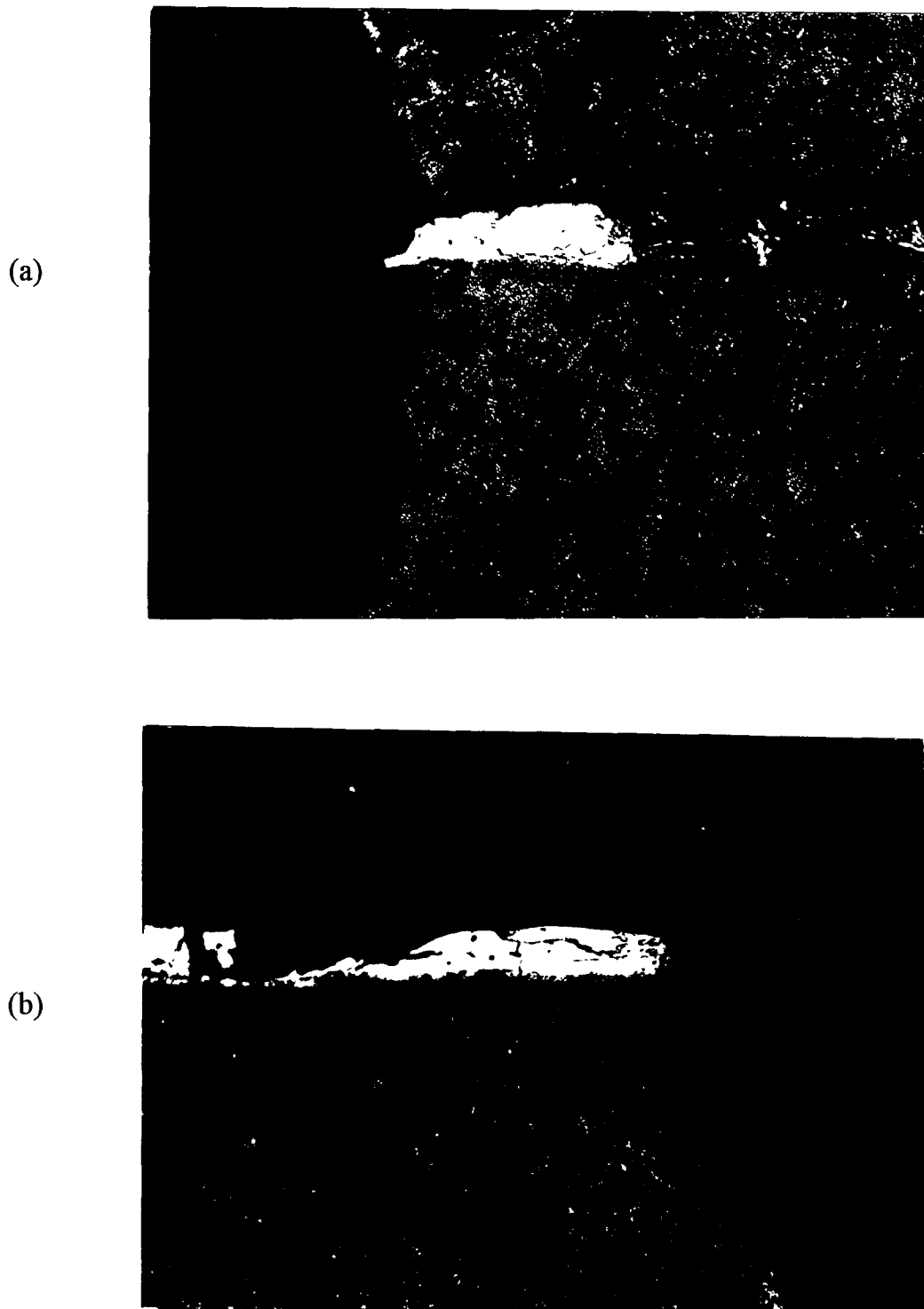


**Figure 5.21(II)** Optical micrographs of specimens after indentation tests using diamond brale with load of 60kgf.  
(a) Specimen 3 ( $\times 300$ ); (b) Specimen 4 ( $\times 300$ ).

visible along the interface between fusion zone and HAZ, indicating the good bonding effect. Moreover, on scrutiny of the deformation around the edge of indentation, the ESD coating specimen demonstrate better resistance to the deformation than the opposite bulk material block used for edge protection in metallographic sample preparation. This is obviously the demonstration of the hardening and strengthening effects of ESD.

## **CHAPTER 6**

### **DISCUSSION**

#### **6.1 Surface Alloying and Microstructure of ESD Coating System**

##### **6.1.1 Surface Alloying**

Surface alloying is the main process in ESD, determining the characteristics of the coating system. Namely, it is the process of surface metallurgical reaction and formation of resultants metallurgically bonded to the surface. It involves the participation of transferred matter, original surface and environment medium. Since the surface alloying is performed at the surface within quite a limited depth while obtaining metallurgical bonding, it serves as a unique surface modification technique which can be used to achieve surface of wide ranges of structures, compositions and thus desired properties.

In ESD, surface alloying is performed between melting droplets transferring from electrode and a subsurface region in the atmospheric media. It proceeds in each spark-induced tiny melting pool on a large substrate surface. As droplets and melting pool are of such small size that the ration of surface area to volume becomes quite high, the atmospheric media plays an important role in the surface alloying.

By considering the above features and the specific characters of electric sparking, the surface alloying in ESD can be reviewed to have the following characteristics:

- a. extremely low heat input;
- b. rapidly heating to high temperature;
- c. short duration of surface alloying in tiny melting pool;
- d. exceptionally rapid solidification;
- e. producing metallurgical bonding.

Obviously, the material systems, process parameters and operating methods will finally determine the processes and results of surface alloying.

In addition to the major alloying reaction in the melting pool, there are reactions in the sparking gap among the transferring droplets, materials vapors and environment media.

Therefore, surface alloying in ESD is of extreme complexity and lack of further knowledge. Investigation of the resultants of ESD by use of modern material analysis techniques such as x-ray diffraction will probably get more understanding.

Anyway, the specific characteristics of surface alloying in ESD indicate that a fused, metallurgically bonded coating with no detectable thermal distortion or changes in metallurgical structure of the substrate can be produced. Moreover, such surface coating can be designed in a wide range of materials composition, and in optimum conditions, achieves an exceptionally fine-grained, homogeneous coating that approach as amorphous structure which is believed to have superior surface performance. However, the unwelcome results may be easily produced if far deviation from the optimum conditions.

### **6.1.2 Materials Systems**

Materials systems determine the metallurgical results of surface alloying and the optimum of ESD processes. Up to now, a wide range of materials have been used satisfactorily in ESD process.

In general, the materials sources for ESD come from the following three parts.

#### **6.1.2.1 Electrodes**

Electrodes for ESD process may be nearly any electrically conductive metal or

cermet capable of being melting in electric sparks. Materials which have been successfully applied include most commercially available bare metals, welding electrodes and many materials adapted or fabricated into electrode forms.

### **1. Composition**

**A. Hardfacing Materials:** Materials most frequently used for electrodes are those hardfacing materials such as the refractory metal carbides and the cobalt-base and nickel-base hardfacing alloys.

**B. Corrosion Resistant Materials:** The most commonly used materials for improving corrosion resistance of surfaces include: chromium and aluminum alloys, and noble metals, such as iridium, platinum, silver, gold and etc.

**C. Other Materials:** The materials used for other purposes vary widely, such as refractory metals for diffusion barriers, structural materials for buildup of selected surfaces, and materials for special surface modification.

**D. Limitation:** Some materials even though electrically conductive, may be unsuitable for ESD application. R. N. Johnson reported in one of his papers[18]:

- a. no significant quantity of chromium-silicide can be successfully deposited although electrodes were gradually consumed.
- b. carbon or graphite which does not have a molten phase at atmospheric pressures, does not transfer from an electrode in significant quantities.
- c. graphite electrodes have been used, however, to thinly carburize some strong carbide formers such as titanium.

**E. Special Problem:** If low-melting-point metals and their alloys are used as alloying materials, "adhesion" of the electrodes at the point of sparking is sometimes observed. This adhesion is stronger the lower the melting point of the electrode and the higher the pulse energy. This can be avoided by reducing the pulse energy and increasing the amplitude of the electrode vibrations. If multi-zone or sandwich structural coating system is required, electrode materials system will be

more complicated.

Anyway, the selection of electrode materials should be based on the requirements of service and the compatibility with the substrate. An important point as to the selection of electrode materials should be borne in mind: much advantage may be gained by formulating materials which take into account the nature of the ESD process and the effect of reaction with the sparking environment. Further study of ESD metallurgy is the crucial approach to establish the principles of formulating materials system.

## **2. Geometry**

**A. Size:** Like welding electrodes, usual ESD electrodes are rods or tubes from 0.5 mm to 25mm, and the usual size ranges from 3mm to 6mm.

**B. Limitation:** Just for the same reasons as in welding process, there are also limitations to the diameter and length of the ESD electrodes.

The surface deposited with a small electrode has a better finish and density is much better. However, a high pulse energy requires electrodes of a larger cross-section if it is necessary to avoid overheating and extending the duration of the pulses. For the same reason, and also in order not to increase the resistance of circuit, it is desirable to avoid long electrodes (the alloying electrodes should not be longer than 20-30mm). The optimum electrode size generally decreases with increasing melting point, increasing resistant ratio, decreasing heat conductivity of the electrode materials. Electrode geometries other than rods or tubes also have been used but are usually confined to vibrating or oscillating electrode motions rather than rotating.

### **6.1.2.2 Substrates**

As with electrodes, substrate materials must also be electrically conductive and capable of being melted.



### **1. Materials Successfully Deposited**

Most structural alloys, such as iron-, nickel-, cobalt-, copper-, aluminum-, titanium-, zirconium-, and refractory metal-base alloys have been successfully coated by ESD process.

### **2. Materials Unsatisfactorily Deposited**

Attempt to apply materials over graphite substrates or over bismuth telluride have not yet been satisfactory.

### **3. Geometry**

The substrate geometries that can be coated by ESD are limited only by the access to the surface using an appropriate electrode.

**A. Successful Application:** ESD coatings have been applied to variety of complex shape, including inside diameters of the tubes or holes, just as arc-welding.

**B. Unsuccessful Application:** Some geometries of surface are difficult to coat by ESD. Excessively rough surfaces or wavy surfaces with a period less than the diameter of the electrode, may lead to the result that the electrode contacts only the high points and therefore only deposits those areas. Apart from this, substrate surfaces usually require little or no preparation for coating other than assuming a reasonable cleanliness and freedom from severe oxidation, as is required for most welding process.

**C. Special Problem:** ESD coating of a cutting-edge or a sharp corner will result in some erosion or rounding of the edge due to the concentration of the spark and the restricted flow of heat from the edge. This effect can be minimized by placing another edge or a sacrificial material in intimate contact and flush with the edge to be protected.

#### **6.1.2.3 Environment Media**

Environment can have significant effect on the deposition characteristics and the

composition of ESD coatings.

As indicated earlier, ESD process are usually conducted in gas medium such as air, argon, nitrogen, CO<sub>2</sub>, helium and various mixture of gases commonly used in the arc-welding process. But most present applications have been in air or argon, with argon used approximately 90% of the time. The advantages of choosing argon lies in the following aspects:

- a. no dissociation of argon is necessary before ionization, so a stable gas conduction path is more easily formed which allows current flow at reduced voltage.
- b. in argon medium, spray transfer mechanism results in better surface finish, except that the deposition rate and transfer efficiencies for all but the refractory alloys and compounds are less.
- c. argon as an inert medium eliminates the contamination from environment which may affects the process, and make the processing of a unit area last longer and the layer deposited thicker.

However, in non-inert medium, contamination by the medium such as nitriding and oxidation in air as we did in this research appears to enrich the surface with hard compounds so as to improve the hardness of the surface. But in many circumstances, such surface layers become brittle and may even peel off if the nitrides form a net along the grain boundaries; and oxidation films on the surface prevent the cohesion of surfaces; an oxide or other films formed on the surface of particles flying towards the cathode or deposited on it can become nuclei for pores or cavities. As shown in our results, the coatings present some brittleness and occasional separation, for which the interference of air should take some responsibility. Therefore many researchers recommend the use of inert gas medium to achieve better surface quality.

In fact, the influence of environment is of complexity, for different materials

systems, and many factors may result in different situations. A recent paper has shown that an atmosphere of CO<sub>2</sub> presents slightly better results over argon and N<sub>2</sub> and may be used in all of the future ESD coatings.

Therefore further study is necessary. If the hardening effect, caused by atmospheric medium such as air and other gases easily and economically available, can be fully utilized in producing well-qualified surfaces, ESD process will show even greater prospect.

### **6.1.3 Microstructure of ESD Coating Systems**

It is important to recognize the fact that the transfer process does not produce a layer of electrode material, as such on the substrate surface. The process should be rather regarded as one in which the substrate is progressively enriched with transferred matter. Since reaction with atmospheric gases may further modify the surface composition and the alloyed material is rapidly chilled from the melting state, the identity of the electrode material may be completely lost. In general, a lot of factors have shown their effects on the structure and characteristics of the surface coating system, but the common points always exist.

#### **6.1.3.1 General Description**

The spark, though intense, is only a few micro-seconds in duration. The resulting material transfer is equally rapid and self-quenching is extremely rapid. Total effects or changes in metallurgical structure of the substrate are typically negligible. The rapid quench rate results in an extremely fine-grained coating structure that approaches (and with some materials, becomes) an amorphous materials or metallic glass. Such kind of structure is believed to contribute to the excellent wear and corrosion properties of the ESD coatings.

### 6.1.3.2 Distinguishment of ESD Coating Structure

#### 1. Fusion Zone

Fusion zone of ESD coating system generally comprises of three structural layers:

##### A. Outmost Layer

- a. Appearance:** Due to its resistant to general etching solutions, this layer usually appears to be "white" in the optical micrograph. However, the appearance of the layer varies with the applied materials systems and etching methods.

Although fine-grained, and in some materials, amorphous structures are expected, it is usually difficult to be distinguished by general methods. For some hardfacing materials as shown in our results, the dispersing hard particles is visible in their featureless matrix in SEM micrograph. The dispersion of such hard particles including their density, size and figure, will have great effects on the structure and performance of the achieved coating system. According to our results, the structure with hard particles of small size and smooth geometrical figure in homogeneous dispersion, appears to have better coating quality and surface performance.

It has been reported that, for some materials systems, such as Ni-Ti surface alloys, investigation by x-ray diffraction (XRD) from surface sequentially polished throughout the thickness of the coating reveals that different alloy phases could be formed on the same material substrate of different surface smoothness.

Pores representing bubbles of trapped gases or cavities associated with non-sufficient overlap and sometimes a network of micro-cracks are visible.

- b. Composition and Properties:** As indicated above, due to the nature of the process (including thermal effects) and reaction with the sparking

environment, this layer approaches the composition of electrode materials but not exactly the same. Surface analysis have shown that in many cases, the properties obtained in this layer are nearly that for the transferred materials. Therefore, this layer can be expected to take the most important part in improving the surface performance.

### **B. Middle Layer**

In this layer, alloying of the substrate with the electrode materials occurs in the very short transfer time, diluting the deposit with substrate materials. Subsequent layers rapidly diminish this effect so that the coating approaches the electrode materials.

- a. Appearance:** This layer is also featureless. Sometimes it is difficult to distinguish from the outmost layer.
- b. Composition:** Along the depth of this layer, composition changes rapidly from nearly that of electrode to nearly that of substrate, and different material combinations exhibit different changing characteristics. In most circumstances, new phases or compounds resulting from alloying present in this layer. From the transient curves by EDS analysis, it is obvious that if intermetallic phases are formed during ESD process, the composition will show step changes along the depth or just a rapid fall in the concentration from electrode materials to substrate materials.

It is important to appreciate that since the heat pulses are extremely brief, the opportunity for diffusion, particularly for solid diffusion, is very restricted. Alloying matter from the electrode therefore cannot penetrate appreciably into the heat-affected zone. However, the rapid transition of composition in this layer does indicate the occurrence of reactional liquid diffusion and its contribution to surface alloying.

- c. Properties:** The change of composition results in transition in properties. The microhardness tests show that dilution of the coating by the substrate material provides a transition layer in the coating structure that exhibits property gradients as a transitional "bridge" between the substrate and the surface.

### **C. Bottom layer**

This layer formed at the bottom of melting pools does not get chances to proceed alloying with transferred matters due to the very short time of sparking and exceptionally rapid quenching by the substrate. However, diffusion may occur in the upper part of the layer.

- a. Appearance:** This layer is thin and featureless, and in some circumstances distinguishable from the upper layers by their interface usually made of the compounds or new phases. Fine-grained or even amorphous structure can be expected. But microcracking and porosity sometimes present along the interface.
- b. Composition:** Composition of this layer approaches that of the substrate. In many circumstances, small gradients of elements from electrode materials in the upper part of the layer are presented on the EDS profile, indicating the limited penetration of those alloying elements, or more exactly their diffusion towards the bulk materials.
- c. Properties:** Transition of properties resulting from diffusion and thermal effect can be expected. However, in some circumstances, there is a "weak valley" at the interface between this layer and the upper layer, followed by an increase till the fusion line. Especially, for some substrate materials such as prehardened steel, the "weak valley" may be so large that this region even presents weakening effects with respect to the substrate, which is referred as "softening" in some literature. Such problem can be solved

by sufficient alloying with the hard electrode materials.

Overall, the inherent transition in properties and the metallurgical bonding are the principle reasons that ESD coatings exhibit such outstanding resistance to damage and spalling in severe mechanical deformation under conditions that destroy most other coatings. The amount of substrate materials fusing into the layer should be controlled to eliminate over-dilution while achieving sufficient metallurgical bond strength. If multi-coatings using different electrode materials or several-stage process is applied, the sequence and the duration for each step in the procedure should be carefully determined in order to reach the optimum.

## **2. Heat Affected Zone (HAZ)**

HAZ usually appears small-grained, narrow, and "dark" at the bottom in the optical micrograph. In cases of sparking overlap or multi-stage deposition, it is a little wider.

This zone is heated to subcritical temperatures high enough to cause some tempering, but no composition changes happen. Due to the thermal effect of the sparking, though very small, some microstructure changes and thus the resulting changes of properties of the substrate material will happen. All the changes depend on material system. For steel, the maximum hardness attainable in this zone is accordingly that of fully quenched steel, while the hardness of fusion zone is augmented by alloying with electrode matter.

Anyway, HAZ of ESD coating system does not show any harmful effect. Instead, it also serves as a good transition "bridge" connecting fusion zone and the substrate.

### 6.1.2.3 Coating Thickness

#### 1. Practical Coating Thickness

Practical coating thickness normally ranges from about  $3\mu\text{m}$  to  $250\mu\text{m}$ , and some deposits of thickness greater than  $1\text{mm}$  have also been obtained for some nickel-base alloys. However, for applications, thickness of less than  $100\mu\text{m}$  are most desirable and practical. Hardfacing materials usually should be applied at the lowest thickness that will meet the service requirement, as thicker coatings tend to be more brittle and have higher internal stresses that can result in cracking of some materials. Our specimens achieve coating thickness of about  $20\text{-}30\mu\text{m}$  with some microcracking.

#### 2. Major Factors

The thickness of ESD coating varies with power setting and sparking duration. Usable coating thickness are strongly dependent upon materials.

**A. Sparking Power and Time:** An increase in the power generally increases the thickness, but at the expense of greater surface roughness and even may results in a reduction of hardness.

For any given set of deposition parameters, the coating thickness will increase with sparking time until a maximum is reached. Continued sparking will get little or no thickness increase and may even result in thickness reduction as a result of spark erosion beginning to dominate the transfer process. This sets a limit to the thickness that can be achieved.

**B. Materials:** Ductile structural materials or materials with low thermal expansion coefficients can normally be applied much thicker, as will be discussed in the following.



#### 6.1.3.4 Softening in ESD Coating System [9]

For steel which has the  $\alpha$ - $\gamma$  transformation in such temperature range, the intensive heating and rapid chilling of microvolume of the surface material always result in the martensite formation with some retained austenite or possibly tempering action, depending on material composition. For example, on high-speed steel or soft steel, the thermal effect leads to the formation of large quantities of retained austenite which produces softening near the interface. It is important to realize that if the quantity of transferred hard material is too small to offset the softening due to austenite formation, the effect of sparking is to soften rather than harden the tool. The basis of this statement is the fact that if tool steel is quenched rapidly from high temperatures a considerable proportion of soft austenite is retained in the structure. The temperature and quenching rates involved in spark treatment are abnormally great and an unusually high proportion of austenite is retained. Since, in general, spark treatment is applied to tools already hardened by conventional means, there is inevitably a tendency for softening to occur. Although, prolonging sparking, using increasing power setting or both may produce intense surface hardening, the subsurface band of comparatively soft material is indeed a characteristic feature of spark-treated tool steel, no matter how hard the outlayer may be.

It has been reported that the surface hardness of high-speed steel can be fully restored by heat treatment after sparking and it may well prove to be of practical benefit to reharden the tool in this way. It should, however, be noted that although a single tempering period produced very little softening of the general steel, repeated heat treatment at the same temperature is likely to cause a progressive fall of hardness and this may be a limiting factor if applied to tools requiring periodic regrinding and resparking. So further work is needed.

## 6.2 Diffusion in ESD

Diffusion is usually considered very effective and important for achieving good surface coating quality and performance because diffusion can build a transition zone which has homogeneously changing gradient of composition and the resulting properties. As we have mentioned before, diffusion process in ESD is quite limited largely due to the extremely short duration of sparking and the exceptionally rapid quenching.

In our ESD specimens, diffusion region does exist in the fusion zone. According to the theory of diffusion, reactional diffusion, especially in the state of liquid, seems to perform in the ESD processes. It can be assumed that reactional diffusion commences from the moment when transferred droplets enter the melting pool. The reactional liquid diffusion facilitates the instantaneous process of surface alloying. However, the following rapid solidification sets a great limit to further diffusion in solid state. If ESD is performed by multi-stage, the current-stage deposition may induce the development of its former diffusion region by providing the temperature and time for solid diffusion again. The similar effect results from the overlap deposition. Therefore, the distinguishable diffusion phenomena can be attributed some extent to our two-stage deposition. At the meantime, as it is shown in our results, the diffusion region does not uniformly distribute through the whole surface coating structure. This again indicates the limit of solid diffusion and the disadvantage of manual operation as well.

In fact, the diffusion process is also largely dependent upon the materials system. If electrode material and substrate material have good mutual diffusivity in the processing conditions, then more obvious diffusion and thus better coating structure can be expected. In case when electrode material is not so compatible with the substrate materials, an inter-layer material which has good compatible with both of them while does not do harm to the designed surface performance can

be applied to produce sandwich-structural coating system. This may be a useful approach to achieve ESD surface coating systems of various desired performances.

### **6.3 Metallurgical Bonding**

Metallurgical bonding as a result of surface alloying is one of the major advantages of ESD. As co-grains are produced along the fusion line, the surface coating is well bonded or welded to the substrate. In this sense, ESD is really a kind of microwelding process. Therefore, some knowledge of welding metallurgy can be applied to explain the metallurgical bonding of ESD.

The co-grains nucleate and grow on the unfused surface of the substrate. Due to the exceptionally low heat input and extremely small size of melting pools with respect to the surface area of the substrate, the grain sizes are extremely small, and there is almost no preferential orientation for grain growth. In particular cases, the grains are so fine that the coating may approaches the amorphous structure.

Moreover, in most cases, HAZ of ESD coating is quite narrow without any visible cracking. It does not have any harmful effect on the bonding. In this sense, metallurgical bonding of ESD coating is better than that of general fusion welding deposition.

In our cases as mentioned before, there is almost no compositional variation in two side subregions (i.e. bottom layer in fusion zone and HAZ) across the fusion line. Therefore, very good bonding can be produced, though two different structures and interference of atmospheric media may have some influence. As confirmed by our results, the metallurgical bonding of ESD coating should be quite good.

Anyway, the knowledge of welding metallurgy, especially that of materials weldability is helpful in considering coating materials system to build good metallurgical bonding by ESD.

#### 6.4 Microcracking in ESD Coating Structure

The observed microcracks in the coating result from stresses caused by thermal effect while sparking, or formation of heterogeneous phases and compounds, or even porosity and cavities. The stresses are usually related to the material system and thickness of the coating, and the process parameters.

The stresses that build up in the coating are more easily relieved and less prone to cracking in the ductile materials, which can absorb more crack-propagating energy to reduce the cracking tendency than low ductile & hard materials. Materials with lower thermal expansion coefficients will produce generally lower stresses and therefore less cracking tendency at the same coating thickness than materials with high thermal expansion coefficients.

Most hardfacing materials are brittle with quite different thermal expansion coefficients from that of the substrate materials. Moreover, alloying and interference of the atmospheric media may result in brittle phases or compounds, which become the origin of cracking.

It has been shown that stresses usually build up in the coating with increasing thickness. So for the same materials, comparatively thick coating suffers higher stresses and more cracking tendency.

Process parameters and operation methods have great influence on the cracking in surface coating structure.

One of the typical effects lies in the cracking orientations. As shown in the general ESD coating microstructure, there exist two main kinds of microcracks. One kind originates and propagates in the parallel direction to the surface, while the other kind is in the vertical direction to the surface. In some circumstances, their form cracking networks, which are most unwelcome for the surface coating structure.

Figure 6.1 published by R. N. Johnson [4], shows the results of different

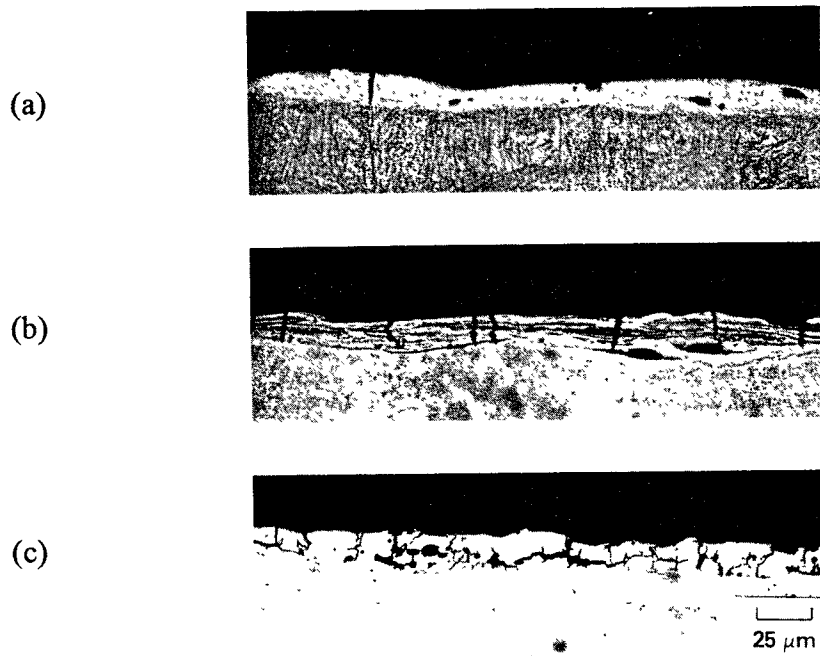


**Figure 6.1** Variation in stress relief cracking in chromium carbide deposited on Type 394 SS as a result of varying ESD parameters.



**Figure 6.2** Cr3-15% ESD coating on Type 316 SS.

coating stresses in the same thickness of chromium carbide deposits on Type 304 stainless steel but with different ESD process parameters. The phenomenon of special interest here is that the direction of stress-relief cracking presents much different effects.

- a. Figure 6.1(c): The cracking structure is obviously undesirable and, as expected, performs poorly in the wear test.
- b. Figure 6.1(a): The cracks perpendicular to the coated surface does not propagate either parallel to the interface or into the substrate.
- c. Figure 6.1(b): The structure is found to perform significantly better in wear rate, galling resistance, and friction coefficients in high temperature sodium than either of the other two structure, including crack-free deposits.

This interesting phenomenon can be explained, according to our results, by the assumption that the vertical cracks shrift part of the shear stresses produced by wear, or most part of tensile stresses caused by bending moments to the sublease or even the substrate which has comparatively better ductility to dull the tips of cracks. Whereas, the hard upper layers with inserted vertical microcracks still demonstrate good resistance to wear deformation. Then, the bonding strength of the surface coating structure is quite important for such "load shrift". Fortunately, metallurgical bonding by ESD makes surface coating of much higher bonding strength than most other coating processes. That is why ESD surface coatings achieve much better surface performances.

Some researchers, therefore, indicate that the stress-relief cracking that sometimes occurs, particularly with hardfacing materials, is not necessarily objectionable. In fact, chromium carbide coating specifications for sodium-cooled nuclear reaction components now specify that the coating must have an average crack density similar to shown in Figure 6.2 [4].

Anyway, microcracks seem to be the inherent defect of ESD coating system. However, through optimization of process parameters and control, desirable surface coating structure can be achieved to meet the service requirement. Besides, further study of ESD metallurgy may find even better approaches to solve such problem as done in welding.

## **6.5 Process Parameters and Their Effect**

In order to produce a well-performed layer on the substrate surface, it is essential to obtain an appreciable transfer of material from the electrode to the substrate. Among the various electrical parameters, the decisive ones are the following [3, 12, 19, 20, 21]:

### **6.5.1 Electrical Power and Spark Energy**

#### **6.5.1.1 Production**

The energy available at the time of occurrence of a spark is the charge stored in the condensers, given by:

$$E = \frac{1}{2}CU^2 \quad (6.1)$$

where  $C$  is the capacitance of the condenser and  $U$  the breakdown voltage.

The total electrical energy over a set period is given by:

$$Q = Ef = \frac{1}{2}CU^2f \quad (6.2)$$

where  $f$  is spark frequency, which is proportional to the energy per spark.

#### **6.5.1.2 Dissipation**

During the sparking, the energy is dissipated in the following ways:

- a. melting and vaporizing some material on the anode;
- b. ionization of the vapor and its transfer to the cathode;

- c. heating the substrate;
- d. losses such as those in the leads connecting the condensers to electrodes; breakdown of dielectric medium; radiation from the spark channel.

#### **6.5.1.3 Distribution**

The distribution of the energy depends upon the following elements: length of the spark gap, the duration of the sparking, the properties of the electrodes and the equipment used.

#### **6.5.1.4 Effect**

It is expected that for a particular set of electrode materials, an increase in the energy of sparking would cause great melting and vaporization of the materials from the anode and this in return would intensify the transfer of material, thus increase the thickness of the layer. But at the same time the roughness of the surface layer increases. A layer of thickness more than 1 mm is so rough that it can not be used in practice. However, the rate of transfer is not directly determined by the energy of sparking and can vary considerably, depending on the individual values of capacity and voltage. Moreover, to each electrical power, there corresponds a maximum thickness of the layer. The more the electrical power is increased then the more the specific time for maximum deposition is reduced.

#### **6.5.1.5 Limitation**

The total energy or heat input that can be used is limited because of the unique properties and advantages inherent to the ESD process. At some point with increasing spark energy and increasing spark frequency, for example, the rapid solidification of the deposit would no longer occur, heat-affected zones would become significant and substrate temperature would increase to levels that allow



metallurgical changes or thermal stress buildup. In other words, the process would become indistinguishable from other arc-welding process. Another reason is the thermal fatigue which dominates the process as the energy increases.

### 6.5.2 Capacitance

The spark energy can be increased by increasing the value of the capacitance or by producing sparks at a higher breakdown voltage. When the spark energy is set, different combination of the two parameters will have different effect on material transfer.

At the moment of discharge, a great capacity effects a greater flow of current which produces a greater electrical power. Therefore the capacity has the the same influence on the hardened layer as the electric power. The greater is the capacity of the capacitor bank, the thicker but also rougher is the surface. Equipment for practical applications must have a capacity between 0 and 100 $\mu$ F. In the early investigation of the effect of different circuit capacities when the breakdown voltage kept constant, it was found that substrate gain increased with capacity (or energy) over the range investigated for the short time of sparking. However, the weight gain is not proportional to the capacity (or energy).

As indicated above, for any value of electrical power, there is a limit to the quantity of material which can be transferred to the cathode. But it is clear that amount of material transferred is larger with higher capacities than with lower capacities before the limit is reached. This limit is reached earlier with higher capacities and gives the weight gain-capacity curves their characteristics shape, as shown in Figure 6.3 [12].

It is thus recommended by some researchers to use higher capacities to achieve the maximum transfer and more efficiency. However, higher capacitors usually result in long duration spark and more pulse energy which cause largely

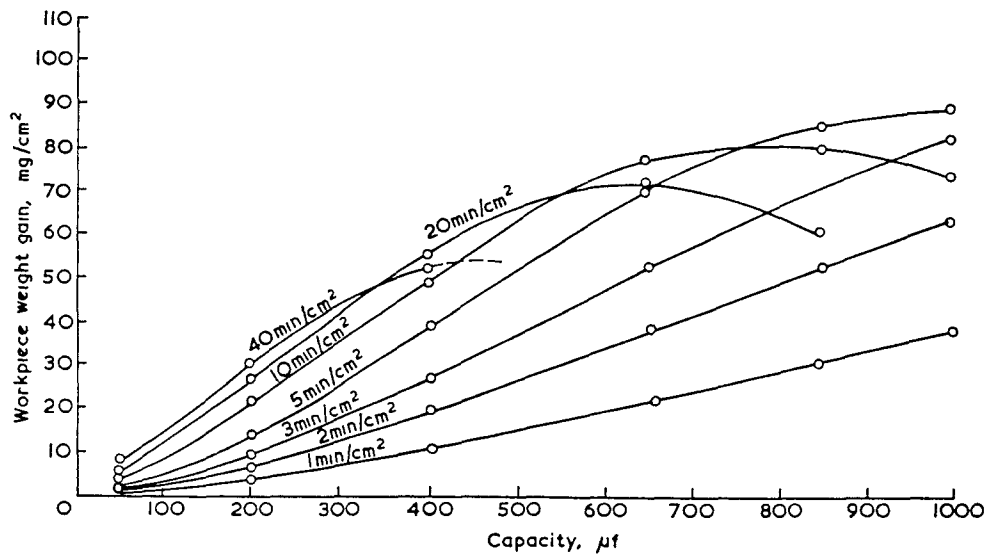


Figure 6.3 Material transfer vs. circuit capacity.

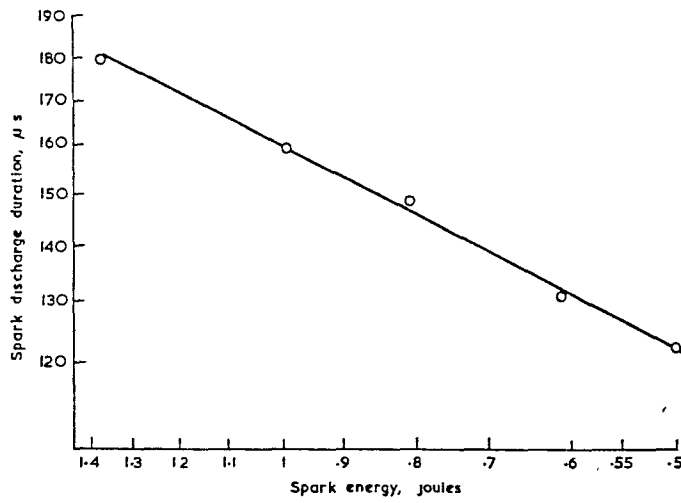


Figure 6.4 Material transfer vs. spark energy.

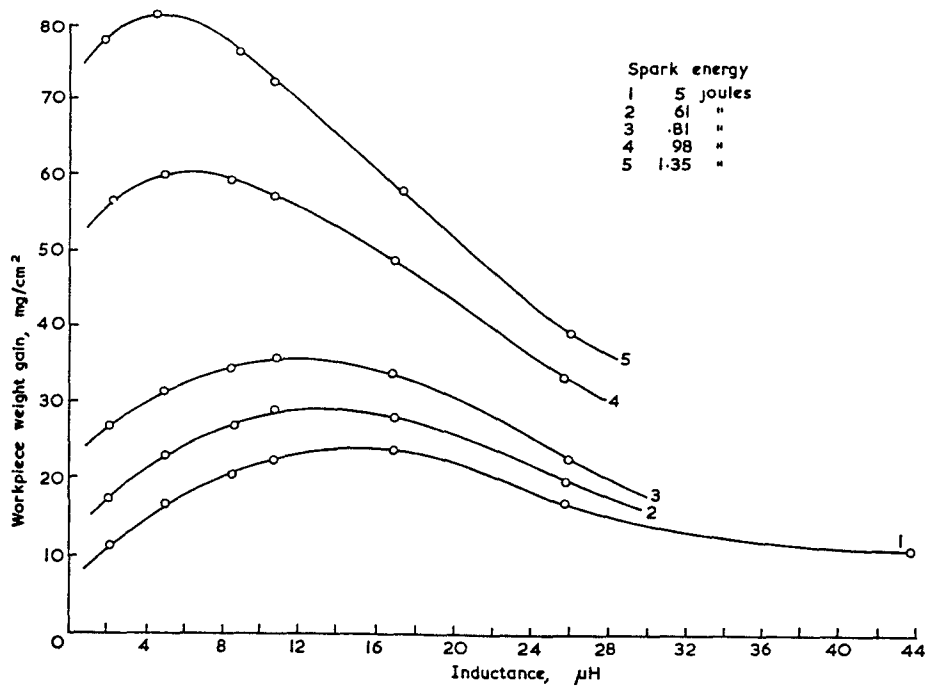


Figure 6.5 Material transfer vs. discharge inductance.

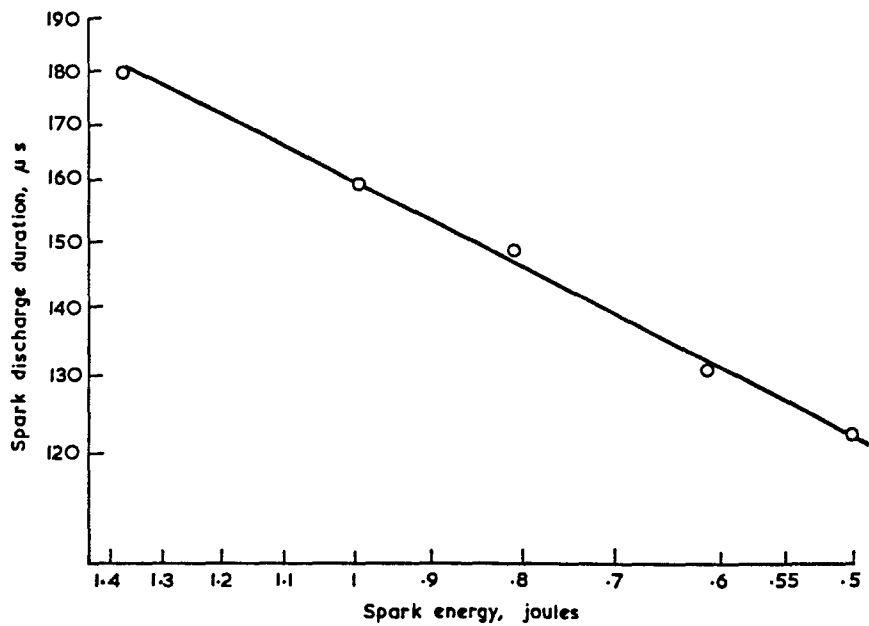


Figure 6.6 Spark duration vs. spark energy for maximum transfer.

globular transfer and rough surface deposits. Therefore other researchers conclude that much smoother, more wear-resistant surfaces can be achieved by using small capacitors charged to a high voltage in a well-designed low inductance circuit.

### **6.5.3 Voltage and Spark Gap**

When the capacity is constant, there is an increase in the rate of transfer with increasing values of spark voltage for short time of treatment, as in the case of capacity variation. However, it is found that in this case with the substrate weight gain per unit of energy does not increase with an increase in sparking voltage, as it does with increasing capacity, but remains almost constant for short time of sparking. It would apparently that the losses in the spark gap increase almost proportionally to the increase in energy, because of the increasing length of spark with voltage.

The increase of breakdown voltage will lead to the commensurate increase of the length of spark gap. When the breakdown voltage in the gap remains constant, the length of the spark gap is not expected to increase. Loss of energy in the spark gap concerned with breakdown of the dielectric and the loss of material in the spark gap increase commensurately with the increase of spark gap.

The same spark energy obtained with higher voltage and lower capacities will entail longer spark gaps and consequently larger losses in the gap than with lower voltages and higher capacities. The efficiency of transfer would therefore be higher in the latter case, as shown in Figure 6.4 [12].

### **6.5.4 Duration of the Sparking**

The material transfer is mainly dependent on the spark energy and its duration which is limited to a few micro-seconds, much less than that of arc. The duration of sparking can be changed by altering the value of the inductance  $L$  in the

discharge circuit.

In early experiments done by C.S.Kahlon, the sparking duration is given by  $\pi(LC)^{1/2}$ . Figure 6.5 [12] shows the observed substrate weight gain vs. the inductances for different values of energies. Figure 6.6 [12] illustrates the relationship between the energy of spark and its duration for maximum transfer. The curves indicate that:

- for each value of spark energy there is an optimum spark duration time for maximum weight gain.
- the feature at the energy loads is of importance. The optimum inductance value is very low and any increase in this value creates a very rapid decline in weight gain. This is related to the occurrence of erosion.

### 6.5.5 Sparking Time

The quality of the layer is largely determined by the time of sparking. To obtain the best quality such as wear resistance, it seems obviously important that a maximum transfer of material is obtained. Figure 7 [21] shows that:

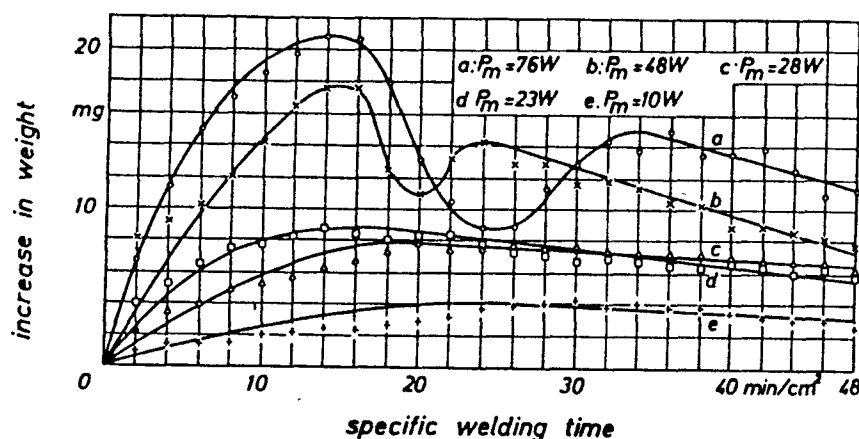


**Figure 6.7** Increase in weight of the workpiece depending on the specific sparking time, for different electrical powers  $P_m$  [21].

- a. only in the first stage of the process is the thickness of the layer proportional to the spark time
- b. there is a maximum weight gain;
- c. beyond the maximum comes a decrease of the thickness and then a second maximum followed by a slight, constant drop in the weight of substrate.

This phenomenon can be generally explained by the breakdown and erosion due to thermal fatigue, and the effect of splattering of melting materials as well. Although there is a linear relationship between the decrease of the electrode weight and the sparking time, there is no corresponding linear build-up of material on the substrate. Therefore it is not possible to reach a particular thickness by an increase of sparking.

As it can be observed in ESD processes, with prolonged time of sparking, dark spots appear on the substrate surface, indicating breakdown of the layer; with further sparking, these spots grow in size and measurements of weight of the substrate begin to show a decrease. It has been proved that thermal fatigue plays an important part in limiting amount of material transfer and in causing a subsequent substrate weight loss. Once breakdown has started to occur the sharp edge offered to the spark will further hasten the erosion of the deposit. It is important, therefore that the substrate is not oversparked if the strengthened layer is to be preserved intact.

The precise moment of completion of the ESD process can be determined by the outward appearance of the spark which gradually loses its brilliance and form after a certain time and this is followed by the appearance of the defective spots.

#### **6.5.6 Amplitude and Frequency of the Vibrating Electrode**

For most early ESD equipment and some still marketed today, spark frequency is controlled by the vibrating frequency of the electrode. The manner and the time of

contacts between the electrode and the substrate thus depend on the amplitude of the vibrating electrode. It is recommended to choose the amplitude between 0.6 and 2.0 mm. With the hand method, using an electrode vibrator and a constant frequency of oscillation of the electrode, force applied to the handle of the vibrator. Changes in the amplitude of oscillation result in corresponding changes of time of charging the condenser, and therefore the voltage of the initial discharge. The different results in respect to increased life of tool after ESD process are explained by the fluctuation in voltage of the initial discharge. The coefficient of increase of life usually ranges from 1.5 to 3.5.

Improved operating efficiency, both with regard to electrical power utilization and production rate would probably result from increased frequency. The limiting value would be set by the electrical circuit requirement such as an optimum quench time between sparks.

In most modern equipment, the spark frequency is controlled electronically independent of the electrode motion. But the electrode still contacts the substrate surface during ESD process, and it is necessary to maintain a continued electrode motion to prevent welding the two surface together.

## **CHAPTER 7**

### **CONCLUSIONS**

An investigation of surface coating microstructure and properties developed by electro-spark deposition on low alloyed steel with some hardfacing materials has been conducted, and reached the following conclusions.

1. Electro-Spark Deposition is one of the very few methods, unusually versatile and effective in achieving various surface performances with extremely low cost.
2. ESD surface coating is achieved with such a low total heat input that changes in metallurgical structure of bulk substrate are negligible and no thermal distortion is detectable.
3. ESD surface coating is made of two-structural zones. The fusion zone of great interest usually comprises of three sublayers. The outmost layer approaches the composition of electrode materials, and thus presents the similar properties. The middle layer shows the transition of composition and properties with formation of certain new phases or compounds in some material systems, and can be taken as a major transitional layer including alloyed and diffusion region. The bottom layer consists of diffusion region at the upper part and the following fused but non-alloyed bulk region. The lower zone is the narrow heat-affected zone adjoining the bulk substrate. Detail structure varies with the applied material system, operating methods and process parameters.
4. Surface alloying predominates ESD process, whereas reactional diffusion, especially in the liquid state, plays roles in the process.
5. Microcracking and porosity seem inherent to ESD process, whereas their influence on surface quality can be minimized through optimization of



process parameters and control. In particular, microcracks in vertical orientation is not necessarily objectionable.

6. ESD surface achieves a fused metallurgical bonded coating of high bonding strength and spalling resistance. It can be of strong wear resistance, and of corrosion resistance or other properties depending upon material systems applied.
7. Air does not seem to be a very good gas medium for ESD due to the consequent nitriding and oxidation that are usually unwelcome for many material systems.
8. ESD surface usually has matte appearance with a variable range of surface roughness.
9. Operating methods, process parameters and control are of extreme importance to ESD surface coating quality.

## **CHAPTER 8**

### **RECOMMENDATION FOR FUTURE WORK**

The future work can be directed in the following aspects:

1. Develop theory of ESD metallurgy and further study the nature of ESD surface structures, especially of those amorphous phases if available.
2. Investigate the changes of materials properties while undergoing ESD process in order to collect data on practical examples and on relevant works in industry applications.
3. Develop approaches to perform micro-metallurgical processes in the surface layers of substrates in order to produce amorphous structures with specified properties on the surface or by depositing materials of specified composition and properties directly onto the surface.
4. Further investigate the effect of environment medium such as nitrogen, oxygen, argon and CO<sub>2</sub> on surface microstructure and properties.
5. Develop new ESD processing methods such as multi-stage coating process; Search for optimum process parameters, and establish an economical and effective ESD process to meet service requirements of engineering practice.
6. Push the advance of ESD equipment for higher quality, better reproducibility, higher production efficiency and lower lost.

## WORKS CITED

1. Lazarenko, B. R. *Electro-spark Machining of Metals*. Consultants Bureau, NY, Vol.2 (1964).
2. Welsh, N. C. "Spark-Hardening of Metals." *J. Inst. Met.* 88 (1959): 103-111.
3. Barash, M. M., and C. S. Kahlon. "Experiments with Electric Spark Toughening." *Int. J. Mach. Tool Des. Res.* 4 (1964): 1-8.
4. Johnson, R. N. "Principles and Application of Electro-Spark Deposition." *Surface Modification Technologies*, TMS (1988): 189-213..
5. Johnson, R. N. "Tribological Coatings for Liquid Metal and Irradiation Environments." *Conference Proceedings on Coatings and Bimetallics for Aggressive Environments*, ASM (1985): 113-123.
6. Rawdon, H. S. "In Discussion of Paper by Ban." *Trans. Amer. Inst. Min. Met. Eng.* 79 (1924): 37.
7. Welsh, N. C. "Frictional Heating and Its Influence on the Wear of Steel." *Journal of Applied Physics*, 28 (1957): 960-968.
8. Welsh, N. C. "Surface Hardening of Non-Ferrous Metals by Spark Discharge." *Nature*, 181 (1958): 1005-1006.
9. Welsh, N. C., and P. E. Watts. "Spark Hardening of Cutting Tools, Austenite Formation and Edge Erosion." *J. Iron and Steel Inst.* May (1961): 30-37.
10. Welsh, N. C., and P. E. Watts. "The Wear Resistance of Spark-Hardened Surface." *Wear*, 5 (1962): 289-307.
11. Lazarenko, B. R., and N. I. Lazarenko. "Electric Erosion of Metals." *Gosenergoizdat*, 1 (1944).
12. Kahlon, C. S. "Electric Spark Toughening of Cutting Tools and Steel Components." *Int. J. Mach. Tool Des. Res.* 10 (1970): 95-121.
13. Johnson, R. N. "Development of Low Friction Materials for LMFBR Components." *Proc. Int. Conf. on Liquid Metal Technology in Energy Production*, CONF-760503, US-ERDA (1976): 95-121.

14. Johnson, R. N. "Coatings for Fast Breeder Reactor Components." *Thin Solid Films*, 118 (1984): 31-47.
15. Johnson, R. N., and G. L. Sheldon. "Advances in the Electrospark Deposition Coating Process." *J. Vac. Sci. Tech. A*4(6) (1986): 2740-2746.
16. Brown III, E.A., and G. L. Sheldon. "A parametric Study on Improving Tool Life by Electrospark Deposition." *Wear of Materials*, 2 (1989): 547-555 .
17. Polyachenko, A.V. *New Methods of Electrical Working of Materials*, Mashgiz, Moscow (1955):366.
18. Natesan, K., and R. N. Johnson. "Development of Coatings with Improved Corrosion Resistance in Sulfur-Containing Environments." *Surface and Coatings Technology*, 43/44 (1990): 821-835.
19. Sheldon, G. L. and R. N. Johnson. "Electro-Spark Deposition—A Technique for Producing Wear Resistant Coatings." *Wear of Materials*, ASM (1985): 388-396.
20. Nosov A.V., and D.V.Bykov. *Working Metals by Electrosparking*. Abridged Translation from Russian, Department of Scientific and Industrial Research, HMSO, London (1956).
21. Stein, H.-U. "Spark Hardening—A Technique for Producing Wear-Resistant Surface." *Science and Technology of Surface Coatings*, Academic Press, NY (1974): 129-135.
22. Budinski, Kenneth G. *Surface Engineering for Wear Resistance*, Prentice-Hall, Inc. (1988).
23. Johnson, Cornelius A. "Metallography Principle and Procedures." *Leco Corporation Manual*, Leco Corporation (1991).
24. *Metals Handbook*, 9th Edition, Vol.10 (1986).
25. Carter, V. E. *Metallic Coatings for Corrosion Control*, Newnes-Butterworth (1977).
26. Sheldon, G. L., R. Wang, and K. A. Clark. "Characteristics of Ni-Ti Surface Alloys Formed by Electrospark Deposition." *Surface Coating Technology*, 36 (1986): 445-454.

27. Vaidyanathan, S. "Reducing Wear of High-Speed Steel Cutting Tools by Spark Hardening." *Wear*, 16 (1970): 255-260.
28. Sisson, Richard D. *Conference Proceedings on Coatings and Bimetallics for Aggressive Environments*, ASM (1986).
29. Yang, Wenge. "Development of Plasma Ion Nitriding Process Parameters to Increase Durability of Machine Components." *Master Thesis*, New Jersey Institute of Technology (1991).
30. Kees, Kenneth Paul. "Hard-Facing with Electro-Spark Deposition." *Master Thesis*, Washington State University (1983).
31. Topinka, Wayne Allen. "Wear Resistant Surface Coatings Deposited on Ti-6Al-4V by Electrospark Alloying." *Master Thesis*, Washington State University (1988).
32. *Surface Texture*, ANSI/ASME B46.1-1985.
33. Schey, John A. *Tribology in Metalworking*, ASM (1983).